BIOTECH STUDIES

VOL 32 ISSUE 2 DECEMBER 2023 ISSN 2687-3761 E-ISSN 2757-5233

Published by Field Crops Central Research Institute, Ankara, TURKEY

TAGEM JOURNALS

Aims and Scope

"Biotech Studies" is the successor to the "Journal of Field Crops Central Research Institute" which has been published since 1992. The journal publishes articles on agro-biotechnology, plant biotechnology, biotechnology for biodiversity, food biotechnology, animal biotechnology, microbial biotechnology, environmental biotechnology, industrial biotechnology and bioprocess engineering, applied biotechnology, omics technologies, system biology, synthetic biology, nanobiotechnology and bioinformatics.

The journal of Biotech Studies has been published twice a year (June & December). Original research papers, critical review articles, short communications and scientific research of the journal are published in English. It is an international refereed journal.

The journal is aimed for researchers and academicians who work in or are interested in the topics of research in biotechnology.

Biotech Studies is indexed in Scopus, ULAKBIM TR Index, Scientific Indexing Services, and CrossRef.

Further information for "***Biotech Studies***" is accessible on the address below indicated:

http://www.biotechstudies.org/

You can reach table of contents, abstracts, full text and instructions for authors from this home page.

Corresponding Address

Address : Field Crops Central Research Institute, (Tarla Bitkileri Merkez Araştırma Enstitüsü)
Şehit Cem Ersever Cad. No:9/11
Yenimahalle, Ankara, Türkiye
Web : www.biotechstudies.org
E-mail : info@biotechstudies.org
Phone : + 90 312 327 09 01-2222
Fax : + 90 312 327 28 93

BIOTECH STUDIES

UN SDG Publishers Compact

As a Publisher, Biotech Studies is pleased to declare its commitment to the United Nations Sustainable Development Goals (UN SDGs) Publishers Compact. The purpose of this Compact is to accelerate progress to achieve SDGs by 2030. Signatories aspire to develop sustainable practices and act as champions of the SDGs during the Decade of Action (2020-2030), publishing books and journals that will help inform, develop, and inspire action in that direction. Furthermore, as a signatory of SDG Publishers Compact, Biotech Studies commit to:

1. **Committing to the SDGs**: Stating sustainability policies and targets on our website, including adherence to this Compact; incorporating SDGs and their targets as appropriate.
2. **Actively promoting and acquiring content** that advocates for themes represented by the SDGs, such as equality, sustainability, justice and safeguarding and strengthening the environment.
3. **Annually reporting on progress towards achieving SDGs**, sharing data and contribute to benchmarking activities, helping to share best practices and identify gaps that still need to be addressed.
4. **Nominating a person who will promote SDG progress,** acting as a point of contact and coordinating the SDG themes throughout the organization.
5. **Raising awareness and promoting the SDGs among staff** to increase awareness of SDG-related policies and goals and encouraging projects that will help achieve the SDGs by 2030.
6. **Raising awareness and promoting the SDGs among suppliers,** to advocate for SDGs and to collaborate on areas that need innovative actions and solutions.
7. **Becoming an advocate to customers and stakeholders** by promoting and actively communicating about the SDG agenda through marketing, websites, promotions, and projects.
8. **Collaborating across cities, countries, and continents** with other signatories and organizations to develop, localize and scale projects that will advance progress on the SDGs individually or through their Publishing Association.
9. **Dedicating budget and other resources towards accelerating progress** for SDG-dedicated projects and promoting SDG principles.
10. **Taking action on at least one SDG goal**, either as an individual publisher or through your national publishing association and sharing progress annually.

Besides these 10 action points, Biotech Studies endorses the SDGs, and explicitly concentrate on eight of 17 goals:

BIOTECH STUDIES

Editorial Information

BIOTECH STUDIES

Editorial Information

Technical Editors

BIOTECH STUDIES

Volume 32 Issue 2 December 2023

CONTENTS

Biotech Studies 32(2), 41-48
http://doi.org/10.38042/biotechstudies.1300663

BIOTECH STUDIES

RESEARCH PAPER

The preparation, characterization, and antibacterial activity evaluation of nanoliposomes incorporated with terebinth extract

Ali Yılmaz[1], Nagihan Nizam[2], Meltem Macit[3], Gülengül Duman[3], Münevver Müge Çağal[4]*

[1]Department of Food Engineering, Graduate School of Natural and Applied Sciences, Gaziantep University, 27310, Gaziantep, Türkiye.
[2]Department of Biotechnology, Graduate Education Institute, Bursa Technical University, 16310, Bursa, Türkiye.
[3]Faculty of Pharmacy, Yeditepe University, 34755, Istanbul, Türkiye.
[4]Department of Bioengineering, Faculty of Engineering and Natural Sciences, Bursa Technical University, 16310, Bursa, Türkiye.

How to cite:
Yılmaz, A., Nizam, N., Macit, M., Duman, G. & Çağal, M. M. (2023). The preparation, characterization, and antibacterial activity evaluation of nanoliposomes incorporated with terebinth extract. *Biotech Studies*, *32*(2),41-48.
http://doi.org/10.38042/biotechstudies.1300663

Article History
Received 29 August 2022
Accepted 25 April 2023
First Online 28 April 2023

Corresponding Author
Tel.: +90 532 6516983
E-mail: munevver.cagal@btu.edu.tr

Keywords
Terebinth (*Pistacia terebinthus*)
Liposome
Microfludizer
Antibacterial activity

Abstract

Nanoliposomes are drug release systems that increase bioavailability and are used for encapsulation of therapeutic active ingredients. Terebinth, which is a medicinal plant that grows in many parts of Türkiye, has antibacterial, antioxidant, and anti-inflammatory activity. The antibacterial activity of nanoliposomes incorporated with ethanol extract of terebinth leaves (TLE) was investigated to determine the effects of formulation.

The nanoliposome formulation was prepared in two steps which were high pressure and high intensity homogenization techniques. Characterization parameters (zeta potential, particle size and distribution, polydispersity index, and encapsulation efficiency) were determined. After third cycle of microfluidization, the zeta potential charge of nanoliposome dispersion was measured -66.6 mV and 91.13 nm in size. The PDI was 0.231. Also, the nanoliposome encapsulation efficiency was calculated as 91.90%. The TLE was encapsulated with nanoliposomes and their antibacterial activity was examined by disk diffusion and minimum inhibition concentration tests against *Escherichia coli* ATTC 25922 and *Staphylococcus aureus* ATTC 25923. Nanoliposome encapsulated TLE (NLTLE) has antibacterial activity against *S. aureus* ATTC 25923. While NLTLE has less active substance, it displays the same antibacterial activity as TLE.

Introduction

Liposomes are tiny spherical structures made of amphipathic lipids organized in one or more bilayers. It is also less immunogenic, biodegradable, and biocompatible. (Ulrich, 2002, Vemuri & Rhodes, 1995; Vuillemard, 1991). Liposomes have many advantages with their structural features, compositions, types and preparation methods. Today, it can be used in many different fields such as food, cosmetics, medicine, pharmacy, and textile (Banerjee, 2001; Betz et al., 2005; Cui et al., 2015; Martí et al., 2012; van Balen et al., 2004). The material being evaluated can be enclosed in a liposome and delivered at the desired place when liposomes are used as medication delivery systems(Pierre & Costa, 2011; Puglia & Bonina, 2012). Similar to this, liposomes are used to encapsulate the substances such as peptides, antibiotics, bioactive chemicals, extracts, and essential oils. Studies indicate that raising the antibiotic concentrations (either passively or actively targeted) near the infection site increases the bactericidal activity, particularly when

liposomes are chosen as antimicrobial drug carriers. It can also lessen the toxicity of the potentially harmful antibacterial active ingredient, which is another contribution (da Silva Malheiros et al., 2010; Engel et al., 2017; Lagacé et al., 1991;Low et al., 2013). Nowadays, nano-sized liposomes have been formed, and their efficacy has been investigated (Tometri et al., 2020). Nanostructures enhance the activity of the encapsulated active material when utilized as a drug carrier. Especially, the microfluidization process is preferred for encapsulation. This technique has several benefits, including high encapsulation efficiency, ability to encapsulate large molecules, to obtain liposome dispersions in nano sizes and long-term stability (Gibbs et al., 1999; Hintz et al., 2015; Hughes, 2005; Torchilin, 2005; Zoghi et al., 2018; Zylberberg & Matosevic, 2016).

The liposomal encapsulation is commonly used with extracts and essential oils from medicinal plants. One of them is *Pistacia terebinthus* L. (Terebinth), which grows naturally in Türkiye, and is used in various fields due to their antibacterial, anti-inflammatory, and cytotoxic activities. The aromatic feature and various medicinal properties of the terebinth are due to the fact that it is a plant rich in phenolic compounds, especially in tannins (Baytop, 1984; Bozorgi et al., 2013; Pelvan & Demirtaş, 2018).

In this study, high pressure and high intensity homogenization (microfluidization) procedures were used to develop a nanoliposome formulation. The physical characteristics of the nanoliposome system were evaluated. Then, the formulation was used to encapsulate the ethanol extract of the terebinth, and its antibacterial activity against gram (+) and gram (-) bacteria were examined.

Materials and Methods

Materials

Terebinth leaves used in the study were obtained from Gaziantep Pistachio Research Institute. The chemicals used in the experiments had analytical purity. Ethanol (99.9%) was obtained from ISOLAB (Wertheim, Germany), L-α-phosphatidylcholine (soybean lecithin, ≥30% enzymatic), and sodium carbonate from Sigma-Aldrich (Missouri, USA).

Preparation of Terebinth Extracts and Their Nanoliposomal Forms

In the first step, microemulsions were made to produce nanoliposomes. For initial homogenization, 200 mL of distilled water and 4 g (2% w/v) of L-phosphatidylcholine material were mixed. For the next 5 min, a direct-end sonicator (IKA- T-18 Digital Ultra-Turrax Homogenizer, a high-speed homogenizer, Staufen, Germany) was used at 70% power (Hafner et al., 2011). The high-pressure homogenizer microfluidizer (M-110EH-30 Microfluidizer High Pressure Homogenizer, Westwood, USA) was used to mechanically prepare liposomes as secondary homogenization. The microfluidization technique was applied on this mixture for three cycles, under a 15000 psi pressure (Macit et al., 2021). After that, to improve its stability and eligibility for encapsulation, the resultant liposome dispersion was lyophilized (Christ Alpha 1-4 LSC Freeze-Dryer, Harz, Germany). For this process, liposome dispersion was kept at -80 °C for overnight. Then, the frozen liposome was lyophilized.

The method used by Doğan et al. (2017) was modified and used in the ethanol extraction of the terebinth leaves. The leaves were dried in an oven at 40 ℃ for 12 h. Then, 200 mL of 90% ethanol solution was added to 20 g of terebinth leaves and stirred at room temperature for 24 h (Stuart/UC 152, Staffordshire, United Kingdom). Subsequently, the mixture obtained by passing through ordinary filter paper was centrifuged at 4500 rpm for 15 min at room temperature (Beckman-Coulter Allegra X30R, Indiana, USA). The mixture obtained after centrifugation was separated from the ethanol part with the help of a rotary evaporator (BUCHI rotary evaporator/R360-E, Flawil, Switzerland). The extract was lyophilized (Toros / TRS 2/2V, Istanbul, Turkey). After lyophilization, powdered TLE weighed as 5.7 g. The lyophilized process was carried out in order not to deteriorate the structures of the TLEs stored for use in the studies.

For encapsulation, lyophilized nanoliposomes were dissolved with autoclaved water at a ratio of 1:10 (w:v) using direct-end sonicator (Bandelin/GM4200, Berlin, Germany) in 5 min under ultrasonic conditions, with an ultrasonic power of 70 W. The nanoliposomes were stored at +4 °C till their characterization analysis and antibacterial experiments.

Analysis of Vesicle Size, Zeta Potential (Z-Potential), and Encapsulation Efficiency (EE)

The mean diameter, zeta potential and PDI values of liposomes were measured by dynamic light scattering (DLS) performed on Malvern Zetasizer (Malvern brand ZS 501).

The encapsulation efficiency analysis was modified and carried out by taking the studies of Kamra et al. (2005) and Nii & Ishii (2005) as an example. The nanoliposome formulations were centrifuged at 18,000 rpm at 5 °C for 60 min. The sediment portion of the mixture was separated and fragmented using ethanol. After this, 1 mL of ethanol-lyzed nanoliposome solution was taken and compared with a UV visible spectrophotometer (VWR/UV-1600PC, Pennsylvania, USA) at 340 nm wavelength.

For this process, lyophilized TLE was dissolved in water instead of ethanol, which is its main solvent. After adding 1.0 g of powdered TLE into 50 mL autoclaved water, it was allowed to dissolve well in the mixer for 90 min. The resulting precipitates were centrifuged at 4500 rpm for 30 min at 26 ℃ and separated from their residues. Since the main solvent of TLE is not water, only a part of the first 1.0 g of TLE was dissolved. To calculate the weight of the solute fraction, it was obtained by

subtracting the amount of TLE that precipitated in the water after centrifugation from the initial powdered TLE. The amount of solute dissolved in 50 mL of distilled water was found to be 0.19 g.

Scanning Electron Microscope (SEM)

The characterization of the nanoliposome-encapsulated terebinth leaf ethanol extract (NLTLE) was performed via an SEM instrument (GeminiSEM 300, Carl Zeiss, Germany). 5 µL of NLTLE was first added to one side of carbon tape, which was adhesive on both sides and placed on an aluminum stub for drying at ambient temperature. Then, the samples were coated with gold under argon vacuum conditions. Gold sputtering thickness was 3.6 nm, obtained in 50 seconds. The accelerating voltage was 5 kV for all experiments. The mean particle sizes of NLTLE were measured using the ImageJ software with the data obtained from the different SEM images of samples.

Antibacterial Activity Determination

Gram (-) bacteria for antibacterial activity; *E. coli* ATTC 25922 and gram (+) bacteria *S. aureus* ATTC 25923 were chosen. Bacterial cultures were obtained from the culture collection unit in the Department of Bioengineering at Bursa Technical University, Bursa, Türkiye. Disc diffusion method (Bauer, 1966) and minimum inhibition concentration method were used to determine the inhibition effect of NLTLE prepared in the study on test bacteria. In the disc diffusion test, a nutrient liquid (NB) (Merck) medium was used for the growth of bacteria. *E. coli* and *S. aureus* were incubated in NB medium at 37 °C for 24 h. A nutrient agar was used in the disc diffusion test. The cultures obtained were adjusted according to the Mc Farland turbidity standard no. 0.5 and 100 µL of each was spread on separate media with the help of the Dragalski loop. Then, sterile discs with a diameter of 6 mm (OXOID, Antimicrobial Susceptibility Test Discs) were placed on the surface of the media at certain intervals. 18 µL of NLTLE, TLE, and nanoliposome formulation (NLF) were added to the placed discs with micropipettes and impregnated. Ofloxacin and distilled water were used for a positive control (PC) and negative control (NC) on the empty disc, respectively. At the end of the application, the petri dishes were incubated at 37 °C for 48 h. At the end of the incubation, the diameter of the zones formed around the disc was measured. The disc diffusion test was performed in three replicates for each bacteria and test substance. Test groups were evaluated statistically using the Kruskal-Wallis rank sum test.

The minimum inhibition concentration (MIC) values were determined by the broth microdilution method according to the CLSI M7-A7 (2006) protocol. Nine dilutions were made for NLTLE, TLE, NLF, and ofloxacin in the value range of 100-0.781 µL/mL. Bacterial suspensions were adjusted to 0.5 McFarland standard turbidity. In brief, the wells of 96-well plates were dispensed with 95 µL of nutrient broth and 5 µL of the bacteria. 100 µL of nine different TLE concentrations were added to it. The same procedures were used with nine different concentrations of NLTLE. The last well was used as a NC. The 96-well microplate was held for 40 sec at 150 rpm on a microplate shaker and incubated in a 37 °C for 24 h. After incubation, each microplate was read in a microplate reader at 600 nm absorbance (Biotek EPOCH microplate spectrophotometer, Vermont, USA). The MIC was evaluated as the lowest concentration of the compounds to inhibit the growth of microorganisms. The MIC test was performed in three replicates for each bacteria and test substance.

Results

Characterization of Nanoliposomes

Particle sizes and zeta potential were determined for each step of the liposome dispersions prepared in two steps. The mean value of the zeta potential of the dispersion prepared in the first stage was measured as -55.0 mV, and the mean size value was measured as 440.6 nm.

Microfluidization, which is a high-pressure homogenization technique, was used as the second homogenization to obtain nanoliposomes. According to the zeta potential data, the mean value of the zeta potential charge was found to be -25.7 mV in three measurements of liposome charges obtained from the first cycle of the microfluidization technique. It has been understood that the first cycle liposomal dispersion with a zeta potential of less than -25 mV is stable

for storage processes, but the number of cycles should be increased for better stability. The average size of the obtained product was 144.9 nm, and the polydispersity index was 0.671 nm. The mean value of the zeta potential charge of the same product of the liposomes after the second cycle was measured as -56.0 mV, and the mean size value was 107.0 nm. The PDI was found to be 0.235. In the second cycle, the size of the liposome vesicles began to approach the nanoscale. Finally, the mean value of zeta potential charge after the third cycle was measured as -66.6 mV and the mean size value was 91.13 nm. The PDI was found to be 0.231 (Table 1).

Table 1. Analysis of nanoliposomal forms

Formulations	Zeta Potantial (mV)	Average Size (nm)	Polydispersity Index (PDI)
DES	- 55.0	440.60	0.626
MFT (Cycle 1)	- 25.7	144.90	0.671
MFT (Cycle 2)	- 56.0	107.00	0.235
MFT (Cycle 3)	- 66.6	91.13	0.231

DES: Direct-End Sonicator, **MFT:** Microfludization Technique

The liposome encapsulation efficiency was calculated for ten different nanoliposomal formulation, and the highest value was reported as 91.90%. NLF2 formulation (0.9 mL TLE), which has the highest value in the formulation prepared with this technique, was used

in characterization studies (Table 2). Besides, considering the amount of encapsulated substance according to the selected nanoliposome formulation (NLF2), the amount of encapsulated terebinth leaves in 1.5 mL was calculated as 3.14 mg. We used almost the same amount of TLE all experiments with encapsulated or unencapsulated.

Table 2. Encapsulation efficiency of nanoliposome formulations

Nanoliposome Formulation	Absorbance Amount (nm)	Encapsulation Efficiency (%)
NLF1 (1 mL TLE)	2.280	77.24
NLF2 (0.9 mL TLE)	2.713	**91.90**
NLF3 (0.8 mL TLE)	2.475	83.84
NLF4 (0.7 mL TLE)	2.238	75.81
NLF5 (0.6 mL TLE)	2.520	85.37
NLF6 (0.5 mL TLE)	2.319	78.56
NLF7 (0.4 mL TLE)	1.941	65.75
NLF8 (0.3 mL TLE)	1.525	51.66
NLF9 (0.2 mL TLE)	1.488	50.41
NLF10 (0.1 mL TLE)	1.441	48.81

The resulting formulation was used for morphological characterization and visualized by SEM. The sizes of NLTLE particles were measured between 130 and 340 nm with the Image-J program on the SEM image. Considering the size difference between the liposome particles compared to the initial nanoliposomes (91.13 nm), it was observed that the nanoliposome increased in size after encapsulation with TLE. Figure 1 shows the SEM image of the NLTLE.

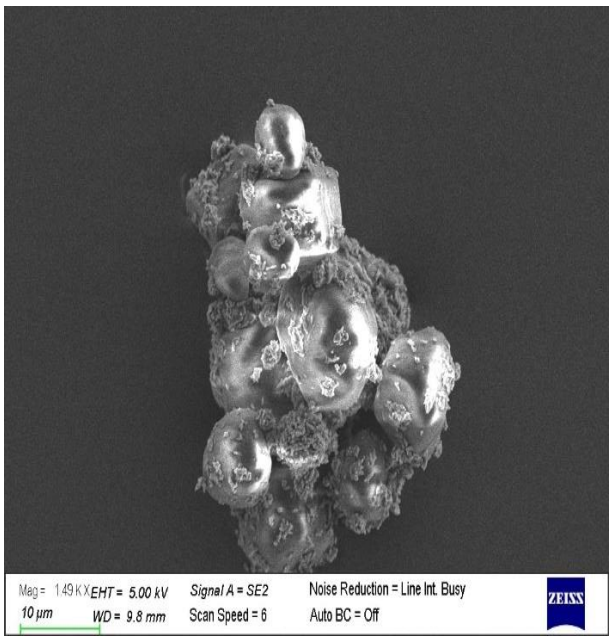

Figure 1. SEM image of nanoliposome-encapsulated terebinth leaf ethanol extract (NLTLE).

Determination of Antibacterial Activity

In terms of bacterial groups, the more antibacterial effect was observed in *S. aureus.* The highest effect was determined at the 48th h for both bacterial groups (Table 3). The amounts used for disc diffusion were calculated from the prepared solutions. It was calculated that there was 68.4 µg of TLE in 18 µL of extract taken for the test. The amount of TLE encapsulated in NLTLE was calculated as 37.7 µg. When evaluated together with the control groups, a statistically significant difference was found between the groups only in *S. aureus* at the 16th h, and *E. coli* at the 24th and 48th h ($p<0.05$) (Figure 2).

Table 3. Comparison of the antibacterial activity with the disc diffusion test

Bacteria Type	Hour	Zone Diameters (mm)				
		NLTLE	TLE	NLF	PC	NC
***E. coli* ATTC 25922**	16	10.67 ±3.21^{a}	9.3 ±0.58^{b}	-	38.01 ±1.00^{ac}	-
	24	11.67 ±2.51^{a}	9.3 ±0.58^{b}	-	38.67 ±1.15^{c}	-
	48	12.67 ±2.08^{a}	11.01 ±0.00^{b}	-	39.01 ±1.00^{c}	-
***S. aureus* ATCC 25923**	16	15.01 ±2.00^{a}	16.67 ±1.15^{b}	-	31.33 ±1.52^{c}	-
	24	15.67 ±2.52^{a}	16.67 ±1.15^{b}	-	33.33 ±0.00^{c}	-
	48	17.01 ±2.65^{a}	18.01 ±1.00^{b}	-	33.33 ±0.58^{c}	-

NLTLE: Nanoliposome-encapsulated terebinth leaf ethanol extract; TLE: Terebinth leaf extract; NLF: Nanoliposome formulation; PC: Positive control (Ofloxacin); NC: Negative control (UV distilled water); -: no microbial growth was observed; ac: Different lowercase letters in the same row indicate a statistically significant difference ($P<0.05$) between the data

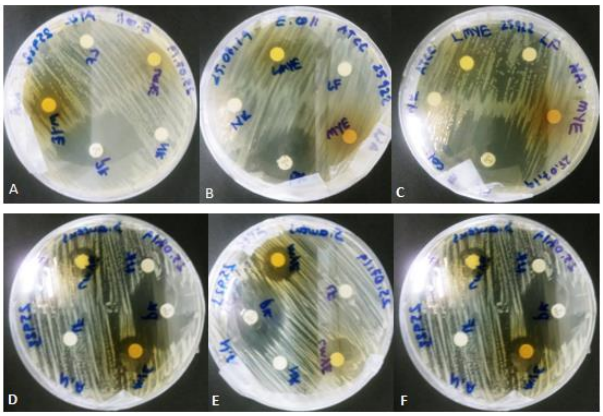

Figure 2. The results of disc diffusion test for *E.coli* ATTC 25922 (A, B, C) and *S. aureus* ATCC 2592 (D, E, F).

The results of the MIC values are presented in Table 4. The amount of encapsulated terebinth leaf for *E. coli* was 2.69 µg and 3.77 µg for *S. aureus*. In addition, the minimum value for TLE was found to be 0.152 mg for *E. coli* and 0.228 mg for *S. aureus.* Results were determined by the broth dilution method with standards approved by the Clinical and Laboratory Standards Institute (CLSI, 2006).

Table 4. Antibacterial activity results for tested samples as MIC

Bacteria Type	Test Samples	MIC (mg)
E. coli ATTC 25922	TLE	0.152
E. coli ATTC 25922	NLTLE	0.114
S. aureus ATCC 25923	TLE	0.228
S. aureus ATCC 25923	NLTLE	0.0838

NLTLE: Nanoliposome-encapsulated terebinth leaf ethanol extract; TLE: Terebinth leaf extract

Discussion

There are many studies on formulations that will both contribute to the effectiveness of antimicrobial agents and controlled release by encapsulation (Engel et al., 2017; Ferreira et al., 2021; Lopes et al., 2019) Principally, with the use of nano-sized liposomes, there is a potential to increase bioavailability after encapsulation (Kırtil & Öztop, 2014). In this study, the preparation stages of nanoliposomes, their characterization, and their effects on the antimicrobial activity of terebinth plant extract were determined.

The study of liposome average size and its distribution is of interest because of its impact on the liposome stability (Were et al. 2004). The effect of preparation methods for the encapsulation of liposomes on the average size and size distribution are shown in Table 1. According to the results, the average particle size of nanoliposomes after three cycles of microfluidization was 91.13 nm. The particle size was reduced by microfluidization process. These results show that microfluidization operating conditions used were adequate for the nanoliposomes (Kumar et al. 2022).

Moreover, the zeta potential is usually used as an indicator of accessible charges in the liposome surface (Awad et al., 2005; De Mello et al. 2013). When the zeta-potential is more than ± 61 mV, the solution is highly compatible with water and the particles are kept very stable (Duman et al., 2014; Heo et al. 2020). The zeta potentials of nanoliposomes were -66 mV, which indicates that they are very compatible for encapsulation.

Looking at the PDI, the measured value indicates that the sample has a very wide particle size distribution if it is greater than 0.7 nm. If this value is less than 0.05 nm, it is called monodisperse. It shows that such dispersions have particles of the same size. Therefore, different algorithms for size distribution are studied with PDI value data among 0.05-0.7 nm. In table 1, the values of the physical properties (zeta potential, size distribution, and surface charge) of the obtained liposomes were compared. It is seen that the dimensions of the liposomes prepared in the first step are 440.6 nm. Looking at the zeta potential graph, it was determined that the liposomal dispersion obtained in the first cycle of the microfluidization technique was stable for storage processes. However, the number of cycles has been increased for better stability and reduced size. In the second cycle, the size of the liposome vesicles began to approach the nanoscale. When the zeta potential and size distribution of the liposome prepared in the third cycle are examined, it is seen that nanoliposomes are formed 91.13 nm, 0.231 PDI, and the liposome load -66.6 mV is stable. Therefore, nanoliposomes taken in the third cycle were used for encapsulation.

In the encapsulation stage, it was dissolved in water instead of ethanol, which is the main solvent of lyophilized TLE. This process was done hence the solvent of the nanoliposomal formulation was water. In addition, the emergence of ethanol-induced effects in antibacterial activity tests was also prevented. Encapsulation efficiency is determined by using organic solvents to release any lipophilic substance trapped between the liposomes bilayer and decompose the liposomal bilayer. The double layer is dissolved in the presence of organic solvents and detergents (Mozafari, 2008). However, not all organic solvents and detergents dissolve lipids with the same efficiency.

In most of the studies, various chemicals such as methanol, isopropanol, Triton-X 100, and Tween-20 are used as lipid solvents. In addition, few studies mention the need to investigate the use of ethanol as a less toxic alternative (Carugo et al., 2016; Demircan, 2016). In this study, ethanol was preferred as the lipid solvent because it is less toxic. The liposome encapsulation efficiency was calculated, and the highest value was reported as 91.90%. In table 1, it is thought that the main reason for the decrease in yield after a certain rate is due to aggregation and deterioration in the liposome structure.

When antibacterial assays were compared, it was observed that TLE and NLTLE were more effective on gram (+) bacteria than gram (-) bacteria (Table 3). It has been observed that two times less concentration of the formulation compared to the extract provides higher antimicrobial activity against *S.aureus*. These results obtained in our study are similar to the antimicrobial activities in the literature (Durak et al., 2015; Tohidi et al., 2011, Sethi et al., 2011). The study of Kavak et al. (2010) supports these results. According to the study, the ethanol extract of the leaf of the terebinth plant showed antibacterial activity against *S. aureus.* On the other hand, the extract had no antibacterial effect on *E. coli.*

In another study conducted by Cui et al. (2015), antimicrobial effects of clove oil containing liposomes were tested against *S.aureus* ATCC 25923 and *E.coli* ATCC 25922. As a result, the liposomal formulation has shown antibacterial activity against only *S.aureus* ATCC 25923 which is gram (+) bacteria. Because, *S.aureus* ATCC 25923 has pore-forming toxins, it can form pores in liposomes. Therefore, toxins can increase the release of substances and interact more easily with active substances. Accordingly, encapsulated TLE has more antibacterial activity on to *S. aureus*.

Overall, this study showed that nanoliposomal formulation increased the bioavailability of TLE at antibacterial tests.

Conclusion

Results presented in this study indicate that nanoliposomes may be good candidates for the encapsulation of bioactive compounds such as TLE. However, data presented in this study also show that preparation of liposomes plays a critical role in terms of

formulation. Here, nanoliposomal formulation with microfluidization allowed significantly decreased liposome size and displayed the best stability of liposomes. According to the antibacterial tests results of NLTLE showed similar activity with TLE although that contains 50% less TLE. These results showed that the decrease in the amount of active substance in encapsulation with nanoliposome did not decrease in the activity, on the contrary, it increased it (Table 5).

Table 5. Effect of TLE and NLTLE on bacteria by amount

Type	Amount of TLE	Bacteria	
		E. coli	*S. aureus*
TLE	68.4 µg	11.01 ± 0.00[b]	1.00 ± 18.01[b]
NLTLE	37.7 µg	12.67 ± 2.08[a]	17.01 ± 2.65[a]

As a conclusion of this study, it has been demonstrated that nanoliposome prepared with microfluidization as a drug carrier is more economical in terms of reducing the amount of active substance and can be used by increasing the bioavailability and antibacterial properties at the same time.

Author Contributions

First Author: Data Curation, Formal Analysis, Investigation, Methodology; Second Author: Data Curation, Formal Analysis, Investigation, Methodology; Third Author: Data Curation, Formal Analysis; Fourth Author: Supervision, Writing - review and editing; and Fifth Author: Investigation, Conceptualization, Writing - review and editing.

Conflict of Interest

The authors declare that they have no known competing financial or non-financial, professional, or personal conflicts that could have appeared to influence the work reported in this paper.

References

Awad, D., Tabod, I., Lutz, S., Wessolowski, H., & Gabel, D. (2005). Interaction of Na2B12H11SH with liposomes: Influence on zeta potential and particle size. *Journal of organometallic chemistry*, 690(11), 2732-2735. https://doi.org/10.1016/j.jorganchem.2005.01.013

Banerjee, R. (2001). Liposomes: applications in medicine. *Journal of Biomaterials applications*, *16*(1), 3-21. https://doi.org/10.1106/RA7U-1V9C-RV7C-8QXL

Bauer, A. W. (1966). Antibiotic susceptibility testing by a standardized single diffusion method. *Am. J. Clin. Pathol.*, 45, 493-496.

Baytop, T. (1984). *Therapy with medicinal plants in Turkey*. Istanbul, CA.: Faculty of Pharmacy Pub.

Betz, G., Aeppli, A., Menshutina, N., & Leuenberger, H. (2005). In vivo comparison of various liposome formulations for cosmetic application, *International journal of pharmaceutics*, *296*(1-2), 44-54. https://doi.org/10.1016/j.ijpharm.2005.02.032

Bozorgi, M., Memariani, Z., Mobli, M., Salehi Surmaghi, M. H., Shams-Ardekani, M. R., & Rahimi, R. (2013). Five Pistacia species (P. vera, P. atlantica, P. terebinthus, P. khinjuk, and P. lentiscus): a review of their traditional uses, phytochemistry, and pharmacology. *The Scientific World Journal*, 2013. https://doi.org/10.1155/2013/219815

Carugo, D., Bottaro, E., Owen, J., Stride, E., & Nastruzzi, C. (2016). Liposome production by microfluidics: potential and limiting factors. *Scientific reports*, 6, 25876. https://doi.org/10.1038/srep25876

CLSI, W. (2006). Clinical and laboratory standards institute methods for dilution antimicrobial susceptibility tests for bacteria that grow aerobically. *Approve Standard M7-A7, CLSI, seventh edition, PA*, USA.

Cui, H., Zhao, C., & Lin, L. (2015). The specific antibacterial activity of liposome-encapsulated Clove oil and its application in tofu, *Food Control*, *56* (2015), 128-134. https://doi.org/10.1016/j.foodcont.2015.03.026

da Silva Malheiros, P., Daroit, D. J., & Brandelli, A. (2010). Food applications of liposome-encapsulated antimicrobial peptides, *Trends in Food Science & Technology*, *21*(6), 284-292. https://doi.org/10.1016/j.tifs.2010.03.003

de Mello, M. B., da Silva Malheiros, P., Brandelli, A., Pesce da Silveira, N., Jantzen, M. M., & de Souza da Motta, A. (2013). Characterization and antilisterial effect of phosphatidylcholine nanovesicles containing the antimicrobial peptide pediocin. *Probiotics and antimicrobial proteins*, 5, 43-50. https://doi.org/10.1007/s12602-013-9125-3

Demircan, E. (2016). *Liposome Encapsulation of Phenolic Compounds Obtained from Apple Peels* (Doctoral thesis). Istanbul Technical University, Institute of Science and Technology, Istanbul.

Doğan, C., Çelik, Ş., & Doğan, N. (2017). Determination of total phenolic compound amounts and antioxidant activities of Siirt region Melengic. *Harran Tarım ve Gıda Bilimleri Dergisi/*Harran Journal of Agricultural and Food Science, 21(3), 293-298. https://doi.org/10.29050/harranziraat.339340

Duman, G., Aslan, İ., Yekta Özer, A., İnanç, İ., & Taralp, A. (2014). Liposome, gel and lipogelosome formulations containing sodium hyaluronate. *Journal of liposome research*, 24(4), 259-269. https://doi.org/10.3109/08982104.2014.907305

Durak, M. Z., & Uçak, G. (2015). Solvent optimization and characterization of fatty acid profile and antimicrobial and antioxidant activities of Turkish *Pistacia terebinthus L*. extracts. *Turkish Journal of Agriculture and Forestry*, 39(1), 10-19. https://doi.org/10.3906/tar-1403-63

Engel, J. B., Heckler, C., Tondo, E. C., Daroit, D. J., & da Silva Malheiros, P. (2017). Antimicrobial activity of free and liposome-encapsulated thymol and carvacrol against *Salmonella* and *Staphylococcus aureus* adhered to stainless steel. *International journal of food microbiology*, 252, 18-23. https://doi.org/10.1016/j.ijfoodmicro.2017.04.003

Ferreira, M., Ogren, M., Dias, J. N., Silva, M., Gil, S., Tavares, L., & Aguiar, S. I. (2021). Liposomes as antibiotic delivery systems: A promising nanotechnological strategy against antimicrobial resistance. *Molecules,* 26(7), 2047**.** https://doi.org/10.3390/molecules26072047

Gibbs, F., Kermasha, S., Alli, I., Mulligan, C.N., B. (1999). Encapsulation in the food industry: a review. *International journal of food sciences and nutrition*,

50(3), 213-224. https://doi.org/10.1080/096374899101256

Hafner, A., Lovrić, J., Pepić, I., & Filipović-Grčić, J. (2011). Lecithin/chitosan nanoparticles for transdermal delivery of melatonin. *Journal of microencapsulation*, 28(8), 807-815. https://doi.org/10.3109/02652048.2011.622053

Heo, S. H., Park, S. I., Lee, J., Kim, M., & Shin, M. S. (2020). Antimicrobial Effect of Supercritical Robinia pseudo-acacia Leaf Extracts and Its Transdermal Delivery System with Cell Penetrating Peptide. *International Journal of Advanced Culture Technology*, 8(1), 226-235 https://doi.org/10.17703/IJACT.2020.8.1.226

Hintz, T., Matthews, K. K., & Di, R. (2015). The use of plant antimicrobial compounds for food preservation. *BioMed research international*, 2015. https://doi.org/10.1155/2015/246264

Hughes, G. A. (2005). Nanostructure-mediated drug delivery. *Nanomedicine: nanotechnology, biology and medicine*, 1(1), 22-30. https://doi.org/10.1016/j.nano.2004.11.009

Kamra, M., Diwan, A., & Sardana, S. (2018). Novel topical liposomal gel of benzoyl peroxide and resveratrol for treatment of acne. *Asian Journal of Pharmaceutical Research and Development*, 6(2), 27-42. https://doi.org/10.22270/ajprd.v6i2.362

Kavak, DD, Altıok, E., Bayraktar, O., & Ülkü, S. (2010). *Pistacia terebinthus* extract: As a potential antioxidant, antimicrobial and possible β-glucuronidase inhibitor. *Journal of Molecular Catalysis B: Enzymatic*, 64(3-4), 167-171. https://doi.org/10.1016/j.molcatb.2010.01.029

Kirtil, E., & Oztop, MH (2014). Liposome as Encapsulation Agent and Its Use in Foods: Structure, Characterization, Production and Stability. *Academic Food Journal/Academic FOOD,* 12(4).

Kumar, A., Dhiman, A., Suhag, R., Sehrawat, R., Upadhyay, A., & McClements, D. J. (2022). Comprehensive review on potential applications of microfluidization in food processing. *Food Science and Biotechnology*, 31, 17-36. https://doi.org/10.1007/s10068-021-01010-x

Lagacé, J., Dubreuil, M., & Montplaisir, S. (1991). Liposome-encapsulated antibiotics: preparation, drug release and antimicrobial activity against Pseudomonas aeruginosa, *Journal of microencapsulation*, *8*(1), 53-61. https://doi.org/10.3109/02652049109021857

Lopes, N. A., Pinilla, C. M. B., & Brandelli, A. (2019). Antimicrobial activity of lysozyme-nisin co-encapsulated in liposomes coated with polysaccharides. *Food Hydrocolloids*, 93, 1-9. https://doi.org/10.1016/j.foodhyd.2019.02.009

Low, W. L., Martin, C., Hill, D. J., & Kenward, M. A. (2013). Antimicrobial efficacy of liposome-encapsulated silver ions and tea tree oil against *Pseudomonas aeruginosa*, *Staphylococcus aureus* and *Candida albicans*, *Letters in applied microbiology*, *57*(1), 33-39. https://doi.org/10.1111/lam.12082

Macit, M., Eyupoglu, O. E., Macit, C., & Duman, G. (2021). Formulation development of liposomal coffee extracts and investigation of their antioxidant capacities. *Journal of Drug Delivery Science and Technology*, 64, 102605 https://doi.org/10.1016/j.jddst.2021.102605

Martí, M., Rodríguez, R., Carreras, N., Lis, M., Valldeperas, J., Coderch, L., & Parra, J. **L**. (2012). Monitoring of the microcapsule/liposome application on textile fabrics, *Journal of the Textile Institute*, *103*(1), 19-27. https://doi.org/10.1080/00405000.2010.542011

Mozafari, MR, Flanagan, J., Matia - Merino, L., Awati, A., Omri, A., Suntres, ZE., & Singh, H. (2006). Recent trends in the lipid - based nanoencapsulation of antioxidants and their role in foods. *Journal of the Science of Food and Agriculture*, *86*(13), 2038-2045. https://doi.org/10.1002/jsfa.2576

Nii, T., & Ishii, F. (2005). Encapsulation efficiency of water-soluble and insoluble drugs in liposomes prepared by the microencapsulation vesicle method. *International journal of pharmaceutics*, 298(1), 198-205. https://doi.org/10.1016/j.ijpharm.2005.04.029

Pelvan, E., & Demİrtaş, İ. (2018). Determination of fatty acid, sterol, tocol compositions, total phenolic contents and antioxidant activities of turpentine (Pistacia terebinthus L.) and pistachio (Pistacia vera) oils grown in Turkey. *GIDA-Journal of Food*, 43(3), 384-392**.** https://doi.org/10.15237/gida.GD18017

Pierre, M. B. R., & dos Santos Miranda Costa, I. (2011). Liposomal systems as drug delivery vehicles for dermal and transdermal applications. *Archives of dermatological research*, 303, 607-621. https://doi.org/10.1007/s00403-011-1166-4

Puglia, C., & Bonina, F. (2012). Lipid nanoparticles as novel delivery systems for cosmetics and dermal pharmaceuticals. *Expert Opinion on Drug Delivery*, 9(4), 429-441. https://doi.org/10.1517/17425247.2012.666967

Sethi, M. H. H. B. A., Rasool, F., & Khurram, M. (2011). Antibacterial activity analysis of extracts of various plants against gram-positive and-negative bacteria. *African Journal of Pharmacy and Pharmacology*, 5(7), 887-893.

Tohidi, M., Khayami, M., Nejati, V., & Meftahizade, H. **(**2011). Evaluation of antibacterial activity and wound healing of *Pistacia atlantica* and *Pistacia khinjuk*. *Journal of Medicinal Plants Research*, 5(17), 4310-4314.

Tometri, S. S., Ahmady, M., Ariaii, P., & Soltani, M. S. (2020). Extraction and encapsulation of *Laurus nobilis* leaf extract with nano-liposome and its effect on oxidative, microbial, bacterial and sensory properties of minced beef, *Journal of Food Measurement and Characterization*, *14*(6), 3333-3344. https://doi.org/10.1007/s11694-020-00578-y

Torchilin, V. P. (2005). Recent advances with liposomes as pharmaceutical carriers. *Nature reviews Drug discovery*, 4(2), 145-160. https://doi.org/10.1038/nrd1632

Ulrich, A. S. (2002). Biophysical aspects of using liposomes as delivery vehicles, *Bioscience reports*, *22*(2), 129-150. https://doi.org/10.1023/A:1020178304031

van Balen, G. P., Martinet, C. A. M., Caron, G., Bouchard, G., Reist, M., Carrupt, P. A., & Testa, B. (2004). Liposome/water lipophilicity: methods, information content, and pharmaceutical applications. *Medicinal research reviews*, 24(3), 299-324. https://doi.org/10.1002/med.10063

Vemuri, S., & Rhodes, C. T. (1995). Preparation and characterization of liposomes as therapeutic delivery systems: a review, *Pharmaceutica Acta Helvetiae*, *70*(2), 95-111. https://doi.org/10.1016/0031-6865(95)00010-7

Vuillemard, J. C. (1991). Recent advances in the large-scale production of lipid vesicles for use in food products: microfluidization, *Journal of microencapsulation*, *8*(4), 547-562. https://doi.org/10.3109/02652049109021878

Were, L. M., Bruce, B., Davidson, P. M., & Weiss, J. (2004). Encapsulation of nisin and lysozyme in liposomes enhances efficacy against *Listeria monocytogenes*. *Journal of food protection*, *67*(5), 922-927.

Zoghi, A., Khosravi-Darani, K., & Omri, A. (2018). Process variables and design of experiments in liposome and nanoliposome research. *Mini reviews in medicinal chemistry*, 18(4), 324-344. https://doi.org/10.2174/1389557516666161031120752

Zylberberg, C., & Matosevic, S. (2016). Pharmaceutical liposomal drug delivery: a review of new delivery systems and a look at the regulatory landscape. *Drug Delivery*, 23(9), 3319-3329. https://doi.org/10.1080/10717544.2016.1177136

Biotech Studies 32(2), 49-58
https://doi.org/10.38042/biotechstudies.1310004

BIOTECH STUDIES

RESEARCH PAPER

Biochemical characterization of *Walterinnesia morgani* (desert black cobra) venom (Serpentes: Elapidae)

Naşit İğci

[1]Department of Molecular Biology and Genetics, Faculty of Science and Arts, Nevşehir Haci Bektaş Veli University, 50300, Nevşehir, Türkiye.

How to cite

İğci, N. (2023). Biochemical characterization of *Walterinnesia morgani* (desert black cobra) venom (Serpentes: Elapidae). *Biotech Studies, 32(*2), 49-58. https://doi.org/10.38042/ biotechstudies.1310004

Article History
Received 13 December 2022
Accepted 09 May 2023
First Online 29 May 2023

Corresponding Author
Tel.: +90 535 3195334
E-mail: igcinasit@yahoo.com.tr

Keywords
Chromatography
Enzyme activity
SDS-PAGE
Snake venom
Zymography

Abstract

Snake venom contains various bioactive proteins and peptides, of which enzymes make up a significant portion. Desert Black Cobra (*Walterinnesia morgani*) is a venomous snake distributed mainly in the Middle East including southeastern Türkiye. The aim of the present study is to investigate the key enzyme activities and protein profile of *W. morgani* venom originating from Sanliurfa province. After the determination of the protein content, the venom sample was subjected to enzymatic activity assays to assess phospholipase A_2, protease, L-amino acid oxidase, hyaluronidase, 5'-nucleotidase and, phosphodiesterase activities by a spectrophotometry-based method. Protease activity was also assessed by gelatin zymography. Additionally, the fibrinogenolytic activity of the venom was evaluated using fibrinogen zymography and SDS-PAGE methods. The protein profile was obtained by SDS-PAGE (both reduced and non-reduced) and reversed-phase HPLC methods. According to the results, 11 protein bands between approximately 12-240 kDa were observed on non-reduced SDS-PAGE gel while there were nine bands between 12-140 kDa on the reduced gel. Venom proteins of *W. morgani* were found predominantly between 25-12 kDa. Proteins were separated into at least 19 major and minor protein groups (peaks) by HPLC analysis. The venom of *W. morgani* showed all tested enzyme activities at varying levels.

Introduction

Snake venom is a complex cocktail consisting of various bioactive proteins and peptides as major constituents, and other organic molecules and inorganics as minor components (Chippaux, 2006; Igci & Ozel Demiralp, 2020). Enzymes make up a significant portion of snake venom proteins. The main enzyme families found in snake venoms are metalloproteinase (SVMP), serine proteinase (SVSP), phospholipase A_2 (PLA_2), L-amino acid oxidase (LAAO), hyaluronidase, phosphodiesterase (PDE), and 5'-nucleotidase (Chippaux, 2006). Annually, more than 420,000 venomous snakebite cases occur globally, of which about 20,000 are fatal (Kasturiratne et al., 2008). Although snake venom components are responsible for their toxicity, they also have diagnostic and therapeutic potential. The drugs targeting the cardiovascular system such as captopril, eptifibatide, and tirofiban were developed based on the peptides found in viper venoms. Moreover, viper venom proteases are used in the diagnostic test for coagulation disorders (Von Reumont et al., 2022).

Walterinnesia morgani (Mocquard, 1905) (Desert Black Cobra), a venomous snake, is mainly encountered in the Middle East including southeastern Türkiye, Iran, Iraq, Syria, Saudi Arabia, and Kuwait (Nilson & Rastegar-Pouyani, 2007). It is is the only member of the Elapidae family in Türkiye, occurring in Sanliurfa and Kilis provinces (Üçeş & Yıldız, 2020; Yıldız, 2020). Populations of *W. morgani* had known as *W. aegyptia* until it was described as a separate species (by combination) in 2007 (Nilson & Rastegar-Pouyani, 2007). It does not cause so many snakebite cases (based on the literature record) possibly due to its

cryptic nocturnal lifestyle but its bite shows neurotoxic effects such as respiratory distress, limb weakness, and numbness (Amr et al., 2020).

The venom arsenals of *W. morgani* and *W. aegyptia* were characterized by a recent proteomic study at the protein family level (Calvete et al., 2021). Three-finger toxin, PLA_2, cysteine-rich secretory protein (CRISP), Kunitz-type serine proteinase inhibitor-like protein, SVMP, LAAO, PDE, acetylcholinesterase, nerve growth factor, 5'-nucleotidase, endonucleotidase, vascular endothelial growth factor protein classes were identified in *W. morgani* venom. Moreover, some of the venom proteins (eg. PLA_2, PDE, three-finger toxins, Kunitz-type protease inhibitor) of a closely-related species *W. aegyptia* were purified and characterized previously (Abid et al., 2020; Al-Saleh et al., 2011; Duhaiman et al., 1996; Lee et al., 1976; Samejima et al., 1997; Simon & Bdolah, 1980; Tsai et al., 2008). However, no study has been published until now regarding the comprehensive enzymatic and fibrinogenolytic activities of *W. morgani* venom. While clinical cases of Desert Black Cobra envenomation are not very common, its venom is understudied and contains different types of biologically active proteins and peptides as other snake venoms. The aim of the present study is to achieve biochemical characterization of *W. morgani* venom originating from southeastern Türkiye in terms of the key snake venom enzyme activities and protein profile.

Materials and Methods

Chemicals

All chemicals used in experiments were molecular biology or liquid chromatography grade. Bis(4-nitrophenyl) phosphate, hexadecyltrimethylammonium bromide (CTAB), tris, hyaluronic acid, fibrinogen from human plasma, phosphate-buffered saline (PBS), glycine, sodium dodecyl sulfate, calcium chloride, L-leucine, O-dianisidine dihydrochloride, and 40% acrylamide/bis solution were purchased from Sigma-Aldrich (Merck-Millipore). Bovine serum albumin (BSA) standard (2 mg/mL), horseradish peroxidase (HRP), and Bradford reagent were from Thermo Scientific, and ammonium persulfate and Coomassie brilliant blue G-250 were from AppliChem and Amresco, respectively. Triton X-100 and gelatin were purchased from Bio-Rad. Other chemicals were obtained from Merck (Merck-Millipore).

Preparation of the venom sample

Venom was milked from one adult individual of *W. morgani* collected from Keberli Village, Sanliurfa province (southeastern Anatolia) following appropriate ethical procedures as described before by Igci and Demiralp (2012). The venom sample was centrifuged at 5,000 x g speed for 5 min at 4°C and the supernatant was lyophilized by using a bench-top freeze-dryer (Millrock). Lyophilized venom was stored at -20°C until use. The species of the snake was identified according to Nilson and Rastegar-Pouyani (2007).

Determination of the protein concentration

Venom was reconstituted in deionized water at 10 mg/mL concentration. Protein content was determined using Bradford's method (Bradford, 1976) in 96-well plate format. 10 µl BSA standards (between 200-1000 µg/mL range) and venom sample were transferred to wells, then 200 µl of Bradford reagent (Thermo Coomassie Plus) was added to each well. After 15 min incubation at room temperature, absorbance at 595 nm wavelength was measured by using a multi-plate reader spectrophotometer (Perkin Elmer, Victor3). The experiment was carried out in triplicate and mean values were used for calculations.

Sodium dodecyl sulfate-polyacrylamide gel electrophoresis (SDS-PAGE)

Discontinuous SDS-PAGE was performed using standard procedures as described by Özel Demiralp et al. (2014) using Bio-Rad Mini-Protean Tetra Cell vertical electrophoresis system. 20 µg venom sample was loaded onto gel (4% stacking, 12% running gel) in reduced (by dithiothreitol) or non-reduced conditions. Electrophoresis was carried out at 100 V constant voltage. The gel was stained with 0.12% (W/V) Coomassie Brilliant Blue G-250 using the "blue-silver" method (Candiano et al., 2004). Bio-Rad Precision Plus Unstained Protein Standard was used to assess the molecular weights of protein bands. Density graphics of gel lanes were created using GelAnalyzer 19.1 software (Lazar & Lazar, 2022).

High performance liquid chromatography (HPLC)

The crude venom of *W. morgani* was separated by the reversed-phase HPLC (RP-HPLC) method using the C18 column (Agilent Poroshell 120 SB-C18, 2.7 µm, 4.6x10 mm). After filtration through a 0.45 µm polytetrafluoroethylene membrane (Agilent), 75 µg protein was injected and chromatographic separation was performed on Agilent 1220 Infinity HPLC system equipped with a diode array detector (DAD). The chromatogram was recorded at 215 nm wavelength and processed with the aid of ChemStation software (Agilent). The reversed-phase separation was achieved using a gradient method using mobile phases A (deionized water + 0.1% TFA) and B (acetonitrile + 0.1% TFA) with a flow rate of 1 mL/min. The gradient was applied as follows: 1 min B 5%, 2-20 min B 30%, 21-50 min B 80%, 51-54 min B 5%, B 5% for 1 min.

Determination of the enzyme activities by spectrophotometry

Spectrophotometric measurements of enzyme activities were performed using Perkin Elmer Victor3 or Lambda25 instruments and appropriate blank tubes were included in each assay. Three technical replicates were included where needed.

Phospholipase A_2 (PLA_2) activity

PLA_2 activity was determined using a commercial kit according to the manufacturer's instructions (Cayman secretory PLA_2 assay kit). The colorimetric assay uses a 1,2-dithio analog of diheptanoyl phosphatidylcholine as a substrate and 5,5'-dithio-*bis*-(2-nitrobenzoic acid) (DTNB) for the detection of free thiols released after PLA_2 activity at 405 nm. Absorbance values were recorded every minute for 10 min and calculations were done using the subtracted values of consecutive time points. The results are expressed as µmol(substrate)/min/mL.

Protease activity

Protease activity was determined using a commercial kit according to the manufacturer's instructions (Pierce Colorimetric Protease Assay Kit), which uses succinylated casein as a substrate. After the hydrolysis of casein by proteases, free amino-terminal groups of released peptides react with trinitrobenzene sulfonic acid (TNBSA) which produces yellowish colour. Trypsin equivalents were calculated using the standard curve.

L-amino acid oxidase (LAAO) activity

LAAO activity was measured according to the method published by Bergmeyer et al. (1983) with some modifications. The reaction mixture included 10 mM L-leucine, 0.2 mg/mL *o*-dianisidine dihydrochloride, and 100 U/mL horseradish peroxidase in 0.2 M Tris-HCl buffer (pH 7.6). Venom (50 µg) was added to this solution and absorbance was recorded every minute for 5 min. Means of the subtracted absorbance values of consecutive time points were calculated and the result is expressed as Units/mg (1 Unit = 1 µmol amino acid oxidized in 1 minute in 1 mL).

Hyaluronidase activity

Hyaluronidase activity assay was performed using the turbidimetric method (Ferrante, 1956). Reaction tubes included 50 µg hyaluronic acid and different concentrations of crude venom (between 200-6.25 µg/mL) in 0.2 M acetate buffer (pH 6.0). After 15 min incubation at 37°C, 2.5% CTAB in 2% NaOH was added to stop the reaction. Samples were measured at 400 nm. The remaining hyaluronic acid amount was estimated based on a calibration curve obtained using different concentrations of hyaluronic acid in the same conditions. After calculation, percent inhibition (hydrolyzed hyaluronic acid) values were used for the IC_{50} calculation.

5'-nucleotidase activity

The 5'-nucleotidase activity was assayed based on a phosphate determination method by Eibl and Lands (1969) with some modifications. The 5'-adenosine monophosphate (5'-AMP) was used as substrate. Crude venom (50 µg) was added to the reaction mixture containing 10 mM $MgCl_2$, 50 mM NaCl, 10 mM KCl, 50 mM Tris, and 10 mM 5'-AMP and incubated at 37°C for 30 min. Thereafter, 30 µl of Triton-X was added and mixed, followed by the addition of 300 µl of 2.5% ammonium molybdate solution (in 6 N H_2SO_4) and 1 mL water. After 20 min incubation at room temperature (RT), absorbance was measured at 660 nm. Released inorganic phosphate content was estimated based on a calibration curve established with KH_2PO_4. The result is expressed as µmoles of inorganic phosphate released in a minute.

Phosphodiesterase (PDE) activity

PDE activity was determined based on the method by Trummal et al. (2014), which is modified from the original method by Babkina and Vasilenko (1964). Fifty µl of venom (1 mg/mL) was added to 200 µl of 10 mM bis(4-nitrophenyl) phosphate (in 0.1 M Tris-HCl, pH 8.8) and incubated at 37°C for 30 min. After that, 1.25 mL of 0.1 M NaOH was added to stop the reaction and measured at 400 nm wavelength. Absorbance was recorded every minute for 5 min. Means of the subtracted absorbance values of consecutive time points were calculated and the result is expressed as Units (1 Unit = 1 µmol substrate modified in 1 minute in 1 mL).

Zymography

Protease activity was also determined by gelatin zymography. Gelatin was added and solubilised in the 12% resolving gel solution at a final concentration of 1 mg/mL. 25 µg of venom were mixed with SDS-PAGE loading buffer without reducing agent and electrophoresis was performed as described previously. After that, the gel was incubated in washing buffer containing 2.5% Triton X-100, 50 mM Tris-HCl pH 7.5, 50 mM $CaCl_2$, 1 µM $ZnCl_2$, and 100 mM NaCl for 2 × 30 min at room temperature; followed by the incubation buffer (1% Triton X-100, 50 mM Tris-HCl pH 7.5, 5 mM $CaCl_2$, 1 µM $ZnCl_2$, and 100 mM NaCl) overnight at 37°C. Then it was washed with distilled water for 10 minutes, followed by staining using Coomassie Brilliant Blue G-250 for 60 min. After destaining with distilled water, the resulting gel was visualized.

Determination of the fibrinogenolytic activity

The fibrinogenolytic activity was determined according to the method by Edgar and Prentice (1973) using SDS-PAGE, with some modifications. Human plasma fibrinogen (12.5 µg in 5 µl) was incubated with 5 µl of venom (125 µg/mL crude venom in 50 mM Tris-HCl, pH 7.8) for different time intervals (5, 10, 30, 60, and 120 min) at 37°C. The reaction was stopped by adding 4 µl of SDS-PAGE loading buffer, followed by heating at 95°C for 5 min. Electrophoresis was performed as mentioned before under a constant voltage of 120 V. Additionally, fibrinogenolytic activity was also investigated by using the fibrinogen zymogram gel method applying a similar procedure as

described in the previous section.

Results and Discussion

Venom color and protein content

The color of *W. morgani* venom used in the present study was yellowish. The yellowish color of snake venoms (typical characteristics of Viperid venoms) is generally attributed to the presence of the flavin groups on LAAOs (Chippaux, 2006). The enzymatic activity results (which are discussed below) showed that the venom had a high LAAO activity. On the contrary, Arikan et al. (2008) reported the color of *W. morgani* venom as colorless. These conflicting results may be due to the variation in the venom composition (Arikan et al., 2014; Chippaux, 2006). The protein content of the reconstituted venom sample was determined as 6.36 mg/mL by the Bradford method.

Protein profiles obtained by SDS-PAGE and HPLC

In order to get an overview of the proteome complexity of *W. morgani* venom, reduced and non-reduced SDS-PAGE and C18-RP-HPLC methods were used. The molecular weight distribution of *W. morgani* venom proteins was obtained by SDS-PAGE under reducing and non-reducing conditions. According to the results, 11 protein bands between approximately 12-240 kDa were observed on the non-reduced gel while there were nine bands between 12-140 kDa on the reduced gel (Figure 1, Table 1). High molecular weight bands of non-reduced gel at 240 and 180 kDa were not observable under reduced conditions and there were also other differences between the two gels. Venom proteins of *W. morgani* were distributed predominantly between 25-12 kDa.

Table 1. Molecular weights assigned to *W. morgani* venom protein bands according to protein marker

Band No	Non-reduced (kDa)	Reduced (kDa)
1	240	140
2	180	95
3	95	68
4	60	56
5	35	30
6	26	23
7	24	16
8	18	15
9	17	12
10	15	
11	12	

Arikan et al. (2008) separated the venom proteins of *W. morgani* from Türkiye (*W. aegyptia* name was used in the paper because it was published before the description of *W. morgani*) by polyacrylamide (7.5%) disc gel electrophoresis method and detected 12 protein fractions. Although their method does not allow the assignment of the molecular weights of the protein bands, it is observable from their results that the venom contains both lower and higher-molecular weight proteins, corroborating the results of the present study. In a study by Abd El Aziz et al. (2015), reducing SDS-PAGE analysis of a closely related species *W. aegyptia* venom resulted in six major protein bands at 10, 12, 14, 22, 70, and 130 kDa. Two thinner and faint bands at 180 and 250 kDa were also observed. Additionally, some of the RP-HPLC fractions contained proteins around six kDa and below. Although there are shared bands between *W. aegyptia* and *W. morgani*, prominent differences are observable in SDS-PAGE band profiles. These two species are closely related to each other phylogenetically, on the other hand, they have differences in venom proteins.

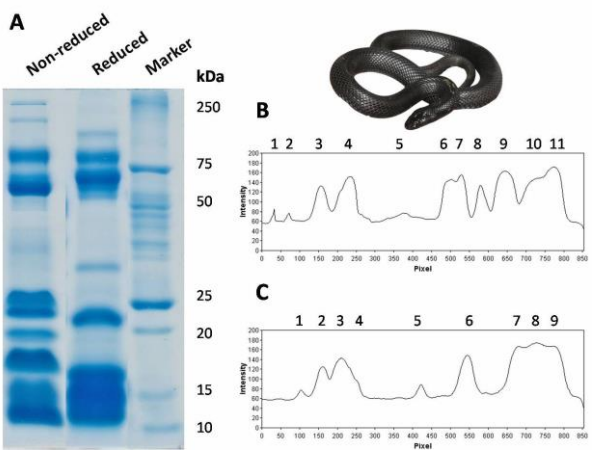

Figure 1. Protein profile of *W. morgani* venom obtained by SDS-PAGE under the reducing and non-reducing conditions. A: Gel images, B: Density plot of non-reduced gel, C: Density plot of the reduced gel. Nine protein bands were observed between 12-140 kDa on the reduced gel while 11 bands between 12-240 kDa were observed on the non-reduced gel. The gel images indicate that one of the major constituents of *W. morgani* venom is three-finger toxins and reveal the presence of high-molecular weight proteins.

Venom proteomes of *W. morgani* and *W. aegyptia* were characterized at the family level by using bottom-up and top-down proteomics in combination (Calvete et al., 2021). Three-finger toxin (3FTx) was the most abundant protein family (~40% of total venom proteins) in *W. morgani* venom. The second most abundant family was PLA_2 (26%) and cysteine-rich secretory protein (CRISP) was the third. Other families identified in *W. morgani* venom were as follows: Kunitz-type serine proteinase inhibitor-like protein (7.2%), SVMP (7.1%), LAAO (6.4%), PDE, acetylcholinesterase, nerve growth factor, 5'-nucleotidase, endonucleotidase, vascular endothelial growth factor. The SDS-PAGE image in Figure 1 shows that most of the venom proteins of *W. morgani* are under 25 kDa. Calvete et al. (2021) identified 3FTx from SDS-PAGE bands of reduced *W. morgani* venom at 10, 14, 18, and 20 kDa. A similar band pattern indicates that the venom sample used in the present study also contains 3FTx as a major venom constituent. Both the SDS-PAGE band pattern and enzyme activity results correlate well with the identified protein families from *W. morgani* venom.

Homodimeric PLA_2 group-I enzyme (named as

WaPLA$_2$) with an estimated molecular mass of 30 kDa was purified from *W. aegyptia* with bactericidal activities (Bacha et al., 2018). PLA$_2$ was identified in *W. morgani* venom from a reduced SDS-PAGE band at approximately 16 and 22 kDa molecular weight and from a 31 kDa band under non-reducing conditions (Calvete et al., 2021). A similar band pattern was observed in this study indicating the presence of dimeric PLA$_2$ enzymes in *W. morgani* venom, and also it was found as one of the major venom constituents according to the band intensities.

The molecular weight of a single-chain phosphodiesterase-I purified from *W. aegyptia* venom was estimated as 158 kDa (Al-Saleh & Khan, 2011). PDEs found in snake venoms generally have higher molecular weights between 90-150 kDa (Al-Saleh & Khan, 2011; Dhananjaya et al., 2010). Although most of the snake venom PDEs are monomeric, some of them were reported as homodimers (Al-Saleh & Khan, 2011). The SDS-PAGE results of the present study showed that *W. morgani* venom has three bands at 95, 180, and 240 kDa under non-reducing conditions whereas 95 and 140-kDa bands were observable in reduced wells in the range where most snake venom PDEs are found (Figure 1). From the results, it is possible that *W. morgani* venom contains single-chain ~ 95 kDa PDE, which is different from *W. aegyptia*. Supporting the results, Calvete et al. (2021) also identified PDE from a reduced SDS-PAGE band with about 97 kDa in *W. morgani* venom.

Based on the enzyme activity results (see the next section) as well as the known molecular weights of SVMPs from other snake venoms, the 240 kDa-band observable on non-reducing SDS-PAGE gel indicating that *W. morgani* venom contains high molecular weight multimeric P-III group SVMP. Calvete et al. (2021) identified SVMP from a non-reduced SDS-PAGE band above 116 kDa and from reduced bands, as well. The present study provides the more approximate molecular weight of the multimeric SVMP found in the venom of *W. morgani*. A ~60 kDa-serine proteinase with factor X activating activity was also purified from *W. aegyptia* venom (Khan & Al-Saleh, 2015). A band at approximately 60 kDa is present in the non-reduced SDS-PAGE gel of *W. morgani* venom, indicating the possibility of the presence of a serine proteinase.

Venoms of the snakes belonging to the family Elapidae may have predominantly proteins below 20 kDa (especially *Naja*, *Bungarus*, *Ophiophagus*) (Nawarak et al., 2003). However, proteins with higher molecular weights can also be found as a major component in the venoms of other Elapids (eg., *Notechis*, *Pseudonaja*, *Oxyuranus*) (Birrell et al., 2007). The presence of the proteins with higher molecular weight in the venoms of *W. morgani* and *W. aegyptia* observed in the present study and the others is a prominent result in this regard, showing the unique venom composition of the genus (Abd El Aziz et al., 2015; Calvete et al., 2021). The genus *Walterinnesia* is considered and used as a basal clade in the phylogenetic trees of Elapids and is recognized as one of the most primitive Elapid species (Keogh, 1998; Wüster et al., 2007). Therefore, investigations on the venom of this genus may provide novel data regarding the venom evolution.

W. morgani envenomation causes generalized limb weakness, numbness, respiratory distress, paraesthesia around the wound, and diplopia, related to its neurotoxic effect (Haidar & Deitch, 2015; Lauer et al., 2011). Edema around the wound can also be seen. These effects mainly originate from the abundant 3FTx proteins in *W. morgani* venom. But other secondary protein families such as PLA$_2$, SVMP, and LAAO also contribute to its physiological effects.

According to the HPLC result recorded at 215 nm, *W. morgani* venom proteins separated into 19 protein groups (peaks) between 15-51 min (Figure 2), which corresponds to 20%-80% acetonitrile concentration in our method. But only two minor peaks were recorded after 60% acetonitrile.

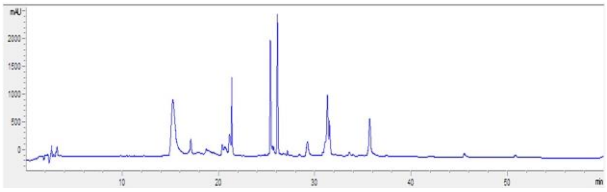

Figure 2. HPLC chromatogram of *W. morgani* venom measured at 215 nm wavelength.

The chromatogram profile obtained at 280 nm was similar, therefore it is not shown. The retention times of each peak are indicated in Table 2. Major and minor peaks were observable on the chromatogram.

Table 2. Retention times of the major and minor RP-HPLC peaks of *W. morgani* venom

Peak No	Retention time (min)	Peak No	Retention time (min)
1	15.2	11*	27.1
2	17.1	12*	28.3
3*	18.7	13	29.2
4	20.3	14	31.2
5*	20.6	15	31.5
6	21.1	16*	33.5
7	21.3	17	35.6
8	25.3	18*	45.5
9	25.7*	19*	50.8
10	26.1		

The general pattern and peak clusters of the chromatogram show similarity to those provided by Calvete et al. (2021). Although chromatographic conditions are different, correlating the retention times and acetonitrile concentration allows a certain degree of comparison. For instance, four region of peak groups is observable on the chromatogram provided by Calvete et al (2021) which is consistent with our results. With a rough estimate, HPLC peaks between 14-22 min obtained in the present study may contain 3FTx, PLA$_2$

may be found in the peaks between 25-27 min, CRISP and SVMP between 30-32, LAAO between 35-37 min retention times. But of course, precise identification can be achieved by mass spectrometry analysis. Both SDS-PAGE and HPLC results indicate that *W. morgani* venom sample investigated in the present study is rich in 3FTx and PLA_2.

Enzyme activities

Enzymatic activities were measured based on spectrophotometric methods. Additionally, protease activity was assessed by gelatin zymography. The results of the enzyme activity measurements by spectrophotometry are summarized in Table 3. Results are generally presented as µmol/min/mL (U/mL). The protein concentration of the venom was calculated as 6.36 mg/mL by Bradford's method and can be used for U/mg calculations. While there is very limited information on the venom of *W. morgani*, there are a few studies on *W. aegyptia* venom, a closely related species aiming to purify and characterize venom proteins. Therefore, the results are compared with those related to *W. aegyptia* venom when available.

Table 3. Enzyme activities of *W. morgani* venom

Enzyme Activity	Activity Values
Phospholipase A_2	68.8 U/ml
Protease (spectrophotometric)	–
Protease (gelatin zymography)	Thin clear band at about 240 kDa
L-amino acid oxidase	4.4 U/ml
Hyaluronidase	IC_{50} = 27.45 µg/ml
Phosphodiesterase	2.93 U/ml
5'-nucleotidase	82.66 U/ml

According to the results of the present study, *W. morgani* venom showed well PLA_2, LAAO, PDE, hyaluronidase, and 5'-nucleotidase activities. These results are similar to those reported by Al-Asmari et al. (1997) obtained for *W. aegyptia* venom. Protease activity was not detected spectrophotometrically in our experimental conditions but a thin clear band at about 240 kDa was observed on gelatin zymogram gel (Figure 3B). There is also a thin band at the same kDa on the non-reducing SDS-PAGE gel, indicating that *W. morgani* venom may contain high molecular weight (approximately 240 kDa) multimeric SVMP. The reason for not detecting the activity in a spectrophotometry-based method can be related to the sensitivity of the assay (the positive control showed activity) or substrate specificity. Gelatin was used as a substrate in zymography whereas casein was used in the spectrophotometric method. Zinc-dependent metalloproteinases (EC 3.4.24) in snake venoms play an important role in the pathology of a venomous snakebite by interfering with the coagulation cascade and causing tissue necrosis and hemorrhage (Chippaux, 2006). SVMPs are mainly found in viper venoms as a major venom protein family. It was concluded that although *W. morgani* venom includes SVMP, its activity is low, which is also the case in the *W. aegyptia* venom (Al-Asmari et al., 1997).

PLA_2 (E.C. 3.1.1.4) is one of the common protein families found in snake venoms that hydrolyses the sn-2 ester bond of glycerophospholipids resulting in the generation of fatty acids and lysophospholipids.Besides their action on the tissue damage in the prey, they have diverse biological activities including procoagulant, anticoagulant, antiplatelet, antimicrobial, myotoxic, and neurotoxic effects(Chippaux, 2006; Kini, 2003). PLA_2 enzymes were purified from the venom of *W. aegyptia* previously (Abid et al., 2020; Bacha et al., 2018; Simon & Bdolah, 1980). PLA_2 activity of the crude venom was calculated as 750 U/mg total protein and about four-fold purification was achieved in the study by Simon & Bdolah (1980). The calculated activity unit value is much higher than that obtained in the present study. The reason for this can be technical variation, different methods were used in these two studies. For example, the specific activity of PLA_2 was calculated as 50 U/mg again for *W. aegyptia* venom. In another study that used a method more similar to the one in this paper, lower activities close to those calculated in this study (when converted to the same unit) were reported across different *Naja* species (Tan et al., 2019). Moreover, enzyme amounts/activities may vary between different species (Chippaux, 2006). Even though they are closely related, it was shown that enzyme abundancies (including PLA_2) varied significantly between *W. aegyptia* and *W. morgani* (Calvete et al., 2021).

LAAO (E.C. 1.4.3.2) is another enzyme family found in snake venoms commonly. *W. morgani* venom has a good level of LAAO activity according to this study. Calvete et al. (2021) identified the enzyme from different SDS-PAGE bands, which are consistent with the results of the present study. LAAOs, which catalyze the oxidative deamination of L-amino acids, have various activities such as hemorrhagic, anticoagulant, antiplatelet, apoptosis-inducing, antibacterial and antiviral effects (Du & Clemetson, 2002). Substrate specifity of *W. morgani* LAAO can be assessed using amino acids other than leucine by additional studies.

Phosphodiesterases (E.C. 3.1.4.1) cleave phosphodiester bonds in nucleic acids and hydrolyze some type of nucleotides, as well. They show diverse biological activities related to nucleotide signaling including platelet aggregation (Chippaux, 2006; Trummal et al., 2014). Phosphodiesterase-I was purified from the venom of *W. aegyptia* (the locality is not clear but published after the description of *W. morgani* so that the taxon was considered as *W. aegyptia*) using preparative native polyacrylamide gel electrophoresis (Al-Saleh & Khan, 2011). They found that the enzyme had a specific activity of 3.4 U/mg (this value corresponded to a three-fold purification). PDE

enzymes were purified from various Viperids and Elapids, as well but Viperids have generally higher activity (Dhananjaya et al., 2010). Along with snake venom PDEs, 5'-nucleotidase (E.C. 3.1.3.5.) is another understudied enzyme class found in snake venoms that cleaves variety of mononucleotides. These enzymes prefer 5'-AMP as a substrate. Therefore, this molecule was used as a substrate to assess the enzymatic activity. Releasing of adenosine by the 5'-nucleotidase activity is thought to contribute to the toxicity of snake venoms (Dhananjaya et al., 2010).

Hyaluronidase (E.C. 3.2.1.35) is another common enzyme family of snake venoms (even across other venomous animal groups). Although its abundance is generally lower than other snake venom proteins, they show significant activity by degrading mucopolysaccharides in the connective tissue of the prey. Therefore, it is thought that this enzyme "helps" venom diffuse through the tissues (Chippaux, 2006). Although hyaluronidase activity of *W. aegyptia* venom was reported (Al-Asmari et al., 1997), there is no information regarding the presence of this enzyme in *W. morgani* venom in the literature. Venom samples were obtained from different parts of Riyadh (Saudi Arabia) in the aforementioned study before the description of *W. morgani*; both species were recorded from the region and specimens identified as *W. morgani* were found genetically identical to *W. aegyptia* from Riyadh and Egypt (Alshammari et al., 2022). Therefore, the species used for the venom source was considered as *W. aegyptia*. Calvete et al. (2021) did not identify the enzyme either by bottom-up or top-down proteomic analyses, possibly due to the low abundance.

In a recent study, proteomic characterization of *W. morgani* venom was achieved and all the enzyme classes assayed in the present study except hyaluronidase were identified at the protein family level (Calvete et al., 2021). As discussed above, SDS-PAGE results also confirm the presence of these enzyme groups in the venom. This study provided the first data on the activities of these enzyme groups in *W. morgani* venom. Additionally, the presence of the enzyme hyaluronidase was reported in *W. morgani* venom for the first time in the present study.

The fibrinogenolytic activity was also assessed by SDS-PAGE and fibrinogen zymography. A slight activity was observed in gelatin zymogram gel while no activity was detected in fibrinogen zymography (Figure 3C). Moreover, SDS-PAGE analysis shows no significant degradation of fibrinogen chains by *W. morgani* venom proteases. Fibrinogen degradation is especially important in the envenomation cases of Viperids (Chippaux, 2006). Although the results of the present study and those in the literature indicate the presence of SVMP and possibly SVSP in *W. morgani* venom, these enzymes do not have (at least prominent) fibrinogenolytic activities according to the results. Supporting these results, lacking the defibrinogenating activity of *W. aegyptia* (a closely related species) was also reported by Al-Asmari et al (1997).

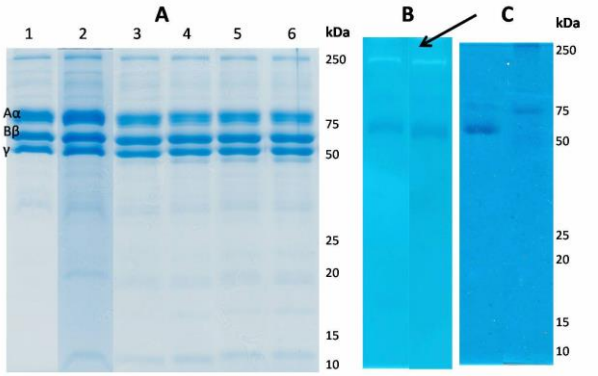

Figure 3. Gel images of SDS-PAGE based fibrinogenolytic activity (A), gelatin zymography (B) and fibrinogen zymography (C). Arrow indicates the slight gelatinolytic activity of *W. morgani* venom. Lane 1: untreated fibrinogen; lanes 2-6: fibrinogen incubated with venom at 5, 10, 30, 60, 120 min, respectively. Aα, Bβ, and γ are symbols denoting the alpha, beta and gamma chains of fibrinogen protein, respectively.

Briefly, the present study revealed the key enzymatic activities of *W. morgani* venom in a comparative manner as well as reported hyaluronidase for the first time and provided additional information on its protein profile. Published studies have been generally focused on the venom of a closely related species *W. aegyptia*. Hence, the data on *W. morgani* venom is limited. Moreover, its fibrinogenolytic activity was assessed for the first time in the literature with this study. There is no data regarding the bioactivity of *W. morgani* in the literature to the best of the author's knowledge. However, a closely related species *W. aegyptia* was shown to possess anticancer and antimicrobial activities (Al-Sadoon et al., 2012; Bacha et al., 2018; Badr et al., 2013). Some interesting molecules such as a peptide named actiflagelin (a member of the 3FTx family), which has sperm motility-enhancing activity have been isolated from *W. aegyptia* venom (Abd El-Aziz et al., 2018). Taking into consideration these findings, *W. morgani* venom may also have potential as a source for natural bioactive molecules.

Conclusion

In conclusion, *W. morgani* venom was found to have all the major enzyme activities important for snake venoms and its venom contains both high and low-molecular weight proteins. The findings of the the present study highlight *W. morgani* venom as a good candidate for use in the discovery of novel bioactive proteins. Analyzing snake venoms in order to obtain an inventory of the protein/toxin classes and assess the variation is not only important for biodiscovery, but also provides insight into the envenomation pathology and contributes to antivenom production. The results are useful in this regard and will guide future purification and characterization studies.

Ethical Statement

Venom was extracted from one adult individual of *W. morgani* collected from Keberli Village, Sanliurfa province (southeastern Anatolia) following appropppriate ethical procedures. Although collecting venom in the nature does not require ethical permission since it can be considered as a specialized secretion, the author obtained ethical permission for animal handling in the laboratory and care as well as the venom milking procedure for various species from Ege University Animal Experiments Local Ethics Committee (2010-43). This study was presented in 1st International Congress on Biotech Studies.

Funding Information

This work was supported by Research Fund of the Nevşehir Hacı Bektaş Veli University (Project number: BAP18F26).

Acknowledgements

The author is grateful to Prof. Dr. Mehmet Zülfü YILDIZ (Adiyaman University Department of Biology) for providing venom sample, Nevşehir Haci Bektaş Veli University (NEVU) Science and Technology Research and Application Center for HPLC analysis, and Ankara University Biotechnology Institute and Prof. Dr. Aslıhan KARATEPE (NEVU Department of Chemistry) for laboratory access. The author also thanks Miss. Fikriye Seda ATASOY for her technical help during some of the experiments. I remember the late Turkish herpetologist Prof. Dr. Bayram GÖÇMEN with respect and thank for his contributions to our studies in the past, as well as his help for obtaining the venom material used in the present study.

References

Abd El Aziz, T. M., Bourgoin-Voillard, S., Combemale, S., Beroud, R., Fadl, M., Seve, M., & De Waard, M. (2015). Fractionation and proteomic analysis of the *Walterinnesia aegyptia* snake venom using OFFGEL and MALDI-TOF-MS techniques. *Electrophoresis*, *36*(20), 2594–2605. https://doi.org/10.1002/elps.201500207

Abd El-Aziz, T. M., Khoury, S. A., Jaquillard, L., Triquigneaux, M., Martinez, G., Bourgoin-Voillard, S., Séve, M., Arnoult, C., Beroud, R., & De Waard, M. (2018). Actiflagelin, a new sperm activator isolated from *Walterinnesia aegyptia* venom using phenotypic screening. *Journal of Venomous Animals and Toxins including Tropical Diseases*, *24*, 2. https://doi.org/10.1186/s40409-018-0140-4

Abid, I, Jemel, I., Alonazi, M., & Bacha, A. B. (2020). A new group II phospholipase A2 from *Walterinnesia aegyptia* venom with antimicrobial, antifungal, and cytotoxic potential. *Processes*, *8*(12), 1560. https://doi.org/10.3390/pr8121560

Al-Asmari, A. K., Al-Abdulla, I. H., Grouch, R. G., Smith, D. C., & Sjostrom, L. (1997). Assessment of an ovine antivenom raised against venom from the desert black cobra (*Walterinnesia aegyptia*). *Toxicon*, *35*(1), 141–145. https://doi.org/10.1016/s0041-0101(96)00068-2

Al-Sadoon, M. K., Abdel-Maksout, M. A., Rabah, D. M., & Badr, G. (2012). Induction of apoptosis and growth arrest in human breast carcinoma cells by a snake (*Walterinnesia aegyptia*) venom combined with silica nanoparticles: Crosstalk between Bcl2 and Caspase 3. *Cellular Physiology and Biochemistry*, *30*(3), 653–665. https://doi.org/10.1159/000341446

Al-Saleh, S. S. M., & Khan, S. (2011). Purification and characterization of phosphodiesterase I from *Walterinnesia aegyptia* Venom. *Preparative Biochemistry & Biotechnology*, *41*(3), 262–277., https://doi.org/10.1080/10826068.2011.575319

Alshammari, A. M., Badry, A., Aloufi, B. H., & El-Abd, E. (2022). Molecular phylogeny of *Walterinnesia aegyptia* (Reptilia, Elapidae) isolated from Ha'il province, Saudi Arabia. Open Journal of Applied Sciences, *12*(10), 1661–1672. https://doi.org/10.4236/ojapps.2022.1210113

Amr, Z. S., Abu Baker, M. A. & Warrell, D. A. (2020). Terrestrial venomous snakes and snakebites in the Arab countries of the Middle East. *Toxicon*, *177*, 1–15. https://doi.org/10.1016/j.toxicon.2020.01.012

Arıkan, H., Göçmen, B., Kumlutaş, Y., Alpagut-Keskin, N., Ilgaz, Ç., & Yıldız, M. Z. (2008). Electrophoretic characterisation of the venom samples obtained from various Anatolian snakes (Serpentes: *Colubridae, Viperidae, Elapidae*). *North-Western Journal of Zoology*, *4*(1), 16–28.

Arıkan, H., Göçmen, B., İğci, N., & Akman, B. (2014). Age-dependent variations in the venom proteins of *Vipera kaznakovi* Nikolsky, 1909 and *Vipera ammodytes* (Linnaeus, 1758) (Ophidia: Viperidae). *Turkish Journal of Zoology*, *38*, 216–221. https://doi.org/10.3906/zoo-1303-17

Babkina, G. T., & Vasilenko, S. K. (1964). Nuclease activity of the venoms of mid-Asia snakes. *Biokhimiya*, *29*, 268–272.

Bacha, A. B., Alonazi, M. A., Elshikh, M. S., & Karray, A. (2018). A novel bactericidal homodimeric PLA_2 group-I from *Walterinnesia aegyptia* venom. *International Journal of Biological Macromolecules*, *117*, 1140–1146. https://doi.org/10.1016/j.ijbiomac.2018.06.024

Badr, G., Al-Sadoon, M. K., & Rabah, D. M. (2013). Therapeutic efficacy and molecular mechanisms of snake (*Walterinnesia aegyptia*) venom-loaded silica nanoparticles in the treatment of breast cancer- and prostate cancer-bearing experimental mouse models. *Free Radical Biology and Medicine*, *65*, 175–189. https://doi.org/10.1016/j.freeradbiomed.2013.06.018

Bergmeyer, H. U., Bergmeyer, J., & Grassl, M. (1983). L-amino acid oxidase. In H. U. Bergmeyer (Ed.), *Methods of Enymatic Analysis Vol. II* (3rd ed., pp. 149–151). Verlag Chemie GmbH.

Birrell, G. W., Earl, S. T. H., Wallis, T. P., Masci, P. P., de Jersey, J., Gorman, J. J., & Lavin, M. E. (2007). The diversity of bioactive proteins in Australian snake venoms. *Molecular & Cellular Proteomics*, *6*(6), 973–986. https://doi.org/10.1074/mcp.M600419-MCP200

Bradford, M. M. (1976). Rapid and sensitive method for the

quantitation of microgram quantities of protein utilizing the principle of protein-dye binding. *Analytical Biochemistry*, *72*(1-2), 248–254. https://doi.org/10.1016/0003-2697(76)90527-3

Calvete, J. J., Pla, D., Els, J., Carranza, S., Damm, M., Hempel, B.-F., et al. (2021). Combined molecular and elemental mass spectrometry approaches for absolute quantification of proteomes: Application to the venomics characterization of the two species of desert black cobras, *Walterinnesia aegyptia* and *Walterinnesia morgani*. *Journal of Proteome Research*, *20*(11), 5064–5078. https://doi.org/10.1021/acs.jproteome.1c00608

Candiano, G., Bruschi, M., Musante, L., Santucci, L., Ghiggeri, G. M., Carnemolla, B., et al. (2004). Blue silver: a very sensitive colloidal Coomassie G-250 staining for proteome analysis. *Electrophoresis*, *25*(9), 1327–1333. https://doi.org/10.1002/elps.200305844

Chippaux, J.-P. (2006). *Snake venoms and envenomations* (1st ed.). Krieger Publishing Company.

Dhananjaya, B. L., Vishwanath, B. S., & D'Souza, C. J. M. (2010). Snake venom nucleases, nucleotidases and phosphomonoesterases. In S. P. Mackessy (Ed.), *Venoms and Toxins of Reptiles* (1st ed., pp. 155-171). CRC Press.

Du, X.-Y., & Clemetson, K. J. (2002). Snake venom L-amino acid oxidases. *Toxicon*, *40*(6), 659–665. https://doi.org/10.1016/s0041-0101(02)00102-2

Duhaiman, A. S., Alhomida, A. S., Rabbani, N., Kamal, M. A., & Al-Jafari, A. A. (1996). Purification and characterization of acetylcholinesterase from desert cobra (*Walterinnesia aegyptia*) venom. *Biochimie*, *78*(1), 46–50. https://doi.org/10.1016/0300-9084(96)81328-9

Edgar, W., & Prentice, C. R. M. (1973). The proteolytic action of ancrod on human fibrinogen and its polypeptide chains. *Thrombosis Research*, *2*(1), 85–95. https://doi.org/10.1016/0049-3848(73)90082-0

Eibl, H., & Lands, W. E. M. (1969). A new, sensitive determination of phosphate. *Analytical Biochemistry*, *30*, 51–57. https://doi.org/10.1016/0003-2697(69)90372-8

Ferrante, N. D. (1956). Turbudimetric measurement of acid mucopolysaccharides and hyaluronidase Activity. *Journal of Biological Chemistry*, *220*, 303–306. https://doi.org/10.1016/S0021-9258(18)65354-2

Haidar, N. A., & Deitch, E. (2015). Snake bites in the Arabian Peninsula, a review article. *Journal of Arid Environments*, *112*(B), 159–164. https://doi.org/10.1016/j.jaridenv.2014.04.010

Igci, N., & Ozel Demiralp, D. (2012). A preliminary investigation into the venom proteome of *Macrovipera lebetina obtusa* (Dwigubsky, 1832) from Southeastern Anatolia by MALDI-TOF mass spectrometry and comparison of venom protein profiles with *Macrovipera lebetina lebetina* (Linnaeus, 1758) from Cyprus by 2D-PAGE. *Archives of Toxicology*, *86*, 441–451. https://doi.org/10.1007/s00204-011-0763-5

Igci, N., & Ozel Demiralp, F. D. (2020). A Fourier transform infrared spectroscopic investigation of *Macrovipera lebetina lebetina* and *M. l. obtusa* crude venoms. *European Journal of Biology*, *79*(1), 14–22. https://doi.org/10.26650/EurJBiol.2020.0039

Kasturiratne, A., Wickremasinghe, A. R., de Silva, Gunawardena, N. K., Pathmeswaran, A., Premaratna, R., Savioli, L., Galloo, D. G., & de Silva, H. J. (2008). The global burden of snakebite: A literature analysis and modelling based on regional estimates of envenoming and deaths. *PloS Medicine*, *5*(11), e218. https://doi.org/10.1371/journal.pmed.0050218

Khan, S. U., & Al-Saleh, S. S. (2015). Biochemical characterization of a factor X activator protein purified from *Walterinnesia aegyptia* venom. *Blood Coagulatin & Fibrinolysis*, *26*(7), 772–777.

Kini, R. M. (2003). Excitement ahead: structure, function and mechanism of snake venom phospholipase A_2 enzymes. *Toxicon*, *42*(8), 827–840. https://doi.org/10.1016/j.toxicon.2003.11.002

Keogh, J. S. (1998): Molecular phylogeny of elapid snakes and a consideration of their biogeographic history. *Biological Journal of the Linnean Society*, *63*(2), 177–203. https://doi.org/10.1006/bijl.1997.0178

Lauer, C., Zickgraf, T. L., & Weisse, M. E. (2011). Case report of probable desert black snake envenomation in 22-year-old male causing profound weakness and respiratory distress. *Wilderness & Environmental Medicine*, *22*(3), 246–249. https://doi.org/10.1016/j.wem.2011.04.003

Lazar Jr., I., Lazar Sr., I. (2022). GelAnalyzer [Internet]. Version 19.1. 2022.

Available from: http://www.gelanalyzer.com/

Lee, C. Y., Chen, Y. M., & Mebs, D. (1976). Chromatographic separation of the venom of Egyptian black snake (*Walterinnesia aegyptia*) and pharmacological characterization of its components. *Toxicon*, *14*(4), 275–278. https://doi.org/10.1016/0041-0101(76)90023-4

Nawarak, J., Sinchaikul, S., Wu, C.-Y., Liau, M.-Y., Phutrakul, S., & Chen, S.-T. (2003). Proteomics of snake venoms from Elapidae and Viperidae families by multidimensional chromatographic methods. *Electrophoresis*, *24*, 2838–2854. https://doi.org/10.1002/elps.200305552

Nilson, G., & Rastegar-Pouyani, N. (2007). *Walterinnesia aegyptia* Lataste, 1887 (Ophidia: Elapidae) and the status of *Naja morgani* Mocquard, 1905. *Russian Journal of Herpetology*, *14*(1), 7–14. https://doi.org/10.30906/1026-2296-2007-14-1-7-14

Özel Demiralp, F. D., İğci, N., Peker, S., & Ayhan, B. (2014). *Temel Proteomik Stratejiler* (1st ed.). Ankara Üniversitesi Yayınevi.

Samejima, Y., Aoki-Tomomatsu, Y., Yanagisawa, M., & Mebs, D. (1997). Amino acid sequence of two neurotoxins from the venom of the Egyptian black snake (*Walterinnesia aegyptia*). *Toxicon*, *35*(2), 151–157. https://doi.org/10.1016/S0041-0101(96)00138-9

Simon, T., & Bdolah, A. (1980). Isolation of phospholipase A from the venom of the desert black snake *Walterinnesia aegyptia*. *Toxicon*, *18*, 369–373. https://doi.org/10.1016/0041-0101(80)90020-3

Tan, C. H., Wong, K. Y., Tan, N. H., Ng, T. S., & Tan, K. Y. (2019). Distinctive distribution of secretory phospholipases A2 in the venoms of Afro-Asian cobras (Subgenus: *Naja*, *Afronaja*, *Boulengerina* and *Uraeus*). *Toxins*, *11*(2), 116. https://doi.org/10.3390/toxins11020116

Trummal, K., Aaspollu, A., Tonismagi, K., Samel, M., Subbi, J., Siigur, J., & Siigur, E. (2014). Phosphodiesterase from *Vipera lebetina* venom – Structure and characterization. *Biochimie*, *106*, 48–55.

https://doi.org/10.1016/j.biochi.2014.07.020

Tsai, H.-Y., Wang, Y. M., & Tsai, I.-H. (2008). Cloning, characterization and phylogenetic analyses of members of three major venom families from a single specimen of *Walterinnesia aegyptia*. *Toxicon*, *51*(7), 1245–1254. https://doi.org/10.1016/j.toxicon.2008.02.012

Üçeş, F., & Yıldız, M. Z. (2020). Snakes of Şanlıurfa province. *Commagene Journal of Biology*, *4*(1), 36–61. https://doi.org/10.31594/commagene.725036

Von Reumont, B. M., Anderluh, G., Antunes, A., Ayvazyan, N., Beis, D., Caliskan, F., et al. (2022). Modern venomics—Current insights, novel methods, and future perspectives in biological and applied animal venom research. *GigaScience*, *11*, 1–27. https://doi.org/10.1093/gigascience/giac048

Wüster, W., Crookes, S., Ineich, I., Mané, Y., Pook, C. E., Trape, J.-F., & Broadley, D. G. (2007). The phylogeny of cobras inferred from mitochondrial DNA sequences: Evolution of venom spitting and the phylogeography of the African spitting cobras (Serpentes: Elapidae: *Naja nigricollis* complex). *Molecular Phylogenetics and Evolution*, *45*(2), 437–453. https://doi.org/10.1016/j.ympev.2007.07.021

Yıldız, M. Z. (2020). Herpetofauna of Kilis province (Southeast Anatolia, Turkey). *Amphibian & Reptile Conservation*, *14*(2), 145–156.

Biotech Studies 32(2), 59-64
http://doi.org/10.38042/biotechstudies.1310572

BIOTECH STUDIES

REVIEW

Food grade microalgae-based biopigments and their production technique versus synthetic colorants

Didar Üçüncüoğlu[1,2]

[1]Department of Food Engineering, Faculty of Engineering, Çankırı Karatekin University, 18100, Çankırı, Türkiye.
[2]Yoka Functional Food, İnd. Trade. Co. Ltd., 18260, Korgun, Çankırı, Türkiye.

How to cite:
Üçüncüoğlu, D. (2023). Food grade microalgae-based biopigments and their production technique versus synthetic colorants. *Biotech Studies*, *32*(2), 59-64. http://doi.org/10.38042/biotechstudies.1310572

Article History
Received 11 January 2023
Accepted 29 May 2023
First Online 05 June 2023

Corresponding Author
Tel.: +90 376 21895008358
E-mail: didaru@karatekin.edu.tr

Keywords
Biotechnology
Microalgae
Biopigment
Synthetic colorants
Food additive

Abstract

In the food industry, synthetic color-active compounds can be added as additives to replace natural colors that are damaged during processing. This addition reduces the batch-to-batch fluctuation and increases the development of new or desired products that are appealing to consumers where natural colors are absent. Synthetic colorants cannot be produced by any bioprocess. In contrast, the Food and Drug Administration declared that algae such as *Chlorella*, *Cryptothecodinium*, *Dunaliella Nannochloropsis*, *Nitzschia*, *Phaeodactylum*, *Schizochytrium*, and *Spirulina* are trustable sources of food pigments as natural sources. These microalgae are photoautotrophic species and can be found on the "Generally Recognized as Safe-GRAS" list of food additives. Microalgae-derived pigments, which are also known as nutraceutical supplements, have been recently used in functional food products. Some of them are used as health and color supporters because of their excellent antioxidant properties that block oxidative reactions in lipid-rich food products. Their unique properties of being harmless to the environment were scientifically proven as well. As a result, the demand for their commercial use is increasing gradually. However, the bioprocess of algae on a huge scale is very limited due to some environmental factors and is hard to produce continuously. The scope of this review was to provide concise knowledge about biopigments extracted from microalgae and their production methods and to clarify the current implementations in the industry. Additionally, food-grade biopigments were compared with synthetic ones. The primary issues with bioprocesses used to produce colorants were highlighted, and as a result, the expected studies were discussed that would be conducted soon.

Introduction

Since color is one of the most valued features by customers, natural or synthetic (artificial) colorants are widely used in the food industry as essential elements in many products. Moreover, colorant usage is also being expanded to include food packaging innovations. Food manufacturers have been using synthetic food colors more frequently than natural food colors to achieve certain features including low cost, improved look, high color intensity, more color stability, and consistency. Several food products on the market may include some unexpected synthetic colors or excessive numbers of the permitted colorants by food regulations. It has been considered that some serious health issues such as mutations, malignancies, decreased hemoglobin concentrations, and allergic reactions could result from this usage (Olas et al., 2021). Therefore, law and education campaigns about food colors applied to consumers and food producers are strongly recommended (Malabadi et al., 2022).

Algae are major elements in the flora of marine and humid environments. Microalgae, which are

phytoplankton, are the main source of ω-3 fatty acids that come from marine and/or aquaculture, in particular (Adarme-Vega et al., 2012). Further implementations have been developed to obtain high-quality and high-value bioactive products for the cosmetic and food supplement industries (Chatterjee et al., 2017). Algal biomass could also be applied for biofuels, biomonitoring, bioremediation, bioplastic production (Zhang et al., 2019), and feeding aquatic organisms (Wang et al., 2020). According to Ruggiero et al. (2015) *Chlorophyta*, *Cryptista*, *Cyanobacteria*, *Euglenozoa*, *Haptophyta*, *Heterokontophyta*, *Glaucophyta*, and *Rhodophyta* are the major phyla which are commonly used in bio-based industrial applications.

Recently, algal outputs have become more popular in many commercial applications such as natural pigment bioproduction. They have been reported as a natural and sustainable food source or as a superfood (Jung et al., 2019; Mouritsen et al., 2020). Moreover, microalgae have been widely evaluated in the production of nutraceuticals (Niccolai et al., 2019) and pharmaceuticals (Debnath & Ghosh, 2023) because of their antioxidant properties and pigment, oil, and vitamin contents.

The objective of this paper is to provide an overview of the biotechnological production of biopigments derived from microalgae and to illustrate how these pigments are now used in the food industry. Moreover, synthetic and food-grade biopigments were contrasted. Also, the anticipated research topics in the near future are discussed for improving algae-based sustainable economy.

To reach these goals, brief information about the biological and taxonomic properties of algae is firstly specified. Then, fundamental algae-based pigment compounds, which were certified as natural food additives, are described chemically and their most common microalgae sources are given. In the second section, bioproduction steps of microalgae are described. Limitations, advantages and disadvantages of different cultivation procedures are discussed. After all, these explanations with the current scientific and industrial background, synthetic colorants are defined with actual European Union legislation. Their ups and downs are also discussed with the food-grade bio-based pigments. Finally, a conclusion has been provided to navigate further research for industrial development.

Algae and algal pigments

Even though the current taxonomic systems for the classification of algae are based on morphological and cytological characteristics such as cell wall constituents and chemical nature of storage products in general, microalgae could also be classified according to their photosynthetic pigments (Levasseur et al., 2020). Microalgae contain pigments produced after photosynthetic reactions, such as chlorophylls (green), carotenoids (yellow to orange), and phycobiliproteins (red to blue) (Siqueira et al., 2018). The microalgae source of these natural colorants was given in **Table 1**. Among them, *Chlorella*, *Cryptothecodinium*, *Dunaliella*, *Nannochloropsis*, *Nitzschia*, *Phaeodactylum*, *Schizochytrium*, and *Spirulina* was declared in the "Generally Recognized as Safe" list as a natural food additive source by the Food and Drug Administration (de Oliveira & Arisseto-Bragotto, 2022).

Table 1. Algal biopigments and their common algae sources

Pigment type (Colorants)	Algal groups	
Chlorophylls Chlorophyll a Chlorophyll b Chlorophyll c_1 Chlorophyll c_2 Chlorophyll d Chlorophyll e Chlorophyll f	Charophyta Chlorophyta Cryptophyta Cyanobacteria Dinophyta Euglenophyta	Heterokontophyta Phaeophyta Rhodophyta Xanthophyta
Carotenoids (Carotenes and Xanthophylls)	Bacillariophyta Charophyta Chlorophyta Chrysophyta	Euglenophyta Phaeophyta Rhodophyta Xanthophyta
Phycobiliproteins	Rhodophyta Dinophyta	Cryptophyta Cyanobacteria

Chlorophylls are responsible for the exact green and are in almost all photoautotrophic organisms. Chlorophylls are gaining great importance not only as a food additive but also as a colorant in the field of pharmaceuticals and cosmetics. *Arthrospira, Chlorella, Gloeothece, Monoraphidium* and *Scenedesmus* are the main microalgae for producing green colorants. Among these, the most well-known microalgae are from the genus *Chlorella*, whose chlorophyll content is about 7% of its biomass (Khanra et al., 2018).

Carotenoid compounds are the most common class of pigments. Most of them share similar chemical structure. Basically, they comprise an eighteen-carbon chain with a conjugated double-bond and two hexacarbonyl rings at each terminal. In this class, carotenoids are divided into carotenes and xanthophylls. The first (carotenes) are oxygen-free hydrocarbons such as α-carotene and β-carotene, and the others (xanthophylls) are oxygenated derivatives of carotene compounds such as astaxanthin, fucoxanthin, lutein, violaxanthin, and zeaxanthin (Haoujar et al., 2019). The main carotenoid sources are the *Chlorophyceae* class. These microalgae can produce both carotenes namely β-carotene and lycopene, and xanthophylls such as antheraxanthin, astaxanthin, lutein, neoxanthin, violaxanthin, and zeaxanthin. However, currently, β-carotene and astaxanthin from the genera *Dunaliella*, *Haematococcus*, and *Scenedesmus* have the highest demand in the global carotenoid market, respectively (Berthon et al., 2017).

Phycobiliproteins, hydrophilic protein pigment complexes present only in Cyanobacteria and microalgae of the *Rhodophyta* phylum as well as in some *Cryptophytes* and *Glaucophytes,* are the last class of pigments found in photosynthetic ones. On an industrial

scale, these pigments are produced from several species of *Arthrospira*, *Aphanizomenon, Porphyridium,* and *Spirulina* (Bhalamur et al., 2018).

For several years, it has been accepted that color-active compounds have beneficial health properties such as oxidation inhibitors, precursors of vitamins, activators of the immune system, and inflammation blockers (Imchen & Singh, 2023). Therefore, they are commonly used in food, pharmaceutical and cosmetic industries as a natural color, food supplement, and a bioactive molecule (García et al., 2017; Hamed, 2016).

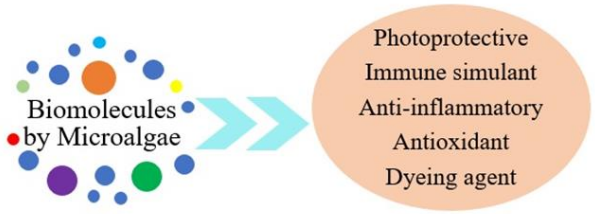

Figure 1. Industrial uses of biomolecules derived from microalgae.

Bio-pigment production

Biopigment production includes cell growth, cultivation and harvest, cell membrane damage, the extraction of pigments and separation, identification, and toxicologic testing for marketing process steps. The primary limitations and bottlenecks for these processes are outlined below along with an explanation.

Cell growth: Microalgae consume natural organic materials and CO_2 as energy and carbon sources. Because of their photoautotrophic structure, they can also produce new carbon sources under sunlight. Therefore, illumination and nutrient supply are the most important steps to start the biomass production during algal cultivation. Optimal light supply differs according to the type of microalgae and the type of end product. Moreover, photosynthesis increases with light supply until photoinhibition is reached. Higher illumination may cause cell death. Photosynthetic organisms naturally contain pigments such as several carotenes, chlorophylls, phycobilin, and xanthophylls for light collection and photoprotection. Photoprotective pigments are astaxanthin, carotene, and other carotenoids (Kratzer & Murkovic, 2021).

Cultivation and harvesting: Microalgae have complex pathways to cultivate. Photoautotrophic cultivation is commonly implemented in open systems (i.e. pools or more commonly 'ponds') on an industrial scale. These media should contain well-balanced salinity or pH to protect the strains from contaminants. Algal cultivation systems are divided into two major groups: indoor photobioreactors and outdoor open pools (ponds). In ponds, mixing, illumination, sterility, and operational costs are very low compared with stirred tank reactors. Even with the high cost of photobioreactors, producers feel comfortable about preferring this reactor type due to the complete sterility. In open systems (large scale), contamination, which is the main bottleneck, is unavoidable (Hu et al., 2018).

Damaging cell membrane and extracting biopigments: High pressure and pulsed electric field processes which are hard to apply to big areas and very expensive have been preferred in industry because of the higher yield. It might be faced with several struggles in separation steps (centrifugation, coagulation, filtration, flocculation, flotation, sedimentation, etc.) from the total bulk product such as cell size, gravity settling, and cell density (Grima et al., 2013). Especially for dye extraction, cell rupture, centrifugation, and solvent extraction usage are common and proper (Monte et al., 2018).

The other major concern is whether microalgal products are rentable or not. Accordingly, algal strains should be optimized genetically to improve the extracted pigment yield. The well-known struggles are the high production costs of cultivation, harvesting (dewatering), and stabilization in product quality (Kratzer & Murkovic, 2021; Lafarga, 2020).

Comparing bio-based pigments and synthetic colorants

Throughout the past two decades, the food sector has been influenced by several sociological, technological, and economic variables. Therefore, with a significant amount of food products being processed to satisfy the demands of brand-new customer categories, the food sector has undergone a quick transformation (Carocho et al., 2014). Hence, food engineers and scientists work hard to produce aesthetically pleasing foods that taste greatly and satisfy consumer demands for quality and cost.

Current statistics are unknown regarding the size of the color market; however, reports show that synthetic, natural, and caramel colors could be implemented in the food industry as food additives on a global scale (da Rosa et al., 2023). Synthetic colors are obtained by chemical synthesis, most often by introducing sulfonic or carboxyl groups into the natural dye molecule. Further, they do not occur naturally in nature. Their main sources are coal or petroleum which could be dangerous (Lis et al., 2020).

In other words, synthetic food colors are created through full chemical synthesis or alteration of several precursor molecules, as opposed to natural food colors which are typically taken from various natural sources and purified. Moreover, their chemical structure does not break down during processing and can be used directly. Due to their more stable colors, bigger synthesis scales, and more affordable manufacturing processes, synthetic colorants have largely replaced natural colorants. However, the negative effects on the environment and human health caused by the excessive use of these chemicals have increased the demand for natural colorants. Thus, intense gradual growth in the 'natural color' market is anticipated (Souza Mesquita et al., 2021).

The European Union has authorized 43 colorants as food additives. Seventeen of them are highly concentrated synthetic pigments. They have no

declared limits on their daily intake levels. Moreover, they are widely available and reachable. However, only some synthetic colors are officially approved by the US and EU, such as Allura red, Brilliant Blue, Erythrosine, Indigo Carmine, Tartrazine, and Sunset Yellow (Olas et al., 2021).

Pigments from nature vary widely in physical and chemical properties. Many of them are extremely sensitive to process and storage conditions such as pH change and light concentration, oxidation, and spontaneous solubility. Initially, natural colors were considered less stable, more difficult to use, and more expensive than synthetic ones. However, considering the consumer's health, it is reasonable to evaluate it for foods and beverages (Downham & Collins, 2000). As a result, it can be accepted that natural colorants or algae-based pigments are preferable to all synthetic colorants due to their superior biocompatibility and lower toxicity (Debnath & Ghosh, 2023).

Table 2. Comparison of using biopigments and synthetic pigments in industry

Parameter	Natural pigments derived from algae	Synthetic dyes and pigments	Reference
Properties	Sensitive to processes	Stable to processes	Malabadi et al., 2022 Olas et al., 2021
Health	Promoting health	allergic, mutagenic, carcinogenic cases may happen	Downham & Collins, 2000 Sharma et al., 2021
Synthesis	Difficult Needs high-quality biotechnological processes	Easy, Semihard Needs chemical reactions in exact conditions	Debnath & Ghosh, 2023 Olas et al., 2021
Costs	Very expensive	Cheap to expensive	Malabadi et al., 2022
Consumer preference	Reasonable to consume	Questionable to consume	da Rosa et al., 2023 Souza Mesquita et al., 2021

Because of all these factors, scientists have focused on research and development activities to find a cost- and environment- effective way and sustainable source for producing natural pigments such as algal bioproducts. Synthetic pigments and biopigments were compared in **Table 2** based on several advantages and disadvantages of them such as process sensitivity, health effects, synthesis type, costs, and consumer preferences. As understood from the table microalgae-based pigment production gains great importance as a natural source.

A growing variety of natural colorants are now being produced on a larger scale in a more environmentally friendly and sustainable way thanks to recent developments in microbial metabolic engineering (Olas et al., 2021; da Rosa et al., 2023).

Conclusion

The use of artificial food colors is still debatable. Current literature clearly shows that using artificial colors might have hazardous and negative impacts on health. Although there are some official requirements for producers, there is not enough information on the possible issues caused by these substances to consumers. The behavior of synthetic dyes should be better understood, which may allow for their incorporation into food products as healthier substitutes.

Microalgae are confirmed crucial resources for innovative food and feed products as superfoods. Up to now, the most cultured species are *Arthrospira*, *Chlorella*, *Dunaliella*, and *Haematococcus*, which can also be cultivated as an energy source under sunlight. Microalgal biomass, as a natural source, includes valuable bioproducts such as pigments, functional food components, and nutraceuticals. The fatty acid-, protein-, and antioxidant-rich extracts can be used as feed and food supplement for daily intake. Microalgae biomass has become a basic component of powders, tablets, and capsules nowadays. Besides, many new products occur in the production of bakeries, meals, and chocolates.

Pigments such as astaxanthin red, lutein yellow, chlorophyll green, or phycocyanin bright blue are natural food dyes used as isolated pigments from microalgae. Biotechnological strategies worldwide, particularly the European Commission Green Deal, target sustainable growth and development. Therefore, algal bioproducts could be used in several areas, especially in food industry. This study described the importance of natural sources to develop a more effective and functional way of obtaining innovative bio-based foods as an example. Despite deep scientific knowledge about microalgae behavior, some gaps are still lacking in optimizing algal bioproducts. Strain selection and growing, harvesting, drying and damaging cell membrane methods are key points that need to be considered when isolating valuable compounds from microalgae.

In conclusion, to overcome the industrial limitations of biotechnological production, researchers and engineers in the industry should concentrate on eliminating the bottlenecks of large-scale harvest and extraction methodologies. It is also crucial to underline the necessity for additional industrial-scale research on algae. Even though several sectors use algae biomass, it is not too much. This is because processing biomass is challenging, yields are low, and product profit margins are therefore low. There is an eminent need to design future studies for the industry using this approach.

Acknowledgements

The author, DU, wants to thank the organizing committee of 1st ICBIOS Congress, held in Turkiye in November 2022, because of the opportunity of presenting the abstract of this study.

References

Adarme-Vega, T. C., Lim, D. K. Y., Timmins, M., Vernen, F., Li, Y., & Schenk, P. M. (2012). Microalgal biofactories: a promising approach towards sustainable omega-3 fatty acid production. *Microbial Cell Factories, 11*(1), 96. https://doi.org/10.1186/1475-2859-11-96

Berthon, J.-Y., Nachat-Kappes, R., Bey, M., Cadoret, J. P., Renimel, I. & Filaire, E. (2017). Marine algae an attractive source to skin care. *Free Radical Research. 510* (6), 555–567. https://doi.org/10.1080/10715762.2017.1355550

Bhalamur, G.L., Valerie, O. & Mark, L. (2018). Valuable bioproducts obtained from microalgal biomass and their commercial applications: A review. *Environmental Engineering Research 230* (3), 229–241. ISSN 1226-1025. http://www.dbpia.co.kr/Article/NODE07417103

Chatterjee, A., Singh, S., Agrawal, C., Yadav, S., Rai, R. & Rai, L.C. (2017). Role of Algae as a Biofertilizer. In Algal Green Chemistry, *Recent Progress in Biotechnology*. https://doi.org/10.1016/B978-0-444-63784-0.00010-2

Carocho, M., Barreiro, M. F., Morales, P. & Ferreira, I. C. F. R. (2014). Adding Molecules to Food, Pros and Cons: A Review on Synthetic and Natural Food Additives. *Comprehensive reviews in food science and food safety*, 13(4), 377–399. https://doi.org/10.1111/1541-4337.12065

da Rosa, M. D. H., Alves, C. J., dos Santos, F. N., de Souza, A. O., Zavareze, E. da R., Pinto, E. & Noseda, M. D. (2023). Macroalgae and Microalgae Biomass as Feedstock for Products Applied to Bioenergy and Food Industry: A Brief Review. *Energies, 16*(4), 1820. http://dx.doi.org/10.3390/en16041820

Debnath, S. & Ghosh, D. (2023). Qualitative and Quantitative Studies on Biopigment Producing Algal Regime from Marine Water Resources of Sundarban Region. *Journal of Pure and Applied Microbiology 17(*1):576-589. https://doi.org/10.22207/JPAM.17.1.55

de Oliveira, A. P. F. & Arisseto-Bragotto, A. P. (2022). Microalgae-based products: Food and public health. *Future Foods*, 6:100157 https://doi.org/10.1016/j.fufo.2022.100157

Downham, A., & Collins, P. (2000). Colouring our foods in the last and next millennium. *International Journal of Food Science & Technology, 35*(1), 5–22. https://doi.org/10.1046/j.1365-2621.2000.00373.x

García, J.L., de Vicente, M. & Galán, B. (2017). Microalgae, old sustainable food and fashion nutraceuticals. *Microbial Biotechnology 100* (5), 1017–1024. https://doi.org/10.1111/1751-7915.12800

Grima, E.M., Fernández, F.G.A. & Robles-Medina, A. (2013). Downstream processing of cell mass and products. In Handbook of Microalgal Culture, 2nd ed. Wiley, 267–309. https://doi.org/10.1002/9781118567166.ch14

Hamed, I. (2016). The Evolution and Versatility of Microalgal Biotechnology: A Review. *Comprehensive Reviews in Food Science and Food Safety 150* (6), 1104–1123. https://doi.org/10.1111/1541-4337.12227

Haoujar, I., Cacciola, F., Abrini, J., Mangraviti, D., Giuffrida, D., Oulad El Majdoub, Y. & Kounnoun, A. (2019). The Contribution of Carotenoids, Phenolic Compounds, and Flavonoids to the Antioxidative Properties of Marine Microalgae Isolated from Mediterranean Morocco. *Molecules*, *24*(22), 4037. http://dx.doi.org/10.3390/molecules24224037

Hu, J., Nagarajan, D., Zhang, Q., Chang, J. S. & Lee, D. J. (2018). Heterotrophic cultivation of microalgae for pigment production: A review. *Biotechnology Advances*, 36, 54–67. https://doi.org/10.1016/j.biotechadv.2017.09.009

Imchen, T. & Singh, K.S. (2023). Marine Algae Colorants: Antioxidant, Anti-Diabetic Properties and Applications in Food Industry. *Algal Research*. 69, 102898 https://doi.org/10.1016/j.algal.2022.102898

Jung, F., Krüger-Genge, A., Waldeck, P. & Küpper, J. H. (2019). Spirulina platensis, a super food? *Journal of Cellular Biotechnology* (5):1, 43-54. https://doi.org/10.3233/JCB-189012

Khanra, S., Mondal, M., Halder, G. & Bhowmick T. K. (2018). Downstream processing of microalgae for pigments, protein, and carbohydrate in industrial application: A review. *Food and Bioproducts Processing*. 110, 60-84. https://doi.org/10.1016/j.fbp.2018.02.002

Kratzer, R., & Murkovic, M. (2021). Food Ingredients and Nutraceuticals from Microalgae: Main Product Classes and Biotechnological Production. *Foods*, 10(7), 1626. https://doi.org/10.3390/foods10071626

Lafarga, T. (2020). Cultured Microalgae and Compounds Derived Thereof for Food Applications: Strain Selection and Cultivation, Drying, and Processing Strategies, *Food Reviews International*, 36:6, 559-583. https://doi.org/10.1080/87559129.2019.1655572

Levasseur, W., Perré, P. & Pozzobon, V. (2020). A review of high value-added molecules production by microalgae in light of the classification. *Biotechnology Advances*, 41:107545, https://doi.org/10.1016/j.biotechadv.2020.107545.

Lis, B., Woźniak, M., Krystofiak, T. & Ratajczak, I. A. (2020). Effect of accelerated aging on the color changes of wood treated with eco-friendly formulations based on propolis and silicon compounds. *BioResources*. 15:3667–77 https://doi.org/10.15376/biores.15.2.3667-3677

Malabadi, R.B., Kolkar K.P. & Chalannavar, R. K., (2022). Plant natural pigment colorants-health benefits: toxicity of synthetic or artificial food colorants. International *Journal of Innovation Scientific Research and Review*. 4:10, 3418-3429. http://www.journalijisr.com

Monte, J., Sá, M., Galinha, C. F., Costa, L., Hoekstrad, H., Brazinha, C. & Crespo, J.G. (2018). Harvesting of *Dunaliella salina* by membrane filtration at pilot scale. *Separation and Purification Technology*, 190, 252–260. http://dx.doi.org/10.1016/j.seppur.2017.08.019

Mouritsen, O. G. & Vinther Schmidt, C. (2020) A Role for Macroalgae and Cephalopods in Sustainable Eating. *Frontiers*. *Psychol*. 11:1402. https://doi.org/10.3389/fpsyg.2020.01402

Niccolai, A., Chini Zittelli, G., Rodolfi, L., Biondi, N. & Tredici, M. R. (2019). Microalgae of interest as food source:

Biochemical composition and digestibility. Algal Research 42, 101617. https://doi.org/10.1016/j.algal.2019.101617

Olas, B., Białecki, J., Urbańska, K., & Bryś, M. (2021). The Effects of Natural and Synthetic Blue Dyes on Human Health: A Review of Current Knowledge and Therapeutic Perspectives. *Advances in nutrition* (Bethesda, Md.), 12(6), 2301–2311. https://doi.org/10.1093/advances/nmab081

Ruggiero, M. A., Gordon, D. P., Orrell, T. M., Bailly, N., Bourgoin, T., Brusca, R. C., Cavalier-Smith, T., Guiry, M. D. & Kirk, P. M. (2015). A Higher-Level Classification of All Living Organisms. *PLoS One 100* (4) https://doi.org/10.1371/journal.pone.0119248

Sharma, M., Usmani, Z., Gupta, V. K. & Bhat, R. (2021). Valorisation of fruits and vegetable wastes and by-products to produce natural pigments, *Critical Reviews in Biotechnology 41*(4):535- 563. https://doi.org/10.1080/07388551.2021.1873240

Siqueira, S. F., Queiroz, M. I., Zepka, L. Q., & Jacob-Lopes, E. (2018). Introductory Chapter: Microalgae Biotechnology - A Brief Introduction. https://doi.org/10.5772/intechopen.73250

Souza Mesquita, L. M., Martins, M., Pisani, L. P., Ventura, S. P. M., & Rosso, V. V. (2021). Insights on the use of alternative solvents and technologies to recover bio-based food pigments. *Comprehensive Reviews in Food Science and Food Safety, 20*(1), 787–818. https://doi.org/10.1111/1541-4337.12685

Wang, A., Yan, K., Chu, D., Nazer, M., Lin, N.T., Samaranayake, E. & Chang, J., (2020). Microalgae as a Mainstream Food Ingredient: Demand and Supply Perspective. Microalgae Biotechnology for Food, Health, and High-Value Products. *Springer*, 29–79 https://doi.org/10.1007/978-981-15-0169-2_2

Zhang, R., Grimi, N., Marchal, L., & Vorobiev, E. (2019). Application of high-voltage electrical discharges and high-pressure homogenization for recovery of intracellular compounds from microalgae *Parachlorella kessleri*. *Bioprocess and Biosystems Engineering, 42*(1), 29–36. https://doi.org/10.1007/s00449-018-2010-4

Biotech Studies 32(2), 65-74
https://doi.org/10.38042/biotechstudies.1332145

BIOTECH STUDIES

RESEARCH PAPER

Effects of nitric oxide, spermidine, and salicylic acid signaling and their crosstalk with each other in the production of commercially important stevioside content and drought stress responses in *Stevia rebaudiana* bertoni

Günce Şahin[1]*

[1]Department of Biology, Faculty of Science and Arts, Bolu Abant Izzet Baysal University, 14300, Bolu, Türkiye.

How to Cite

Şahin, G. (2023). Effects of Nitric Oxide, Spermidine, and Salicylic Acid Signaling and Their Crosstalk with Each Other in the Production of Commercially Important Stevioside Content and Drought Stress Responses in *Stevia rebaudiana* Bertoni. *Biotech Studies, 32(*2), 65-74. https://doi.org/10.38042/biotechstudies.1332145

Article History
Received 01 November 2022
Accepted 01 June 2023
First Online 19 July 2023

Corresponding Author
Tel. : +90 554 450 9688
E-mail: guncesahin@gmail.com

Keywords
Antioxidant activity
Elicitors
Rebaudioside A
Stevioside
Stress mitigation

Abstract

The leaves of *Stevia rebaudiana* Bertoni contain steviol glycosides (SGs), which provide the sweet taste of stevia. However, drought can have a negative impact on the plant's growth and development. To address this issue, signaling molecules such as sodium nitroprusside (SNP), spermidine (SPD), and salicylic acid (SA) are often applied to increase plant tolerance. However, the combined effects of these molecules have not been extensively studied. This research aimed to investigate the effects of controlled elicitation with SA, SNP, SPD, and their combinations on plant performance, SG content, and drought stress mitigation in *Stevia rebaudiana* under drought stress. The elicitor treatments were found to result in a significant increase in SG content, with 0.1 mM SA being the most effective treatment. Additionally, the treatments were able to reduce the stress effects on growth parameters to non-stress levels. The use of SPD, SA+SNP, and SPD+SNP on stressed plants significantly increased CAT and SOD activity, resulting in a more active antioxidant defense system that lowered MDA contents and H_2O_2 generation. These findings suggest that stevia cultivation with controlled elicitation could be used to improve plant growth, tolerance, and SG production under drought stress conditions.

Introduction

Stevia (*Stevia rebaudiana* Bertoni), a perennial herb of the family Asteraceae, is increasing in popularity as a non-caloric natural sweetener that could be utilized as a replacement for manufactured sweeteners and as a natural medication (Vasquez-Hernandez *et al.*, 2019). Diabetes, cancer, obesity, hypertension, and dental decay have been treated using the leaf extract of stevia (Gantait *et al.*, 2015; Álvarez-Robles *et al.*, 2016; Singh *et al.*, 2017). The requirements for steviol glycoside (SG) sweeteners were determined by the Joint FAO/WHO Expert Committee on Food Additives in 2007 (JECFA, 2007). These chemicals are responsible for plant–environment interactions as well as the plant's low caloric content and sweet taste (Jain *et al.*, 2014). The key ingredients in most SG products are rebaudioside A (Reb A) and stevioside (Yoneda *et al.*, 2018). Stevia can be propagated using a variety of plant parts, including seed, leaf, inter-node, node and shoot tip, and stem explants (Uddin *et al.*, 2006; Seyis *et al.*, 2017; Sichanova *et al.* 2022). The stem-cutting procedure has limitations because only a small number of new plants may be reproduced from a single plant. When the seed is utilized, the plants have a low magnitude of sweetness variation (Tadhani *et al.*, 2007; Mathur & Shekhawat, 2013; Moharramnejad *et al.*, 2019).

Climate change and water scarcity issues have affected the productivity of many plant species in semi-arid locations in recent years. Furthermore, due to the anticipated water shortage as a result of global warming, as well as increased competition from agricultural and industrial water consumers, efficient water resource management has become of great importance (Gholami Zali & Ehsanzadeh, 2018). Drought stress (DS), a major constraint to plant growth and development, causes a sharp decline in relative water content and stomatal conductance, limiting plant biomass, yield, and metabolic productivity (Gunes *et al.*, 2007). To protect themselves from dehydration and maintain cell volume, plants undergo an osmotic adjustment process through the accumulation of solutes in their cells (Rahdari & Hoseini, 2012).

Some physical and chemical factors (elicitors) that are commonly used for the synthesis of phenols, flavonoids, stevioside, and other useful chemicals can induce secondary metabolite production in plants, resulting in a protective state against stress factors without limiting plant performance (Mathur & Shekhawat, 2013; Cardenas-Manrquez *et al.*, 2016; Vázquez-Hernández *et al.*, 2019). Elicitors, which set off a cascade of complicated responses at the molecular, biochemical, and physiological levels, have been shown to stimulate certain biosynthetic pathways, resulting in increased levels of stress metabolites, all geared toward environmental acclimatization and adaptation (Giri & Zaheer, 2016).

Exogenous application of signaling molecules such as sodium nitroprusside (SNP) (a commonly used nitric oxide (NO) donor), spermidine (SPD), and salicylic acid (SA) to enhance stress tolerance by triggering plant response is a well-known stress mitigation strategy (Chavoushi *et al.*, 2019). In plants, SA is a key signaling molecule that promotes tolerance to a wide range of biotic and abiotic stressors (Horváth *et al.*, 2007). SA is also involved in the control of a number of physiological processes in plants, including membrane permeability, growth and development, and ion absorption and transport (Raskin, 1992). Under stress conditions, exogenous SA has an effect on the rate of reactive oxygen species (ROS) formation. Furthermore, SA affects antioxidant enzyme activity and boosts plant tolerance to abiotic stressors (Horváth *et al.*, 2007). SA has been discovered to have varied impacts on plant development and stress adaptation depending on the technique, concentration, application time, and plant species (Metwally *et al.*, 2003; Miura & Tada, 2014; Khan *et al.*, 2015).

Some research has highlighted the role of polyamines, particularly SPD (Alcázar *et al.*, 2010; Li *et al.*, 2016; Sequera-Mutiozabal *et al.*, 2017). Because of its cationic nature, SPD interacts with biological molecules and encourages cellular multiplication and morphogenesis when added to culture media (Kevers *et al.*, 2002). Exogenous SPD was reported to partially mitigate the DS-induced loss in photosynthetic efficiency in previous investigations (Yin *et al.*, 2014).

NO, another signaling molecule, is associated with a number of physiological processes including iron availability, growth, germination, and adaptive response to external stresses (Hancock, 2020; Ageeva-Kieferle *et al.*, 2021). From the perspective of abiotic stresses, it has been demonstrated that using the SNP which is NO donor lessens the negative effects of salt, drought, and heavy metals in plants (Arasimowicz & Floryszak-Wieczorek, 2007; Kazemi *et al.*, 2010). However, since NO is a reactive nitrogen species, investigations have revealed that its effects on various cells can be either protective or harmful, depending on the dosage and location of activity. NO also acts as an antioxidant and a signaling molecule, triggering changes in antioxidative gene expression, and protecting plant cells from oxidative damage (Arasimowicz & Floryszak-Wieczorek, 2007).

Exogenously applied elicitors increase secondary metabolite production as a response to stress. Strategies aimed at increasing the SG content of stevia (e.g., employing controlled elicitation) would contribute to enhancing the sweetness and therapeutic benefits of this species (Vasquez-Hernandez *et al.*, 2019). Various relieving agents, including SNP, polyamines, and SA have been used to treat different effects of abiotic stress, including DS, but the combined use of SNP, SPD, and SA under drought stress in stevia has not been reported (Shehab *et al.*, 2010; Bidabadi *et al.*, 2012; Kumar *et al.*, 2012; Yildiztugay *et al.*, 2014; Singh *et al.*, 2017). The vast majority of the scientific literature concentrated on a single application of these agents. Therefore, in the current study, SNP, SPD, SA, and various combinations of two of these signaling molecules (SNP+SA, SPD+SA, SPD+SNP) were exogenously applied to plant cultures. The contents of oxidative stress indicators including malondialdehyde (MDA) and hydrogen peroxide (H_2O_2) were measured to investigate the roles of these signaling molecules. The quantity of stevioside as well as the antioxidant enzyme activities like superoxide dismutase (SOD) and catalase (CAT) was investigated to determine the plant's response to stress. The aim of the present study was to assess the impact of controlled elicitation using SA, SNP, SPD, and their combinations on SG content and plant performance under DS and the potential effects of elicitors on DS mitigation in *Stevia rebaudiana*.

Materials and Methods

Plant Materials

Stevia rebaudiana plantlets were obtained from single-seed descendant seedlings. To obtain a sufficient number of plants, shoot tips of 4-week-old plantlets were transferred to culture vessels containing well-watered vermiculite. The plantlets with well-developed roots were carefully removed from the vessels and transferred to pots containing a soil:vermiculite

mixture (3:1). Before drought stress was applied, the plants were given a 5-day pretreatment with stress relievers, which included SNP (0.1 mM), SPD (0.1 mM), and SA (0.1 mM), as well as SA + SNP (0.1 mM + 0.1 mM), SA + SPD (0.1 mM + 0.1 mM), and SPD+SNP (0.1 mM + 0.1 mM). The required concentrations of elicitor were prepared in sterile distilled water containing 1% Tween 20 (V/V) (Merck, Darmstadt, Germany). All pots were watered every two days until the beginning of the drought stress (DS), which was imposed by restricting water supplies for 12 days. The stress relievers were applied three times by foliar spray (using 10 mL per plant) to each group's 23-day-old plant, until all of the leaves were fully soaked on both sides. After 12 days, the shoot dry weight (SDW), shoot fresh weight (SFW), root dry weight (RDW), root fresh weight (RFW), shoot length (SL), root length (RL), and leaf number (LN) were recorded. Leaves at the same location on many stems were taken from the base, middle, and top parts of the plant in all experiments to avoid confounding variations in the results related to leaf age. The experiment consisted of five biological replicates, each containing six plants kept in a culture room (16-h light/8-h dark photoperiod at 24 ± 2 °C). The treatment concentrations of stress relievers were determined using literature and early experimental efforts (Moharramnejad *et al*., 2019; Pradhan *et al*., 2020).

Quantification of Stevioside Contents

The stevioside content of the samples was determined by a previously described method (Kolb *et al*., 2001). The extracts were made by dissolving exactly 20 mg of dried leaf powder in 20 mL of analytical grade ethanol (70%, V/V). HPLC was performed using a Shimadzu system (LC-8A; Kyoto, Japan) for the quantification of Reb A and stevioside. The ethanol extracts (each 20 µl of the leaf samples) or standard samples were loaded into an HPLC C18 column (Nucleodur HILIC, 250 × 5 mm) under isocratic conditions. Analytical grade acetonitrile: water (80:20, V/V) was used as mobile phase at a flow rate of 2 mL min^{-1}. The peaks were integrated at 200 nm to quantify stevioside content. The results are given in mg/g of dry weight for each sample.

Enzyme Extraction and Protein Determination for Enzyme Assays

Enzyme extraction and protein determination for analyses of CAT and SOD activities were performed as previously described by Şahin (2019). For the enzyme analysis, 0.5 g of fresh weight (FW) of the leaves were homogenized in 2 mL of ice cold 50 mM K-phosphate buffer containing 2 mM Na-EDTA and 1% polyvinylpyrrolidone (PVP); then the homogenate was centrifuged at 4 °C and 12,000 rpm min^{-1} for 10 min. Tissue extracts were kept at –80 °C for determination of CAT and SOD activities. The protein content was determined according to Lowry *et al*. (1951).

Catalase Activities

The CAT activity was determined spectrophotometrically by monitoring the consumption of H_2O_2 at 240 nm (extinction coefficient at 38.9 mM^{-1} cm^{-1}) over a 2-min interval (Chance and Maehly 1955). The values are expressed in units (U) mg^{-1} $protein^{-1}$, FW.

Superoxide Dismutase Activities

The technique described by Giannopolitis and Ries (1977) was used to evaluate SOD activity, which is based on the enzyme's capacity to prevent the photochemical reduction of nitro blue tetrazolium (NBT). The SOD activity was determined spectrophotometrically by measuring absorbance at 560 nm in both the control and main groups. The values are expressed in units (U) mg^{-1} $protein^{-1}$, FW.

H_2O_2 Contents

As previously detailed by Şahin (2019), the H_2O_2 level was detected spectrophotometrically at 415 nm. An H_2O_2 standard curve was used to compute the H_2O_2 content, which was represented as mmol g^{-1} FW.

Malondialdehyde Contents

Trichloroacetic acid (TCA) (1%, W/V) was used to homogenize the leaves. The homogenate in TCA was combined with 0.5% (W/V) thiobarbituric acid (TBA) and incubated at 95 °C in a water bath for 30 min before quick cooling in an ice bath. The absorbance of the supernatant was measured spectrophotometrically at 532 nm. The MDA concentration was determined using an extinction coefficient of 155 mM cm^{-1} after deducting the nonspecific absorbance at 600 nm (Heath & Packer, 1968).

Statistical Analysis

All data were evaluated by analysis of variance (ANOVA), and mean values were compared via Duncan's multiple range tests using SPSS version 16.0 (SPSS Inc., Chicago, IL, USA). Values of $P \leq 0.05$ indicated significance between the treatments and control at a given time. The experiments for the analysis of growth parameters were performed in five replicates. The analyses to determine the contents of oxidative stress indicators, the quantity of stevioside, and antioxidant enzyme activities were performed in three replicates.

Results and Discussion

The SDW, SFW, RDW, RFW, SL, RL, and LN of *Stevia rebaudiana* Bertoni were all measured under different experimental conditions to see how drought stress affects the development and growth of stevia (Figure 1). DS significantly increased RL (from 9.75 to 15.0 cm) but decreased SL (from 18.15 to 10.13 cm) (Figure 2B, C). Compared to the control (non-stressed plants), RFW (from 0.78 to 1.35 g) and RDW (from 0.051 to 0.063 g) were both enhanced.

Figure 1. The effects of different elicitors on morphological changes in *S. rebaudiana* cultivars: (a) SA, (b) DS, (c) control, (d) SA+SPD, (e) SNP, and (f) SDP under drought stress.

The use of SA significantly increased RFW and RDW under drought conditions, compared to non-stressed plants (Figure 2A). Additionally, when compared to drought-stressed plants, the exogenous application of SA resulted in a significant increase in LN, SL, SFW, and SDW, while RFW and RDW remained similar to those of drought-stressed plants.

These findings indicate that the SA treatment had a positive impact on plantlet growth (LN, SL, RL, RFW, and RDW) under drought stress in the current study (Figure 2), which is consistent with its effects on *Phaseolus vulgaris*, *Carthamus tinctorius*, and other plants (Kazemi *et al.*, 2010; Sadeghipour & Aghaei, 2012; Chavoushi *et al.*, 2020). Previous studies have suggested that SA regulates plant growth and development by influencing growth regulators such as auxin, abscisic acid (ABA), and ethylene (Zhu, 2001; Pacheco *et al.*, 2013).

The exogenous application of SPD to drought-stressed plants decreased LN, SL, SFW, SDW, RFW, and RDW when compared to the control. When compared with drought-stressed plants, the SPD application to the plants under drought stress caused no significant effect on LN, but it significantly decreased RL. de Agazio *et al.* (1995) reported that spermidine (Spd) treatment induced 50% inhibition of root extension in maize seedlings. The inhibition of root growth observed during Spd treatment of maize seedlings was observed to be associated with a lignification of the cell wall and a reduction of both the mitotic index and cell elongation.

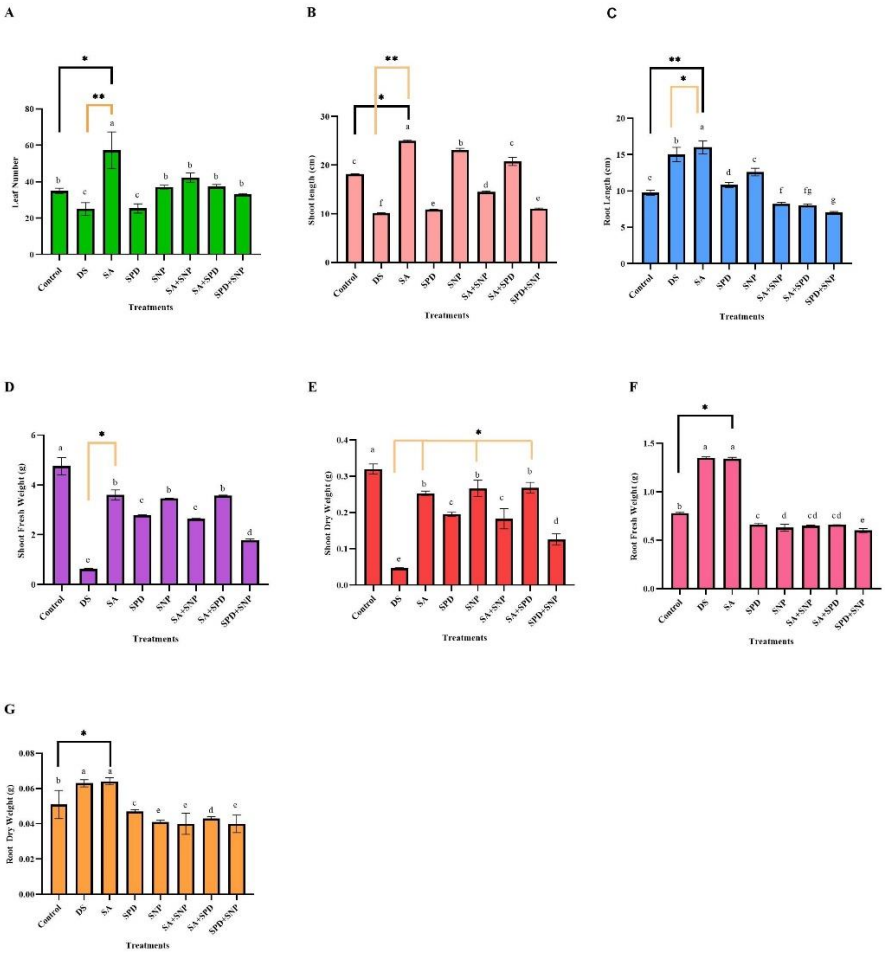

Figure 2. Effects of stress alleviators on growth parameters of plants under drought stress, A: leaf number, B: shoot length, C: root length, D: shoot fresh weight, E: shoot dry weight, F: root fresh weight, G: root dry weight. All mean values which share the same letter are not significantly different; otherwise, they differ significantly at P≤0.05. Values expressed as means ± SD of five replicates.

The application of exogenous SNP to drought-stressed plants resulted in enhanced SL and RL compared to the control plants. Furthermore, it also caused an increase in SFW and SDW when compared to the drought-stressed plants. (Figure 2B, E). A similar result was also reported in a review article (Popova & Tuan, 2010). The study also found that the SNP treatment decreased RDW and RFW, compared with non-stressed and drought-stressed plants. Chavoushi *et al.* (2019) suggest that this effect may be due to the ability of NO to alter the cell cycle and expression levels of root developmental genes.

The DS stimulated root growth and therefore RL, RDW, and RFW. This finding might be linked to the shortage of water, which caused the root to extend and expand in order to efficiently absorb soil moisture (Akinci & Losel, 2009). Under drought conditions, the combined application of SA+SNP, SA+SPD, and SPD+SNP to the plants had no significant effect on LN, but it reduced RL, SDW, RDW and RFW in comparison to the control. The combined application of SA+SNP, SA+SPD, and SPD+SNP increased SFW, SDW, LN, and SL, but decreased RL, RFW, and RDW when compared to the drought-stressed plants. The application of SA+SNP, SA+SPD, and SPD+SNP to plants under drought stress mitigated the negative effects of drought stress on growth parameters (LN, RFW, SFW, RDW, SDW, and RL). The elicitor treatments examined in our study had a considerable positive impact on the morphology of Stevia plants. This observation could be attributed to the elicitation, which led to the reduction of stress effects on practically all growth parameters to a non-stressed level.

In our research, elicitor treatments resulted in significant changes in the SG contents of stevia leaves when compared to the control plants (Figure 3).

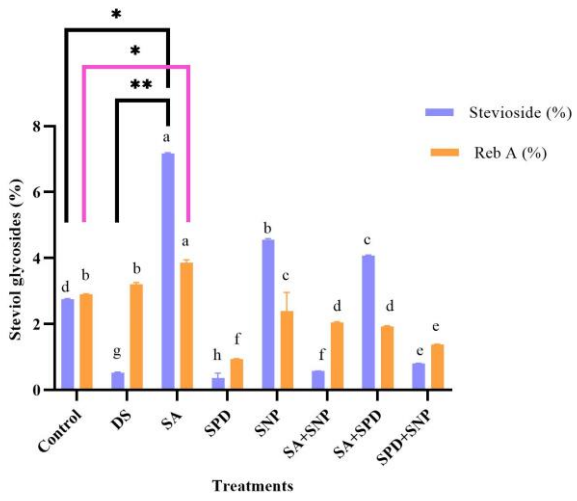

Figure 3. Effects of stress elicitor treatments on stevioside and Reb A content under drought stress. The data are means ± SD from three replicates. Values followed by different letters in the same column are significantly different ($P \leq 0.05$).

The best treatment that increased SG contents was 0.1 mM of SA, with 2.59-fold of stevioside and 1.33-fold of Reb A, which agrees with the findings reported by Vasquez-Hernandez *et al.* (2019), who found that SA-treated plants had a 2.42-fold increase in iso Reb B and a 1.39-fold increase in Reb A.

In addition to the SA findings, SNP and SA+SPD raised the stevioside concentration by 1.65- and 1.47-fold, respectively. The application of combinations of both SPD+SNP and SA+SNP to the plants under drought stress decreased the stevioside and Reb A content compared to the control plants. The decrease in stevioside and Reb A content under the combined treatment of elicitors may be due to a complex interaction between the different elicitors and the plant's response to stress. It is possible that when multiple elicitors are applied together, they may activate different signaling pathways that could compete with each other or interfere with each other's effectiveness. This may result in an overall decrease in the biosynthesis of Stevioside and Reb A. Our findings indicate that elicitors applied foliarly to stevia plants trigger defense mechanisms and cause glycoside accumulation and an increase in antioxidant activity. In addition to the SA results, an increase in endogenous H_2O_2 content (0.81 mmol g^{-1} FW) considerably enhanced the quantity of SGs in the leaves of stevia. These findings clearly demonstrate that elicitors applied foliarly to stevia plants trigger the defense mechanisms, which is in line with the results reported by Javed *et al.* (2018), who showed a high amount of SGs obtained in stevia leaves under various H_2O_2 concentrations. Vasquez-Hernandez *et al.* (2019) showed the relative gene expression linked with SGs biosynthesis. In this work, treatment of stevia leaves with SA (0.1 mM) increased the concentration of SGs, which correlated with the inducement of gene expression associated with the biosynthesis of these compounds and an increase in LN. Hajihashemi and Geuns (2017) clearly indicated that the elicitors examined exerted significant transcriptional control over SG production, comparable to what has been observed with gibberellin treatments on stevia plants. Consequently, the potential metabolic interaction/competition between elicitors and many phytohormonal responses appears to be involved in the physiology of growth regulation via dynamic changes. The interaction of elicitors with other plant growth regulators may be antagonistic or synergistic under optimum and stressed conditions. By signaling crosstalk with other plant growth regulators, SA can control numerous plant responses in both optimum and stressful conditions (Khan *et al.*, 2015). Iglesias *et al.* (2011) have found that SA-mediated auxin signaling inhibition. In *Solanum lycopersicum*, SA caused the production of ABA in plants under normal and saline conditions, which increased the growth properties and facilitated osmotic adaptation (Szepesi *et al.*, 2009).

SA is one of the most important phytohormones that interacts with NO, working as a secondary messenger (Nawaz *et al.*, 2017). NO has been proposed

to operate as a downstream SA-signaling molecule in the mitigation of stimulated oxidation in *Triticum aestivum* seedlings that have been osmotically stressed (Naser Alavi *et al.*, 2014). SA may also promote NO production by increasing the activity of NO-producing enzymes (Zottini *et al.*, 2007). Canola plants under Ni stress treated with SA+NO showed enhanced plant growth (Kazemi *et al.*, 2010). SNP or SA treatment applied to Ni-stressed plants mitigates the harmful effects of Ni. Compared with exogenous stand-alone applications of SA and SNP to Fe-deficient *Arachis* seedlings, the combined application of SA and NO resulted in higher Fe absorption and reduced leaf interveinal chlorosis (Kong *et al.*, 2014). In our research, the application of both SA and/or SNP to the plants significantly increased LN, SL, SFW, and SDW when compared to the drought-stressed plants.

NO, in conjunction with phytohormones and secondary messengers, plays a crucial function in a variety of plant metabolic and physiological processes. Numerous synergistic and antagonistic interactions between NO and all major plant growth regulators have been identified, as summarized elsewhere (Asgher *et al.*, 2017). Bitrián *et al.* (2012) indicate that NO has a role in both stress and developmental responses caused by polyamines (PAs) such as putrescine, SPD, and spermine. It was shown that PAs can cause high NO production in *Arabidopsis* seedlings (Tun *et al.*, 2006). The fact that L-Arg is a common precursor in the production of PAs and NO adds to the evidence that these two signaling molecules are linked (Gao *et al.*, 2009). Concurrent NO and putrescine applications protected *Vigna radiata* from cadmium contamination by a number of mechanisms, including the activation of antioxidants, as well as an increase in phytochelatin production (Nahar *et al.*, 2016). In our research, the application of both SPD+SNP to the plants significantly increased antioxidant enzyme activities.

During the control of plant processes, synergistic or antagonistic interactions between SA and NO have been reported (Durner & Klessig, 1999; Manjunatha *et al.*, 2010; Gémes *et al.*, 2011; Chavoushi *et al.*, 2019). According to findings reported by Kumar and Klessig (2000), SA-stimulated protein kinase appears to work downstream of SA in the signaling pathway of NO in plant defense mechanisms in transgenic tobacco. In *Brassica napus* under Ni stress, the combined application of SA and NO had a synergistic effect (Kazemi *et al.*, 2010). SA is thought to cause stomatal closure by activating peroxidase in guard cells, leading to the generation of extracellular ROS and NO, as well as inactivating K^{+}_{in} channels, resulting in stomatal closure (Khokon *et al.*, 2011). In the current study, the application of both SA+SNP to the plants significantly increased antioxidant enzyme activities.

SA stimulated the generation of ROS, including H_2O_2 (Gémes *et al.*, 2011), and elevated NO synthesis in *Arabidopsis* plants in a dose-dependent manner (Zottini *et al.*, 2007). The accumulation of H_2O_2 was not consistently linked to the stress tolerance induced by SA. Mora-Herrera *et al.* (2005) investigated the sensitivities of two potato cultivars to freezing temperatures and showed that SA may promote freezing tolerance in both cultivars, but only in the less tolerant genotype was it associated by H_2O_2 accumulation. NO, as a free radical, may promote chain reactions triggered by other free radicals, and it can be protective or harmful depending on the concentrations of the reaction product (Lipton *et al.*, 1993). As a result, the cell's fate (adaptation to stress or apoptosis) is determined by the essential balance between the generation of ROS and NO. In the current study, it was found that young stevia leaves accumulated more H_2O_2, which is thought to provide functional cross-tolerance to drought stress after being exposed to SA, SNP, and SA+SPD.

The superoxide dismutase (SOD: 1.15.1.1) activity serves as the first line of defense system, while catalase (CAT: EC 1.11.1.6) is the primary enzyme involved in neutralizing H_2O_2. Compared to non-stressed plants (37.6 U mg-1 protein), the drought stress caused an increase in CAT activity (123.0 U mg^{-1} protein). However, the application of SPD (170.3 U mg^{-1} protein), SA+SNP (150.3 U mg^{-1} protein), and SPD+SNP (166.4 U mg^{-1} protein) to stressed plants resulted in a further increase in CAT activity compared to drought-stressed plants (Figure 4). This increase in CAT activity can help to reduce the high peroxide concentration that occurs under drought stress. The application of SA to plants significantly reduced CAT activity and increased hydrogen peroxide accumulation when compared to DS plants. Similar to our findings, it was found that SA treatment decreased CAT activity and increased hydrogen peroxide accumulation in soybean genotypes under water deficit conditions (Razmi *et al.*, 2017). Safari *et al.* (2022) reported that exogenous SA inhibited CAT enzyme activity in *Impatiens walleriana* under drought stress; similar findings were reported by Antonić *et al.* (2016). These results suggested that the mechanism of action of SA involves binding CAT and inhibiting its activity by increasing the level of H_2O_2.

When compared with non-stressed plants (0.025 U mg^{-1} protein), DS caused an increase in SOD activity (0.045 U mg^{-1} protein). The SOD activity of the stressed plants was increased by the application of SPD (from 0.045 to 0.072 U mg^{-1} protein), SA+SNP (from 0.045 to 0.065 U mg^{-1} protein), and SPD+SNP (from 0.045 to 0.063 U mg^{-1} protein). When compared to DS plants, SNP application to plants significantly reduced CAT and SOD activity. SOD activity was found to be lower in corn (Yildiztugay *et al.*, 2014) and safflower (Chavoushi *et al.*, 2019) after SNP treatment under drought stress, which is similar to our findings. They reported that superoxide anion and NO reacted directly, which decreased superoxide radicals and SOD activity. The SNP can prevent lipid peroxidation by inhibiting membrane peroxidation enzymes and scavenging peroxyl radicals, thus playing a protective role.

The MDA levels of the stevia plants increased significantly (from 4.73 to 14.67 mol g^{-1} FW) as a result of the drought stress, as seen in Figure 4.

When elicitors were added to drought-stressed plants, the increase in MDA content was partially alleviated. In comparison to non-stressed plants, drought-stressed plants increased CAT and SOD activities to regulate the excessive peroxide concentrations. The antioxidant defense system in SPD-,SA+SNP-, and SPD+SNP-treated plants was more active than that of other treatments. These enhanced antioxidant activities due to SPD, SA+SNP, and SPD+SNP treatments resulted in lower MDA contents and H_2O_2 generation. The application of stand-alone or combinations of SA, SNP, and SPD to plants against drought stress led to a modest drop in MDA concentration, which helped offset the damage.

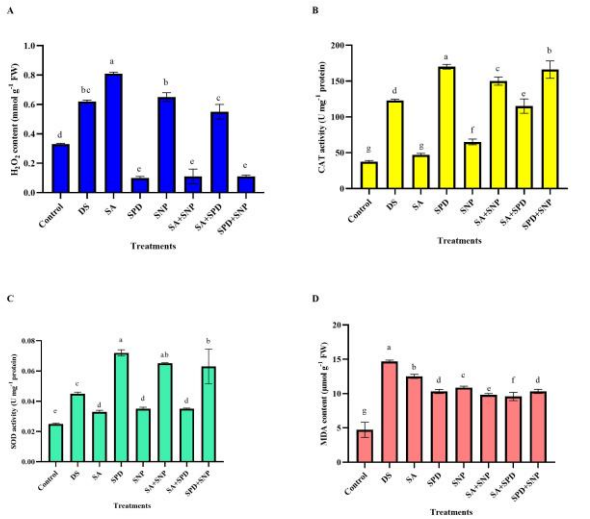

Figure 4. Effects of stress alleviators on A: H_2O_2 content, B: CAT activity, C: SOD activity, D: MDA content under drought stress. All mean values which share the same letter are not significantly different; otherwise, they differ significantly at $P \leq 0.05$. Values expressed as mean ± SD of three replicates.

Conclusion

Our aim was to investigate the changes in SG levels in leaves during pre-adaptation and subsequent drought stress, but we were also interested to know if changes in antioxidant enzymes, hydrogen peroxide, and MDA content could play a role in cell survival during drought stress with elicitor treatments that improved drought acclimation. Our findings demonstrated that elicitors (especially 0.1 mM SA) applied foliarly to stevia plants activated enzymatic defensive systems and stimulated the production of desired metabolites.

As a result, in abiotic stressed plants, the finer details of plant physiology, biochemistry, bioinformatics, and molecular biology techniques in conjunction with the effects of SA, SPD, and NO on plant immune-mediated defense networks can reveal new insights into how these molecules interact with other defense signaling pathways.

Funding Information

This project was supported by TÜBİTAK (The Scientific and Technological Research Council of Turkey, project no: 119Z764).

Acknowledgements

I thank Prof. Dr. Nusret Zencirci for his cooperation and technical assistance during the study. This project was supported by TÜBİTAK (The Scientific and Technological Research Council of Turkey, project no: 119Z764).

References

Ageeva-Kieferle, A., Georgii, E., Winkler, B., Ghirardo, A., Albert, A., Hüther, P., Mengel, A., Becker, C., Schnitzler, J. P., Durner, J., & Lindermayr, C. (2021). Nitric oxide coordinates growth, development, and stress response via histone modification and gene expression. *Plant physiology*, *187*(1), 336-360. https://doi.org/10.1093/plphys/kiab222

Akinci, S., & Losel, D. M. (2009). The soluble sugars determination in Cucurbitaceae species under water stress and recovery periods. *Advances in Environmental Biology*, *3*(2), 175-183.

Alcázar, R., Altabella, T., Marco, F., Bortolotti, C., Reymond, M., Koncz, C., Carrasco, P. & Tiburcio A. F. (2010). Polyamines: molecules with regulatory functions in plant abiotic stress tolerance. *Planta*, *231*, 1237-1249. https://doi.org/10.1007/s00425-010-1130-0

Álvarez-Robles, M. J., López-Orenes, A., Ferrer, M. A. & Calderón, A. A. (2016). Methanol elicits the accumulation of bioactive steviol glycosides and phenolics in *Stevia rebaudiana* shoot cultures. *Industrial Crops and Products, 87*, 273–279. https://doi.org/10.1016/j.indcrop.2016.04.054

Antonić, S., Milošević, A., Cingel, M., Lojić, M., Trifunović-Momčilov, M., Petrić, A., Subotić, A. & Simonović, A. (2016). Effects of exogenous salicylic acid on *Impatiens walleriana* L. grown in vitro under polyethylene glycol-imposed drought. *South African Journal of Botany*, *105*, 226-233. https://doi.org/10.1016/j.sajb.2016.04.002

Asgher, M., Per, T. S., Masood, A., Fatma, M., Freschi, L., Corpas, C. F. & Khan, N.A. (2017). Nitric oxide signaling and its crosstalk with other plant growth regulators in plant responses to abiotic stress. *Environmental Science and Pollution Research, 24*(3), 2273-2285. https://doi.org/10.1007/s11356-016-7947-8

Arasimowicz, M., & Floryszak-Wieczorek, J. (2007). Nitric oxide as a bioactive signalling molecule in plant stress responses. *Plant Science*, *172*, 876-887. https://doi.org/10.1016/j.plantsci.2007.02.005

Bidabadi, S. S., Mahmood, M., Baninasab, B. & Ghobadi, C. (2012). Influence of salicylic acid on morphological and physiological responses of banana (*Musa acuminata* cv. 'Berangan', AAA) shoot tips to *in vitro* water stress induced by polyethylene glycol. *Plant Omics, 5*, 33-39.

Bitrián, M., Zarza, X., Altabella, T., Tiburcio, A. F., & Alcázar, R.

(2012). Polyamines under Abiotic Stress: Metabolic Crossroads and Hormonal Crosstalks in Plants. *Metabolites*, *2*(3), 516–528. https://doi.org/10.3390/metabo2030516

Cardenas-Manríquez, G., Vega-Muñoz, I., Villagómez-Aranda, A., León-Galvan, M., Cruz-Hernandez, A., Torres-Pacheco, I., Rangel-Cano, R., Rivera-Bustamante, R. & Guevara-Gonzalez, R. (2016). Proteomic and metabolomic profiles in transgenic tobacco (*N. tabacum* xanthi nc) to *CchGLP* from *Capsicum chinense* BG-3821 resistant to biotic and abiotic stresses. *Environmental and Experimental Botany, 130*, 33-41. https://doi.org/10.1016/j.envexpbot.2016.05.005

Chance, B. & Maehly, A. (1955). Assay of catalases and peroxidases. *Methods in Enzymology, 2*, 764-775.

Chavoushi, M., Najafi, F., Salimi, A. & Angaji, S.A. (2020). Effect of salicylic acid and sodium nitroprusside on growth parameters, photosynthetic pigments and secondary metabolites of safflower under drought stress. *Scientia Horticulturae, 259*. https://doi.org/10.1016/j.scienta.2019.108823

Chavoushi, M., Najafi, F., Salimi, A. & Angaji, S.A. (2019). Improvement in drought stress tolerance of safflower during vegetative growth by exogenous application of salicylic acid and sodium nitroprusside. *Industrial Crops and Products, 134*, 168-176. https://doi.org/10.1016/j.indcrop.2019.03.071

De Agazio, M., Grego, S., Ciofi-Luzzatto, A. Rea, E., Zaccaria, M.L. & Federico R. (1995). Inhibition of maize primary root elongation by spermidine: Effect on cell shape and mitotic index. *Journal of Plant Growth Regulation*, *14*, 85-89. https://doi.org/10.1007/bf00203118

Durner, J. & Klessig, D. F. (1999). Nitric oxide as a signal in plants. *Current Opinion in Plant Biology, 2*, 369-374.

Gantait, S., Das, A. & Mandal, N. (2015). *Stevia*: a comprehensive review on ethno-pharmacological properties and *in vitro* regeneration. *Sugar Technology, 17*, 95-106. https://doi.org/10.1007/s12355-014-0316-3

Gao, H. J., Yang, H. Q. & Wang, J. X. (2009). Arginine metabolism in roots and leaves of apple (*Malus domestica* Borkh.): the tissue-specific formation of both nitric oxide and polyamines. *Scientia Horticulturae, 119*, 147-15. https://doi.org/10.1016/j.scienta.2008.07.034

Gémes, K., Poór P., Horváth E., Kolbert Z., Szopkó D., Szepesi Á. & Tari, I. (2011). Cross-talk between salicylic acid and NaCl-generated reactive oxygen species and nitric oxide in tomato during acclimation to high salinity. *Physiologia Plantarum*, *142*, 179-192. https://doi.org/10.1111/j.1399-3054.2011.01461.x

Gholami Zali, A., & Ehsanzadeh, P. (2018). Exogenous proline improves osmoregulation, physiological functions, essential oil, and seed yield of fennel. *Industrial Crops and Products*, *111*, 133-140. https://doi.org/10.1016/j.indcrop.2017.10.020

Giannopolitis, C. N. & Ries, S. K. (1977). Superoxide dismutases I. Occurrence in higher plants. *Plant Physiology, 59*, 309-314.

Giri, C. C. & Zaheer, M. (2016). Chemical elicitors versus secondary metabolite production *in vitro* using plant cell, tissue and organ cultures: recent trends and a sky eye view appraisal. Plant *Cell Tiss Organ Culture, 126*, 1-18. https://doi.org/10.1007/s11240-016-0985-6

Gunes, A., Inal, A., Alpaslan, M., Eraslan, F., Bagci, E. G. & Cicek, N. (2007). Salicylic acid induced changes on some physiological parameters symptomatic for oxidative stress and mineral nutrition in maize (*Zea mays* L.) grown under salinity. *Plant Physiology, 164*, 728-736. https://doi.org/10.1016/j.jplph.2005.12.009

Hajihashemi, S. & Geuns, J. M. (2017). Steviol glycosides correlation to genes transcription revealed in gibberellin and paclobutrazol-treated *Stevia rebaudiana*. *Journal of Plant Biochemistry and Biotechnology, 26*, 387-394. https://doi.org/10.1007/s13562-017-0399-5

Hancock, J. T. (2020). Nitric Oxide Signaling in Plants. *Plants*, *9* (11), 1550. https://doi.org/10.3390/plants9111550

Heath, R. L. & Packer, L. (1968). Photoperoxidation in isolated chloroplasts: I. Kinetics and stoichiometry of fatty acid peroxidation. *Archives of Biochemistry and Biophysics*, *125*, 189-198.

Horváth, E., Pál, M., Szalai, G., Páldi, E., & Janda, T. (2007). Exogenous 4-hydroxybenzoic acid and salicylic acid modulate the effect of short-term drought and freezing stress on wheat plants. *Biologia plantarum*, *51*(3), 480-487. https://doi.org/10.1007/s10535-007-0101-1

Iglesias, M. J., Terrile, M. C. & Casalongué, C. A. (2011). Auxin and salicylic acid signalings counteract the regulation of adaptive responses to stress. *Plant Signal Behaviour, 6*, 452-454. https://doi.org/10.4161/psb.6.3.14676

Jain, P., Kachhwah, S. & Kothari, S. (2014). Biotechnology and metabolic engineering of *Stevia rebaudiana* (Bert.) Bertoni: perspective and possibilities. *International Journal of Life Sciences Biotechnology and Pharma Research, 3*, 15.

JECFA (2007). Steviol glycosides. In: 68th JECFA-Chemical and Technical Assessment. Geneva, Switzerland.

Javed, R., Yücesan, B. & Gurel, E. (2018). Hydrogen peroxide-induced steviol glycosides accumulation and enhancement of antioxidant activities in leaf tissues of *Stevia rebaudiana* Bertoni. *Sugar Technology*, 20, 100-104. https://doi.org/10.1007/s12355-017-0521-y

Kazemi, N., Khavari-Nejad, R. A., Fahimi, H., Saadatmand, S. & Nejad-Sattari, T. (2010). Effects of exogenous salicylic acid and nitric oxide on lipid peroxidation and antioxidant enzyme activities in leaves of *Brassica napus* L. under nickel stress. *Scientia Horticulturae, 126*, 402-407. https://doi.org/10.1016/j.scienta.2010.07.037

Kevers, C., Gaspar, T. & Jacques, D. (2002). The beneficial role of different auxins and polyamines at successive stages of somatic embryo formation and development of *Panax ginseng in vitro*. *Plant Cell Tissue Organ Culture, 70*, 181-188.

Khan, M. I. R., Fatma, M., Per, T. S., Anjum, N. A., & Khan, N. A. (2015). Salicylic acid-induced abiotic stress tolerance and underlying mechanisms in plants. *Frontiers in Plant Science*, *6*, 462. https://doi.org/10.3389/fpls.2015.00462

Khokon, M., Okuma, E. I., Hossain, M. A., Munemasa, S., Uraji, M., Nakamura, Y., Mori, I. C. & Murata, Y. (2011). Involvement of extracellular oxidative burst in salicylic acid-induced stomatal closure in *Arabidopsis*. *Plant Cell*

Environment, 34, 434-443. https://doi.org/10.1111/j.1365-3040.2010.02253.x

Kolb, N., Herrera, J. L., Ferreyra, D. J. & Uliana, R. F. (2001). Analysis of Sweet Diterpene Glycosides from Stevia rebaudiana: Improved HPLC Method. *Journal of Agricultural and Food Chemistry, 49*, 4538-4541. https://doi.org/10.1021/jf010475p

Kong, J., Dong, Y., Xu, L., Liu, S. & Bai, X. (2014). Effects of foliar application of salicylic acid and nitric oxide in alleviating iron deficiency induced chlorosis of (*Arachis hypogaea* L.). *Botanical Studuies, 55*, 1-12. https://doi.org/10.1186/1999-3110-55-9

Kumar, D. & Klessig, D. F. (2000). Differential induction of tobacco MAP kinases by the defense signals nitric oxide, salicylic acid, ethylene, and jasmonic acid. *Molecular Plant-Microbe Interact, 13*, 347-351. https://doi.org/10.1094/mpmi.2000.13.3.347

Kumar, H., Kaul, K., Bajpai-Gupta, S., Kaul, V. K. & Kumar, S. (2012). A comprehensive analysis of fifteen genes of steviol glycosides biosynthesis pathway in *Stevia rebaudiana* (Bertoni). *Gene, 492*, 276-284. https://doi.org/10.1016/j.gene.2011.10.015

Li, Z., Zhang, Y., Zhang, X., Peng, Y., Merewitz, E., Ma, X., Huang, L. & Yan, Y. (2016). The alterations of endogenous polyamines and phytohormones induced by exogenous application of spermidine regulate antioxidant metabolism, metallothionein and relevant genes conferring drought tolerance in white clover. *Environmental and Experimental Botany, 124*, 22-38. https://doi.org/10.1016/j.envexpbot.2015.12.004

Lipton, S. A., Choi, Y. B., Pan, Z. H., Lei, S. Z. & Chen, H. S. (1993). A redox-based mechanism for the neuroprotective and neurodestructive effects of nitric oxide and related nitroso-compounds. *Nature, 364*, 626-632. https://doi.org/10.1038/364626a0

Lowry, O. H., Rosebrough, N. J., Farr, A. L. & Randal, R. J. (1951). Protein measurement with the folin phenol reagent. *Journal of Biological Chemistry, 193*, 65-75. https://doi.org/10.1016/s0021-9258(19)52451-6

Manjunatha, G., Lokesh, V. & Neelwarne, B (2010). Nitric oxide in fruit ripening: trends and opportunities. *Biotechnology Advances 28*, 489-499. https://doi.org/10.1016/j.biotechadv.2010.03.001

Mathur, S. & Shekhawat, G. S. (2013). Establishment and characterization of *Stevia rebaudiana* (Bertoni) cell suspension culture: an *in vitro* approach for production of stevioside. *Acta Physiologia Plantarum, 35*(3), 931-939. https://doi.org/10.1007/s11738-012-1136-2

Metwally, A., Finkemeier, I., Georgi, M. & Dietz, K. J. (2003). Salicylic acid alleviates the cadmium toxicity in barley seedlings. *Plant Physiology, 132*, 272-281. https://doi.org/10.1104/pp.102.018457

Miura, K., & Tada, Y. (2014). Regulation of water, salinity, and cold stress responses by salicylic acid. *Frontiers in Plant Science*, 5, 4. https://doi.org/10.3389/fpls.2014.00004

Moharramnejad, S., Azam, A. T., Panahandeh, J., Dehghanian, Z. & Muhammad, A. (2019). Effect of Methyl Jasmonate and Salicylic Acid on *In Vitro* Growth, Stevioside Production, and Oxidative Defense System in *Stevia rebaudiana*. *Sugar Technology, 21*, 1031-1038. https://doi.org/10.1007/s12355-019-00727-8

Mora-Herrera, M. E., Lopez-Delgado, H., Castillo-Morales, A. & Foyer, C. H. (2005). Salicylic acid and H_2O_2 function by independent pathways in the induction of freezing tolerance in potato. *Physiologia Plantarum, 125*(4), 430-440. https://doi.org/10.1111/j.1399-3054.2005.00572.x

Nahar, K., Hasanuzzaman, M., Alam, M. M., Rahman, A., Suzuki, T. & Fujita, M. (2016). Polyamine and nitric oxide crosstalk: antagonistic effects on cadmium toxicity in mung bean plants through upregulating the metal detoxification, antioxidant defense and methylglyoxal detoxification systems. *Ecotoxicology and Environmental Safety, 126*, 245-255. https://doi.org/10.1016/j.ecoenv.2015.12.026

Naser Alavi, S. M., Arvin, M. J. & Manoochehri Kalantari, K. (2014). Salicylic acid and nitric oxide alleviate osmotic stress in wheat (*Triticum aestivum* L.) seedlings. *Journal of Plant Interactions, 9*, 683-688. https://doi.org/10.1080/17429145.2014.900120

Nawaz, F., Shabbir, R. N., Shahbaz, M., Majeed, S., Raheel, M., Hassan, W. & Sohail, M. A. (2017). Cross talk between nitric oxide and phytohormones regulate plant development during abiotic stresses. In M. El-Esawi (Ed.), *Phytohormones-signaling mechanisms and crosstalk in plant development and stress responses* (1st ed., pp. 117-141). InTech. https://doi.org/10.5772/intechopen.69812

Pacheco, A. C., da Silva Cabral, C., da Silva Fermino, E. S. & Aleman, C. C. (2013). Salicylic acid induced changes to growth, flowering and flavonoids production in marigold plants. *Medicinal Plants Research, 7*, 3158-3163.

Popova, L. & Tuan, T. (2010). Nitric oxide in plants: Properties, biosynthesis, and physiological functions. *Iranian Journal of Science and Technology Transaction A: Science, 34*, 173-183.

Pradhan, N., Singh, P., Dwivedi, P. & Pandey, D.K. (2020). Evaluation of sodium nitroprusside and putrescine on polyethylene glycol induced drought stress in Stevia rebaudiana Bertoni under *in vitro* condition. *Industrial Crops and Products,* 154. https://doi.org/10.1016/j.indcrop.2020.112754

Rahdari, P. & Hoseini, M. (2012). Drought stress: a review. *International Journal of Agronomy and Plant Production, 10*, 443-446.

Raskin, I. (1992). Role of salicylic acid in plants. *Annual Review of Plant Physiology and Plant Molecular Biology,* 43, 439-463. https://doi.org/10.1146/annurev.pp.43.060192.002255

Razmi, N., Ebadi, A., Jahanfar Daneshian, J., & Soodabeh Jahanbakhsh (2017). Salicylic acid induced changes on antioxidant capacity, pigments, and grain yield of soybean genotypes in water deficit condition, *Journal of Plant Interactions*, *12*, 457-464. https://doi.org/10.1080/17429145.2017.1392623

Sadeghipour, O. & Aghaei, P. (2012). Impact of exogenous salicylic acid application on sometraits of common bean (*Phaseolus vulgaris* L.) under water stress conditions. *International Journal of Agriculture and Crop Sciences, 4*, 685-690.

Safari, M., Mousavi-Fard, S., Rezaei Nejad, A., Sorkheh K. & Sofo A. (2022). Exogenous salicylic acid positively affects morpho-physiological and molecular responses of *Impatiens walleriana* plants grown under drought stress. *International Journal of Environmental Science and Technology*, *19*, 969-984.

https://doi.org/10.1007/s13762-020-03092-2

Sequera-Mutiozabal, M., Antoniou, C., Tiburcio, A. F., Alcázar R. & Fotopoulos V. (2017). Polyamines: Emerging Hubs Promoting Drought and Salt Stress Tolerance in Plants. *Current Molecular Biology Reports*, *3*, 28-36. https://doi.org/10.1007/s40610-017-0052-z

Seyis, F., Yurteri, E. & Özcan, A. (2017). *In Vitro* Multiplication of *Stevia rebaudiana* (Bertoni) Genotypes Using Different Explants. *International Journal of Crop Science and Technology*, *3*(2), 36-41. https://doi.org/10.26558/ijcst.326792

Shehab, G. G., Ahmed, O. K. & El-Beltagi, H. S. (2010). Effects of various chemical agents for alleviation of drought stress in rice plants (*Oryza sativa* L.). *Notulae Botanicae Horti Agrobotanici Cluj, 38*, 139-148.

Sichanova, M., Geneva, M., Petrova, M., Miladinova-Georgieva, K., Kirova, E., Nedev, T., Tsekova, D., Iwanov, I., Dochev, K., Ivanova, V., & Trendafilova, A. (2022). Improvement of Stevia rebaudiana Bertoni In Vitro Propagation and Steviol Glycoside Content Using Aminoacid Silver Nanofibers. *Plants*, *11*(19), 2468. https://doi.org/10.3390/plants11192468

Singh, G., Singh, G., Singh, P., Parmar, R., Paul, N., Vashist, R., Swarnkar, M. K., Kumar, A., Singh, S. & Singh, A. K. (2017). Molecular dissection of transcriptional reprogramming of steviol glycosides synthesis in leaf tissue during developmental phase transitions in *Stevia rebaudiana* Bert. *Scientific Reports, 7*, 11835. https://doi.org/10.1038/s41598-017-12025-y

Szepesi, Á., Csiszár, J., Gémes, K., Horváth, E., Horváth, F., Simo, M. L. & Tari, I. (2009). Salicylic acid improves acclimation to salt stress by stimulating abscisic aldehyde oxidase activity and abscisic acid accumulation and increases Na^+ content in leaves without toxicity symptoms in *Solanum lycopersicum* L. *Journal of Plant Physiology, 9*, 914-925. https://doi.org/10.1016/j.jplph.2008.11.012

Şahin, G. (2019). Effects of salicylic acid and heat acclimation on thermotolerance and withanolide accumulation under high temperature stress in the Cape gooseberry (*Physalis peruviana* L.) *Turkish Journal of Botany, 43*, 468-474. https://doi.org/10.3906/bot-1901-4

Tadhani, M., Patel, V. & Subhash, R. (2007). *In vitro* antioxidant activities of *Stevia rebaudiana* leaves and callus. *Journal of Food Compostion and Analysis, 20*, 323-329. https://doi.org/10.1016/j.jfca.2006.08.004

Tun, N. N., Santa-Catarina, C., Begum, T., Silveira, V., Handro, W., Floh, EIS, Scherer, G. F. (2006). Polyamines induce rapid biosynthesis of nitric oxide (NO) in *Arabidopsis thaliana* seedlings. *Plant Cell Physiology, 47*, 346-354. https://doi.org/10.1093/pcp/pci252

Uddin, M. S., Chowdhury, M. S. H., Khan, M. M. M. H., Uddin, M. B., Ahmed, R. & Baten, M. (2006). *In vitro* propagation of *Stevia rebaudiana* Bert in Bangladesh. *African Journal of Biotechnology, 5*, 1238-1240.

Vasquez-Hernandez, C., Feregrino-Perez, A. A., Perez-Ramirez, I., Ocampo-Velazqueza, R. V., Rico-García E., Torres-Pacheco I. & Guevara-Gonzaleza R. G. (2019). Controlled elicitation increases steviol glycosides (SGs) content and gene expression-associated to biosynthesis of SGs in *Stevia rebaudiana* B. cv. Morita II. *Industrial Crops and Products, 139*, 111479. https://doi.org/10.1016/j.indcrop.2019.111479

Vázquez-Hernández, M. C., Parola-Contreras, I., Montoya-Gómez, L. M., Torres-Pacheco, I., Schwarz, D. & Guevara-González, R. G. (2019). Eustressors: chemical and physical stress factors used to enhance vegetables production. *Scientia Horticulture*, *250*, 223-229. https://doi.org/10.1016/j.scienta.2019.02.053

Yildiztugay, E., Ozfidan-Konakci, C. & Kucukoduk, M. (2014). Exogenous nitric oxide (as sodium nitroprusside) ameliorates polyethylene glycol induced osmotic stress in hydroponically grown maize roots. *Plant Growth Regulation, 330*, 683-696. https://doi.org/10.1007/s00344-014-9417-1

Yin, Z. P., Li S., Ren, J. & Song, X. S. (2014). Role of spermidine and spermine in alleviation of drought-induced oxidative stress and photosynthetic inhibition in Chinese dwarf cherry (*Cerasus humilis*) seedlings. *Plant Growth Regulation, 74*, 209-218. https://doi.org/10.1007/s10725-014-9912-1

Yoneda, Y., Shimizu, H., Nakashima, H., Miyasaka, J. & Ohdoi, K. (2018). Effect of treatment with gibberellin, gibberellin biosynthesis inhibitör, and auxin on steviol glycoside content in *Stevia rebaudiana* bertoni. *Sugar Technology, 20*(4), 482-491. https://doi.org/10.1007/s12355-017-0561-3

Zhu, J. K. (2001). Cell signaling under salt, water, and cold stresses. *Current Opinion in Plant Biology, 4*(5), 401–406. https://doi.org/10.1016/s1369-5266(00)00192-8

Zottini, M., Costa, A., De Michele, R., Ruzzene, M., Carimi, F. & Lo Schiavo, F. (2007). Salicylic acid activates nitric oxide synthesis in *Arabidopsis*. *Journal of Experimental Botany, 58*(6), 1397-1405. https://doi.org/10.1093/jxb/erm001

Biotech Studies 32(2), 75-82
http://doi.org/10.38042/biotechstudies.1332403

BIOTECH STUDIES

RESEARCH PAPER

Omicron variants bind to human angiotensin-converting enzyme 2 (ACE2) much stronger due to higher number of charged-charged interactions

Sibel Kalyoncu[1]

[1]Izmir Biomedicine and Genome Center, 35340 Izmir, Turkiye

How to cite:
Kalyoncu, S. (2023). Omicron variants bind to human angiotensin-converting enzyme 2 (ACE2) much stronger due to higher number of charged-charged interactions. *Biotech Studies*, *32*(2),75-82. http://doi.org/10.38042/biotechstudies.1332403

Article History
Received 25 April 2023
Accepted 24 July 2023
First Online 24 July 2023

Corresponding Author
Tel.: +90 232 2994168
E-mail: sibel.kalyoncu@ibg.edu.tr

Keywords
Coronavirus disease 2019 (COVID-19)
Severe acute respiratory syndrome coronavirus 2 (SARS-CoV-2)
Omicron
Receptor binding domain (RBD)
Angiotensin-converting enzyme 2 (ACE2)

Abstract

Since the start of COVID-19 pandemic, several mutant variants of SARS-CoV-2 have emerged with different virulence and transmissibility patterns. Some of these variants have been labeled as variants of concern (VOC). There are mainly five strain clades with VOC status: Alpha, Beta, Gamma, Delta, and Omicron. Omicron sub-variants have been currently in circulation around the world, and they show faster transmissibility and lower virulence compared to others. Receptor binding domain (RBD) of SARS-CoV-2 spike protein is the region where it binds to human angiotensin-converting enzyme 2 (hACE2) on the host cell. Mutations on RBD might have direct or indirect effects on differential disease patterns of these variants. In this study, we analyzed sequence and structures of SARS-CoV-2 variants' RBD domains and documented their predicted affinities and contact interactions with hACE2. We found that Omicron sub-variants have much higher hACE2 affinities compared to other VOC strains. To understand reasons behind this, we checked biophysical characteristics of RBD-hACE2 contacts. Surprisingly, number of charged-charged interactions of Omicron sub-variants were on average 4-fold higher. These higher charged residue mutations on epitope region of Omicron sub-variants leading to stronger affinity for hACE2 might shed light onto why Omicron has less severe disease symptoms.

Introduction

On December 2019, the first report of coronavirus disease 2019 (COVID-19) was announced (Li et al., 2020), and more than 6.8 million people worldwide were killed by COVID-19 as of 11 April 2023 (Dong et al., 2020). Although the first vaccinations against the original Wuhan strain started in late 2020, new mutant variants of severe acute respiratory syndrome coronavirus 2 (SARS-CoV-2) are emerging and spreading where early-developed vaccines might not protect as expected (Eyre et al., 2022; Kalyoncu et al., 2023; Markov et al., 2023). There are numerous variants of SARS-CoV-2 of which are labeled as variants of concern (VOC) by World Health Organization (WHO) due to either its increase in transmissibility or virulence (Aleem et al., 2022). Up to now, five main VOCs have been reported with their related strain clades: (i) Alpha (B.1.1.7), (ii) Beta (B.1.351), (iii) Gamma (P.1), (iv) Delta (B.1.617.2), and (v) Omicron. While the former four of them were previously circulating VOCs, Omicron sub-variants are the currently circulating VOCs (Rambaut et al., 2020). The symptoms of Omicron variants are not as severe as other previous VOCs but its transmissibility is higher (Chatterjee et al., 2023).

SARS-CoV-2 is a single-stranded RNA-enveloped virus (Lu et al., 2020). It uses its spike protein for receptor recognition and cell membrane entry. The receptor binding domain (RBD) of its spike protein binds to angiotensin-converting enzyme 2 (ACE2), a cellular receptor, for its viral entry into the host cell (Jackson et al., 2022; Letko et al., 2020). Because the RBD domain of

spike protein is indispensable for the host cell entry, mutations on RBD for emerging new variants should be analyzed in detail to see whether those mutations affect its receptor binding kinetics. It is not known whether ACE2 binding kinetics of variants' RBD domain affect SARS-CoV-2's transmissibility and/or virulence. We hypothesize that stronger binding of RBD-ACE2 decreases the virulence and increases the transmissibility. We tested this hypothesis by investigating the RBD structures of all VOCs and binding kinetics between their RBDs and human ACE2. We found that Omicron strains mostly have a stronger affinity for ACE2 (dissociation constant-K_D in picomolar range) while previous VOCs have much less affinity (K_D in nanomolar range). We also showed that this stronger binding was caused by a higher number of (four fold) charged-charged amino acid interactions and higher positive charges in the RBD-ACE2 interface.

Materials and Methods

Sequence analysis

Amino acid sequences of RBD domains were extracted from NCBI GenBank database with "Severe acute respiratory syndrome coronavirus 2 isolate" term (with organism tax id of txid2697049). First RNA sequences were downloaded from NCBI Genbank (Genbank IDs: OQ415315.1 for Alpha, OM286905.1 for Beta, OK091006.1 for Delta, OM367886.1 for Gamma, OM366054.1 for Kappa, OX315743.1 for BA.1, OX315675.1 for BA.2, OP603965.1 for Omicron BA.4&5, OM739178.1 for Omicron BA.2.12.1, OQ300138.1 for Omicron BQ.1, OQ300139.1 for Omicron XBB). Regions coding for RBD domain of Spike protein were analyzed and translated to corresponding amino acid sequences. GISAID Database was used to confirm the extracted amino acid sequences (Elbe & Buckland-Merrett, 2017). There were some discrepancies between NCBI extracted data and GISIAD database, GISIAD Database was used to correct these discrepancies because it consolidates many isolates (>200) for each reported variant. SnapGene software (www.snapgene.com) was used to align amino acid sequences. EMBL-EBI Simple Phylogeny tool was used to create phylogram plot (Madeira et al., 2022). The graph for the selected country (Turkiye in here) was represented as the proportion of the total number of each strain sequences over time (https://covariants.org/per-country) (Elbe & Buckland-Merrett, 2017). Variants were represented in the graph if they have at least 70 sequences over a period of at least four weeks.

Structure analysis and homology modelling

Three dimensional RBD domain structures of many variants used in this study were already in RCSB PBD database (PDB IDs: 7EKF for Alpha, 7EKG for Beta, 7EKC for Delta, 7SO9 for Gamma, 7VX9 for Kappa, 7UB0 for BA.2, 7NXQ for Omicron BA.4&5, 7XNS for Omicron BA.2.12.1), only Omicron BA.1, BQ.1 and XBB variants were not in the database. Therefore, a homology modeling was used for these three variants. Their structural coordinates were modeled using SWISS-MODEL (Waterhouse et al., 2018). The aim of homology modeling is to get the lowest energy conformation for the given amino acid sequence based on a template structure. There are numerous experimental structures of other SARS-CoV-2 variants which can be used as templates in RCSB PDB database. The template with the highest sequence identity was chosen as the homology modeling template for the selected variant (7WBP for Omicron BA.1, 7XNQ for Omicron BQ.1 and 7YQW for Omicron XBB).

RBD-human ACE2 (hACE2) interaction of the Wuhan strain (PDB ID: 6LZG) was used to generate variants' RBD-hACE2 complex structure. PyMOL was used to align each variant's RBD domain structures onto WT RBD (The PyMOL Molecular Graphics System, Version 2.0 Schrödinger, LLC). Root Mean Square Deviation **(**RMSD) values were used to assess quantitative measures of the similarity between two superimposed/aligned structures. Then, structures of aligned RBD-hACE2 complexes were exported as the final structures for binding interaction analysis.

Electrostatic potential calculations

Adaptive Poisson-Boltzmann Solver (APBS) under PyMOL was used to calculate and display the electrostatic potentials of each molecular surface (Miller et al., 2012). Results were represented as a color-coded electrostatic surface in units of K_bT/e_c where K_b is Boltzmann's constant, T is temperature and e_c is electric charge.

Affinity and interaction prediction

The affinities and interfacial contact numbers of the interacting proteins were calculated using PRODIGY web server (Vangone & Bonvin, 2015; Xue et al., 2016). The PDB file of each variant's RBD-hACE2 complex was imported into PRODIGY, the model was selected as protein–protein, interactor 1 was set to the chain of RBD, interactor 2 was set to the chain of the hACE2, and the temperature was set to 25 °C. The affinities and dissociation constants of each RBD-hACE2 complex were reported. Also, the number of interfacial contacts based on their types (Charged-Charged, Charged-Polar, Charged-Apolar, Polar-Polar, Polar-Apolar, Apolar-Apolar) were reported. Binding affinity were reported in two terms: predicted free energy (ΔG) and dissociation constant (K_D) according to the equation below:

$$\Delta G = RTlnK_D$$

where R is the ideal gas constant (kcal/K mol), T is the temperature (K) and ΔG is the predicted free energy.

Results and Discussion

Since the start of the COVID-19 pandemic, several mutant variants have emerged around the world, and each showed different transmissibility and disease

symptoms. Currently, Omicron sub-variants have been circulating in the population. While Omicron variants show lower disease severity, their transmissibility increases (Rana et al., 2022). The molecular mechanism underlying these evolutionary patterns of Omicron variants is still not known. Here, we try to investigate structural mechanisms behind the virus-host cell interaction of Omicron sub-variants by comparing them to early variants of the SARS-CoV-2. After the SARS-CoV-2 virus enters the body, it directly binds to the human ACE2 receptor on the host cell. The interacting domain of SARS-CoV-2 virus is RBD located on the Spike protein. First, we extracted the coding amino acid sequence information of RBD domains for all variants tested (Figure 1). Amino acids 317-540 of Spike protein were selected as RBD domain according to three dimensional structural patterns. On the sequence alignment, epitope regions where it directly contacts with hACE2 were highlighted along with mutated sites. According to our results, four epitope positions (417, 446, 498, 501) out of 21 showed mutational patterns among different variants (Figure 1). Among these positions, Omicrons sub-variants (BA.1, BA.2, BA.4&5, BA.2.12.1, BQ.1, XBB) showed enriched mutational patterns compared to early variants. For example, positions 440, 498, and 505 clearly evolved to a more basic pattern for all Omicron sub-variants.

The emergence of SARS-CoV-2 variants in Turkey has been parallel to the global pattern (Figure 2A). Evolutionary relationship between variants seemed to align well with their emergence sequence in the population (Figure 2B). And there was a clear distinction between early variants and Omicron sub-variants. From a structural point of view, three dimensional structures of each variants' RBD domain were needed. For most of them, their atomic coordinates were readily available in

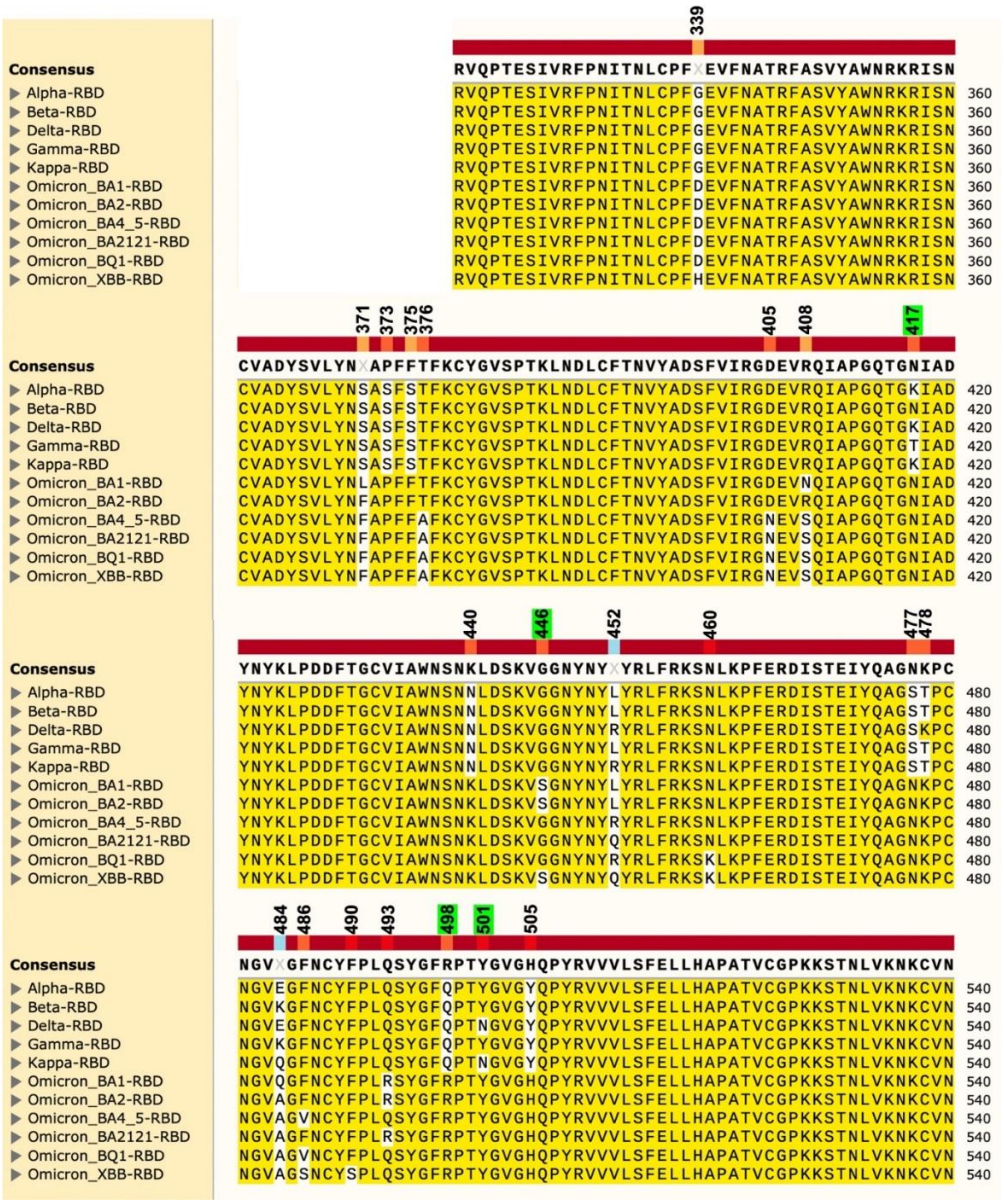

Figure 1. Amino acid sequence alignment of receptor binding domains of SARS-CoV-2 strains. Mutation sites are marked with the residue number, and epitope residues on mutation sites are highlighted with green.

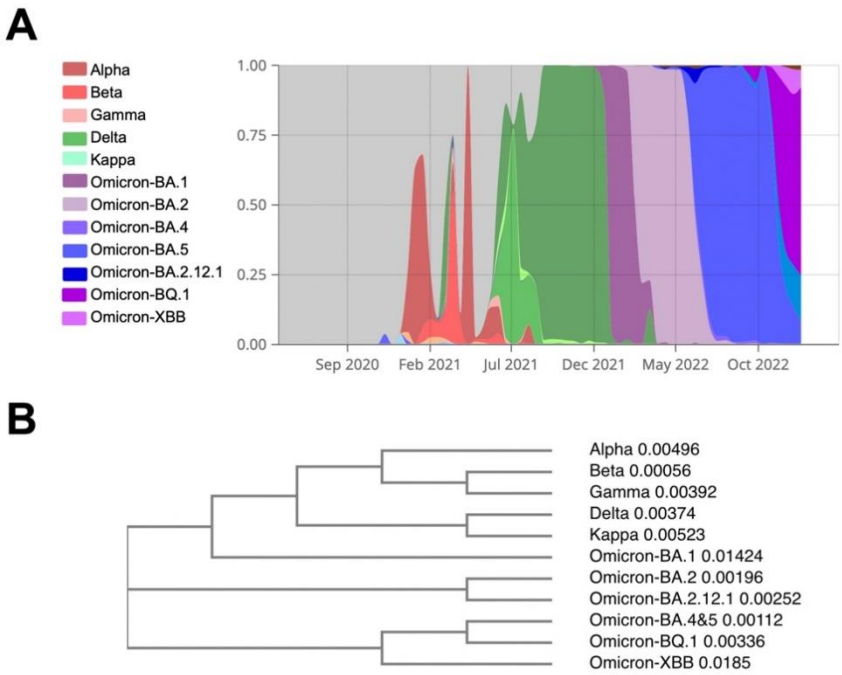

Figure 2. Lineage and structure of SARS-CoV-2 strains. (**A**) Proportion of total number of sequences over time, that fall into strain groups in Turkiye. Data was retrieved from https://covariants.org/ (Elbe & Buckland-Merrett, 2017). (**B**) Phylogenetic tree showing an evolutionary relationship of SARS-CoV-2 strains.

the protein databank, but those of three variants (Omicrons BA.1, BQ.Q, XBB) were absent. Therefore, homology modeling was performed for each of these three variants with templates of >98% sequence identity (Table 1). In comparison to the original Wuhan strain, RMSD values of early variants were clearly lower than those of Omicron sub-variants with the highest structural distance of Omicron BQ.1 (RMSD of 1.904 Å). Most strikingly, the number of amino acid mutations in Omicron sub-variants was 4x-19x times more than early variants.

Epitope surfaces of RBDs where they bind to hACE2 were first analyzed electrostatically by Poisson-Boltzmann Surface Area (PBSA) method. It is commonly used to calculate free energies of various molecules with a solvation contribution and electrostatic analysis (Wang et al., 2017). There was a clear difference in epitope surfaces of VOC strains and Omicron sub-strains (Figure 3). VOC strains, especially early variants (Wuhan, Alpha, Beta, Gamma), have slightly negative to neutral surfaces, while all Omicron sub-variants have

Table 1. Structure information for RBD domains of all strains. Structure similarity to Wuhan RBD was represented as Root Mean Square Deviation **(**RMSD) and the number of amino acid mutations compared to Wuhan RBD was reported. PBD IDs used were given for each RBD structure. The strains with no published structure (Omicron-BA.1/BQ.1/XBB) were homology-modelled by Swiss-Model and their model template PDB IDs along with % sequence identity to those templates were given

	RMSD (Å^2) from Wuhan strain	Structure or homology model template (PDB ID)	% Sequence identity, if homology modelled	Number of mutations compared to Wuhan strain
Alpha	0.209	7EKF	-	1
Beta	0.143	7EKG	-	3
Gamma	0.161	7EKC	-	3
Delta	0.456	7SO9	-	2
Kappa	0.840	7VX9	-	2
Omicron-BA.1	0.234	7WBP	98.6	13
Omicron-BA.2	0.612	7UB0	-	16
Omicron-BA.4&5	1.899	7XNQ	-	17
Omicron-BA.2.12.1	1.671	7XNS	-	17
Omicron-BQ.1	1.904	7XNQ	99.5	18
Omicron-XBB	1.129	7YQW	98.6	19

dominantly positive surfaces at varying patch locations on the epitopes. Among early variants, only Kappa strain has a comparable positive epitope surface. This positive charge dominance in epitope surface probably changes the biophysical characteristics of RBD-hACE2 binding interaction.

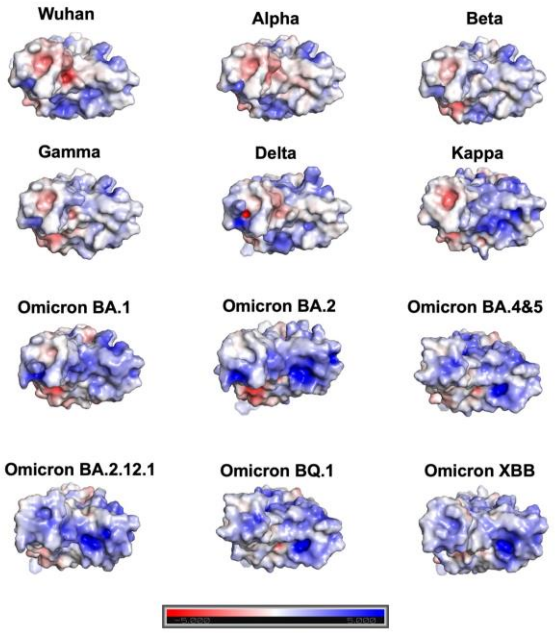

Figure 3. Poisson-Boltzmann Surface Area (PBSA) results of each variant RBD to analyze their electrostatic behaviors. Epitope surfaces where they directly interact with hACE2 were shown for each. More positively charged interaction surfaces of Omicron variants are obvious with more blue patches.

Next, we focused on interaction contacts and affinities of RBD-hACE2. Epitope region of Wuhan strain where hACE2 directly binds was highlighted in the complex structure of Wuhan RBD-hACE2 (Figure 4A). Among those, K417, G446, Q498, and N501 were mutated epitope residues in most of the variants. When RBD domains of all variants were aligned on Wuhan RBD domain with a stationary hACE2, the main regions on the epitope interface seemed to be conserved (Figure 4B). Therefore, we can assume that the same epitope residues dominate the RBD-hACE2 interaction with a possible contribution from nearby conformational residues.

The affinity of protein-protein interactions is an important indicator for association/dissociation kinetics and functional changes. Stronger binding patterns might lead to lower dissociation rates resulting in functional improvements or impairments depending on the mechanism of action (Kastritis & Bonvin, 2013). When we estimated affinities of RBD-hACE2 interaction by Prodigy, there was a clear distinction between Omicron sub-variants and early variants (Table 2). Omicron-subvariants had stronger binding affinities to hACE2 with the highest affinity of Omicron-BA.2.12.1 (K_D of 0.01 nM). While early variants were in nanomolar range for the K_D, Omicron variants showed dissociation constants in picomolar ranges. When averages were taken, Omicron-variants showed more than two times better affinities.

There could be several reasons behind the stronger binding affinities of Omicron variants, but the most obvious cause should be related to changes in epitope-paratope interactions. When we checked epitope-

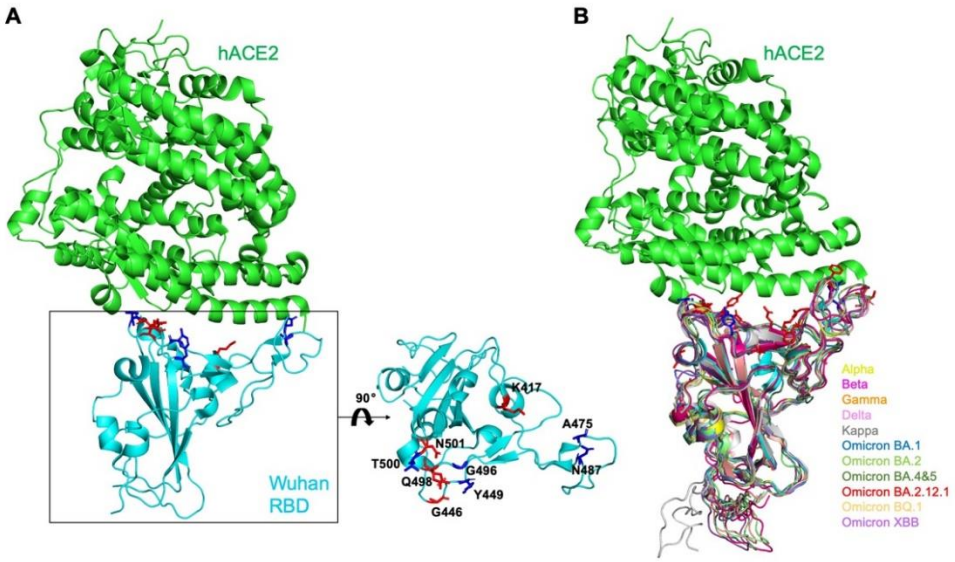

Figure 4. Complex structures of ACE2-RBD. (**A**) Cartoon representation of human ACE2-RBD of Wuhan strain interaction. Epitope residues of Wuhan RBD were labeled as red and blue sticks which represent mutated and unmutated residues, respectively. (**B**) Cartoon representation of human ACE2 with overlayed RBD structures of all other strains.

paratope interactions by physicochemical content types, there was a clear difference in the number of charged-charged contacts (Table 2). While early variants had a frequency of 1.8 charged-charged contacts, Omicron variants had 7.0 of those (more than 3.5 times higher frequency). Other interfacial contact types did not have that much of a significant change. Therefore, we concluded that stronger binding patterns of Omicron sub-variants are mostly due to its increased charged-charged interactions between RBD-hACE2 interface, especially through positively charged surfaces of Omicron RBDs. Accumulation of charged mutations around the epitope region of RBD could be an indicator of this affinity increase.

There are several molecular dynamics (Jawad et al., 2021; Kim et al., 2022) and experimental studies on RBD-hACE2 binding kinetics (Barton et al., 2021; Kim et al., 2022). However, they mostly focus on either the Wuhan strain or early strains, none of those studies discuss recently circulating omicron strains such as BQ.1 and XBB. Our general finding of Omicron strains' higher binding affinity was experimentally confirmed by one of these studies (Kim et al., 2022) but they only discuss the first strain of Omicron.

The first Omicron variant (BA.1) first appeared at the end of 2021 in South Africa and its several sub-variants have been emerging until today (Das et al., 2022). Although there are several mutations (>60) in their genome, all Omicron variants show higher transmissibility along with less disease severity. This is good news for the population because the COVID-19 pandemic might have started to converge into an endemic status (Are et al., 2023). We hypothesized that bio-physical/chemical properties of RBD-hACE2 interaction of Omicron variants might have effects on their disease and transmissibility patterns. We found out that Omicron variants have more positive epitope surfaces, and they also have an overall higher binding affinity to hACE2. The affinity was measured as dissociation constant (K_D), higher the affinity means lower dissociation constant. The affinity is directly related to the dissociation constant (k_{off}) and inversely related to the association constant (k_{on}) (Kastritis & Bonvin, 2013). The higher the affinity is the lower the dissociation and the higher the association of interacting proteins ($K_D=k_{off}/k_{on}$) (Wang et al., 2019). When the association rates are higher, it can attach to the host cells at a higher rate, in this case, hACE2 expressing epithelial cells in the airways (J. Liu et al., 2021). These factors might lead to faster transmissibility due to faster rates of association. On the other hand, lower dissociation rates can cause prolonged actions on the cell probably leading to less disease severity (H. Liu et al., 2021). More experimental research is needed to confirm this theory by investigating the relationship between these RBD-hACE2 affinities and virus variants' transmissibility/virulence patterns.

Conclusion

The COVID-19 pandemic has affected all nations in the world since the start of 2020, but its convergence to an endemic state started after Omicron strains emerged. Omicron strains showed lower disease severity along with rapid transmissibility. There are more than 60 mutations in Omicron variants compared to the original Wuhan strain, but mutations on RBD domain are notable due to their direct contact with the host cell via hACE2. Here, we focused on RBD domains of variants of concern and performed a structural and

Table 2. Interaction information for hACE2 – RBD of each SARS-CoV-2 strain. Prodigy was used to predict affinities/contact numbers for hACE2 based on their three dimensional structures (Vangone & Bonvin, 2015; Xue et al., 2016)

	Affinity to hACE2		**Number of interfacial contacts per type**					
	ΔG (kcal/mol)	K_D (nM)	Charged-Charged	Charged-Polar	Charged-Apolar	Polar-Polar	Polar-Apolar	Apolar-Apolar
Wuhan	-12.4	0.83	3	10	19	5	23	9
Alpha	-12.2	1.00	3	7	22	5	21	12
Beta	-11.8	2.10	0	9	23	5	20	12
Gamma	-12.1	1.40	0	8	23	5	21	13
Delta	-12.7	0.47	2	9	21	5	24	10
Kappa	-12.2	1.20	3	9	20	7	24	12
Omicron-BA.1	-12.5	0.67	7	7	23	5	20	11
Omicron-BA.2	-13.3	0.17	9	5	27	4	21	15
Omicron-BA.4&5	-12.3	0.88	5	8	26	6	21	17
Omicron-BA.2.12.1	-15.2	0.01	11	7	32	4	27	17
Omicron-BQ.1	-12.3	0.91	5	8	26	6	21	17
Omicron-XBB	-12.6	0.61	5	10	24	6	22	11
Average for initial strains	**-12.2**	**1.17**	**1.8**	**8.7**	**21.3**	**5.3**	**22.2**	**11.3**
Average for Omicron strains	**-13.0**	**0.54**	**7.0**	**7.5**	**26.3**	**5.2**	**22.0**	**14.7**

functional analysis of their RBD-hACE2 interaction. We found out that Omicron sub-variants bind to hACE2 at least two times stronger. Also, we showed that this affinity increase is mainly due to a higher number of charged-charged contacts especially with positively charged epitope surfaces between RBD and hACE2. We speculate that stronger affinity of Omicron variants might lead to higher transmissibility and lower disease severity patterns due to their faster rates of association and/or slower rates of dissociation.

Funding Information

This research received support from The Scientific and Technological Research Council of Türkiye (TÜBİTAK) project number 18AG020_IBG-COV-01.

Acknowledgements

The author thanks Prof. Dr. Mehmet Inan (Izmir Biomedicine and Genome Center, IBG) for his valuable comments. The author would like to express her gratitude to Kalyoncu Lab and FARMA group members at IBG.

References

Aleem, A., Akbar Samad, A. B., & Slenker, A. K. (2022). Emerging Variants of SARS-CoV-2 And Novel Therapeutics Against Coronavirus (COVID-19). In *StatPearls*. https://www.ncbi.nlm.nih.gov/pubmed/34033342

Are, E. B., Song, Y., Stockdale, J. E., Tupper, P., & Colijn, C. (2023). COVID-19 endgame: From pandemic to endemic? Vaccination, reopening and evolution in low- and high-vaccinated populations. *J Theor Biol*, *559*, 111368. https://doi.org/10.1016/j.jtbi.2022.111368

Barton, M. I., MacGowan, S. A., Kutuzov, M. A., Dushek, O., Barton, G. J., & van der Merwe, P. A. (2021). Effects of common mutations in the SARS-CoV-2 Spike RBD and its ligand, the human ACE2 receptor on binding affinity and kinetics. *Elife*, *10*. https://doi.org/10.7554/eLife.70658

Chatterjee, S., Bhattacharya, M., Nag, S., Dhama, K., & Chakraborty, C. (2023). A Detailed Overview of SARS-CoV-2 Omicron: Its Sub-Variants, Mutations and Pathophysiology, Clinical Characteristics, Immunological Landscape, Immune Escape, and Therapies. *Viruses*, *15*(1). https://doi.org/10.3390/v15010167

Das, S., Samanta, S., Banerjee, J., Pal, A., Giri, B., Kar, S. S., & Dash, S. K. (2022). Is Omicron the end of pandemic or start of a new innings? *Travel Med Infect Dis*, *48*, 102332. https://doi.org/10.1016/j.tmaid.2022.102332

Dong, E., Du, H., & Gardner, L. (2020). An interactive web-based dashboard to track COVID-19 in real time. *Lancet Infect Dis*, *20*(5), 533-534. https://doi.org/10.1016/S1473-3099(20)30120-1

Elbe, S., & Buckland-Merrett, G. (2017). Data, disease and diplomacy: GISAID's innovative contribution to global health. *Glob Chall*, *1*(1), 33-46. https://doi.org/10.1002/gch2.1018

Eyre, D. W., Taylor, D., Purver, M., Chapman, D., Fowler, T., Pouwels, K. B., Walker, A. S., & Peto, T. E. A. (2022). Effect of Covid-19 Vaccination on Transmission of Alpha and Delta Variants. *N Engl J Med*, *386*(8), 744-756. https://doi.org/10.1056/NEJMoa2116597

Jackson, C. B., Farzan, M., Chen, B., & Choe, H. (2022). Mechanisms of SARS-CoV-2 entry into cells. *Nat Rev Mol Cell Biol*, *23*(1), 3-20. https://doi.org/10.1038/s41580-021-00418-x

Jawad, B., Adhikari, P., Podgornik, R., & Ching, W. Y. (2021). Key Interacting Residues between RBD of SARS-CoV-2 and ACE2 Receptor: Combination of Molecular Dynamics Simulation and Density Functional Calculation. *J Chem Inf Model*, *61*(9), 4425-4441. https://doi.org/10.1021/acs.jcim.1c00560

Kalyoncu, S., Yilmaz, S., Kuyucu, A. Z., Sayili, D., Mert, O., Soyturk, H., Gullu, S., Akinturk, H., Citak, E., Arslan, M., Taskinarda, M. G., Tarman, I. O., Altun, G. Y., Ozer, C., Orkut, R., Demirtas, A., Tilmensagir, I., Keles, U., Ulker, C., Inan, M. (2023). Process development for an effective COVID-19 vaccine candidate harboring recombinant SARS-CoV-2 delta plus receptor binding domain produced by Pichia pastoris. *Sci Rep*, *13*(1), 5224. https://doi.org/10.1038/s41598-023-32021-9

Kastritis, P. L., & Bonvin, A. M. (2013). On the binding affinity of macromolecular interactions: daring to ask why proteins interact. *J R Soc Interface*, *10*(79), 20120835. https://doi.org/10.1098/rsif.2012.0835

Kim, S., Liu, Y., Ziarnik, M., Cao, Y., Zhang, X. F., & Im, W. (2022). Binding of Human ACE2 and RBD of Omicron Enhanced by Unique Interaction Patterns Among SARS-CoV-2 Variants of Concern. *bioRxiv*. https://doi.org/10.1101/2022.01.24.477633

Letko, M., Marzi, A., & Munster, V. (2020). Functional assessment of cell entry and receptor usage for SARS-CoV-2 and other lineage B betacoronaviruses. *Nat Microbiol*, *5*(4), 562-569. https://doi.org/10.1038/s41564-020-0688-y

Li, Q., Guan, X., Wu, P., Wang, X., Zhou, L., Tong, Y., Ren, R., Leung, K. S. M., Lau, E. H. Y., Wong, J. Y., Xing, X., Xiang, N., Wu, Y., Li, C., Chen, Q., Li, D., Liu, T., Zhao, J., Liu, M., Feng, Z. (2020). Early Transmission Dynamics in Wuhan, China, of Novel Coronavirus-Infected Pneumonia. *N Engl J Med*, *382*(13), 1199-1207. https://doi.org/10.1056/NEJMoa2001316

Liu, H., Zhang, Q., Wei, P., Chen, Z., Aviszus, K., Yang, J., Downing, W., Jiang, C., Liang, B., Reynoso, L., Downey, G. P., Frankel, S. K., Kappler, J., Marrack, P., & Zhang, G. (2021). The basis of a more contagious 501Y.V1 variant of SARS-CoV-2. *Cell Res*, *31*(6), 720-722. https://doi.org/10.1038/s41422-021-00496-8

Liu, J., Li, Y., Liu, Q., Yao, Q., Wang, X., Zhang, H., Chen, R., Ren, L., Min, J., Deng, F., Yan, B., Liu, L., Hu, Z., Wang, M., & Zhou, Y. (2021). SARS-CoV-2 cell tropism and multiorgan infection. *Cell Discov*, *7*(1), 17. https://doi.org/10.1038/s41421-021-00249-2

Lu, R., Zhao, X., Li, J., Niu, P., Yang, B., Wu, H., Wang, W., Song, H., Huang, B., Zhu, N., Bi, Y., Ma, X., Zhan, F., Wang, L., Hu, T., Zhou, H., Hu, Z., Zhou, W., Zhao, L., . . . Tan, W. (2020). Genomic characterisation and epidemiology of

2019 novel coronavirus: implications for virus origins and receptor binding. *Lancet*, *395*(10224), 565-574. https://doi.org/10.1016/S0140-6736(20)30251-8

Madeira, F., Pearce, M., Tivey, A. R. N., Basutkar, P., Lee, J., Edbali, O., Madhusoodanan, N., Kolesnikov, A., & Lopez, R. (2022). Search and sequence analysis tools services from EMBL-EBI in 2022. *Nucleic Acids Res*, *50*(W1), W276-279. https://doi.org/10.1093/nar/gkac240

Markov, P. V., Ghafari, M., Beer, M., Lythgoe, K., Simmonds, P., Stilianakis, N. I., & Katzourakis, A. (2023). The evolution of SARS-CoV-2. *Nat Rev Microbiol*. https://doi.org/10.1038/s41579-023-00878-2

Miller, B. R., 3rd, McGee, T. D., Jr., Swails, J. M., Homeyer, N., Gohlke, H., & Roitberg, A. E. (2012). MMPBSA.py: An Efficient Program for End-State Free Energy Calculations. *J Chem Theory Comput*, *8*(9), 3314-3321. https://doi.org/10.1021/ct300418h

Rambaut, A., Holmes, E. C., O'Toole, A., Hill, V., McCrone, J. T., Ruis, C., du Plessis, L., & Pybus, O. G. (2020). A dynamic nomenclature proposal for SARS-CoV-2 lineages to assist genomic epidemiology. *Nat Microbiol*, *5*(11), 1403-1407. https://doi.org/10.1038/s41564-020-0770-5

Rana, R., Kant, R., Huirem, R. S., Bohra, D., & Ganguly, N. K. (2022). Omicron variant: Current insights and future directions. *Microbiol Res*, *265*, 127204. https://doi.org/10.1016/j.micres.2022.127204

Vangone, A., & Bonvin, A. M. (2015). Contacts-based prediction of binding affinity in protein-protein complexes. *Elife*, *4*, e07454. https://doi.org/10.7554/eLife.07454

Wang, C., Greene, D., Xiao, L., Qi, R., & Luo, R. (2017). Recent Developments and Applications of the MMPBSA Method. *Front Mol Biosci*, *4*, 87. https://doi.org/10.3389/fmolb.2017.00087

Wang, Y., Yan, J., & Goult, B. T. (2019). Force-Dependent Binding Constants. *Biochemistry*, *58*(47), 4696-4709. https://doi.org/10.1021/acs.biochem.9b00453

Waterhouse, A., Bertoni, M., Bienert, S., Studer, G., Tauriello, G., Gumienny, R., Heer, F. T., de Beer, T. A. P., Rempfer, C., Bordoli, L., Lepore, R., & Schwede, T. (2018). SWISS-MODEL: homology modelling of protein structures and complexes. *Nucleic Acids Res*, *46*(W1), W296-W303. https://doi.org/10.1093/nar/gky427

Xue, L. C., Rodrigues, J. P., Kastritis, P. L., Bonvin, A. M., & Vangone, A. (2016). PRODIGY: a web server for predicting the binding affinity of protein-protein complexes. *Bioinformatics*, *32*(23), 3676-3678. https://doi.org/10.1093/bioinformatics/btw514

BIOTECH STUDIES

VOL 32 ISSUE 2 DECEMBER 2023 ISSN 2687-3761 E-ISSN 2757-5233

CONTENTS